THERMAL AND OPTICAL STUDIES OF CARBONS OBTAINED FROM HEXANE BY PYROLYSIS

BY

MD. ABDUR RASHID, B.SC. (HONS.), M.SC.

A THESIS PRESENTED TO THE DEPARTMENT OF PHYSICS, BUET, DHAKA IN PARTIAL FULFILMENT FOR THE DEGREE OF MASTER OF PHILOSOPHY.

BANGLADESH UNIVERSITY OF ENGINEERING & TECHNOLOGY

DHAKA

MARCH, 1987.

ACKNOWLEDGEMENT

I am extremely pleased to express my grateful acknowledgement to the following :

Dr. Tafazzal Hossain, my research supervisor, for his valuable help and fruitful suggestions in all stages of the work.

Professor M. Ali Asgar, Head of the department of Physics, BUET, Professor G.U. Ahmad, Dr. Nazma Zaman, Mrs. Dil Afroz Ahmed, Mrs. Fahima Khanam and my wife Hashi, for their helpful advice, inspiration and sincere cooperation.

J. Podder for his keen interest in the work.

Dr. Shamim Jahangir, and Mrs. Nasrin Farooq for their helpful advice and assistance in carrying out Differential thermal analysis (DTA) and Thermogravimetric analysis (TGA).

Mr. Shafiuddin Khan, for drawing the diagrams.

M/S. Shafiul Haque and Sirajul Islam, for developing and printing of the photo-micrographs.

Mr. Md. Abdul Mobin, for typing the manuscript of the thesis.

Bangladesh University of Engineering and Technology, for the award of a grant and financial assistance to me for completing this work.

ABSTRACT

Pyrolysis of hexane has been carried out to examine whether it is possible to carbonise and ultimately to graphitize. Observation for isotropism or anisotropism has been made on the microstructures of carbons produced from hexane, using polarized-light microscopy. Differential thermal analysis (DTA) and Thermogravimetric analysis (TGA) have been employed to ascertain the graphitizability of hexane.

CONTENTS

CHAPTER - 1

INTRODUCTION

A number of workers[1-28] have recognised that the early stages of carbonisation process are important in deciding whether the final product of carbonisation is graphitic or not. Those organic materials which ultimately produce graphitizing carbons pass through a fusion stage during carbonisation. This is a necessary but not the sufficient condition for graphitizable organic materials.

The most remarkable work by Brooks and Taylor[5,6] on the structural conditions for graphitizability have demonstrated the significance of mesophase transformation which takes place as a precursor state in all graphitizable organic materials during carbonisation in the temperature range 350°C - 600°C. This transformation is a liquid state structural transition in which the large planer molecules formed by the reactions of thermal cracking and aromatic polymerization become aligned in a parallel array to form an optically anisotropic liquid crystal.

Mesophase is thus the precursor to graphitization and this phase is formed when an isotropic organic material is converted into a mosaic texture. Nematic mesophases have been considered by Brooks and Taylor[5,6], Dubois et al[11], Honda et al[12] and Marsh et al[13] in their studies on carbon production. This phase separates from the isotropic matrix as anisotropic spherical droplets on carbonisation. With the progress of carbonisation these spherical droplets tend to coalesce under certain pressure and temperature conditions to give a nematic texture. This discovery of conditions

for the formation of the spherical mesophase has received the greatest attention in characterizing graphitizable organic materials.

Abramski and Mackowsky[14] claimed that the size and the mosaic units are related to the degree of plasticity developed by the sample on carbonisation; the higher the plasticity developed the greater the possibility of obtaining order over larger areas resulting in larger mosaic units.

From a thermodynamic standpoint, the effect of pressure is often competatitive with that of temperature. In general, increase in temperature tends to melt a solid and produce a less ordered system; while increase in pressure tends to maintain an ordered phase. This creates the possibility that an isotropic liquid phase of a carbonising system may be favourably transformed under pressure into an optically anisotropic liquid crystal. This crystal describes the effect of pressure on carbonisation and its relationship to the graphitizability of the resulting carbon.

In the initial stages of nucleation and growth, the carbonaceous mesophase appears as small spherules which are suspended in the optically isotropic matrix with a simple structure as illustrated in three dimensions in fig. 1-1. As observed with cross polarisers, the extinction contours are rather simple and define the loci of points where the layers are parallel or perpendicular to the plane of polarization of the incident light. The layer planes of the simple spherules are stacked perpendicularly to the polar diameter and curve to meet the interface of the isotropic phase normally.

As carbonisation progresses with increasing temperature and duration of heat-treatment, the growing mesophase spherules, which are more dense than the isotropic parent phase, sink to the bottom of the container. When the spherules coalesce, larger droplets are produced giving rise to a bulk mesophase as in fig. 1.2. The bulk mesophase is an ensemble of extinction contours, the polarized-light extinction contours display nodes and maltese crosses when observed with cross-polarizers.

The first order red plate i.e. the gypsum plate is inserted at 45^{o} between crossed polars which gives the violet red interference colour at the end of the first order; if it suffers a very small subtractive effect there is a very marked change to orange or yellow; while if it suffers a very small additive effect, the red colour is raised to indigo or blue. Using this method sometimes called sensitive tint method, changes in pleochroism and in extinction contours for coalesced and for deformed mesophase are usually observed.

The process of the formation, coalescence, and deformation of the plastic mesophase establishes the basic elements of the graphite microstructure. The linear stacking discontinuities, that is, the nodal and cross-structures, are essential features of the coalesced mesophase, and the nodal structures are at least found to persist in their basic form upto graphitization temperatures.

The carbonaceous mesophase transformation which determines the morphology of graphitic products is thus considered as a precursor state to all graphitizable organic compounds. Many workers [18, 27] have shown that hetero-atoms such as H_2, O_2, N_2, S etc.

present in the feedstock materials may affect the carbonising and graphitizing behavior of an organic sample. These hetero-atoms can form in part stable volatile by-products during phyrolysis and thus decreases the carbon yield. On the other hand, the hetero-atoms can affect cross-linkage in the specimen and then also reduces the carbonising and graphitizing character of the sample.

The mechanism where hydrocarbons undergo pyrolysis to form elemental carbon is a complex process involving gas-phase decomposition reactions, nucleation of liquid microdroplets, diffusional transport of the nuclei to the surface and dehydrogenation to form carbon[22-25].

It was shown by many authors[18,27] that the increasing pressure not only increase the coke yield but also lowers the temperature at which pyrolysis was completed. Increase of pressure also improves pre-order and graphitizability of the residues. Simultaneously, the microstructure becomes coarser and more isotropic, i.e. the enlarged areas of optical anisotropy exhibit no. preferred orientation.

Little information is available in the open literature on the influence of pressures on the formation of microstructure in the residues. Some results of studies on carbonisation[28] under increasing pressure gave the following findings :

(i) Increasing pressure does not only increase the coke yield but also lowers the temperature at which pyrolysis is completed.

(ii) Increasing pressure changes mesophase microstructure.

(iii) Increasing pressure causes a pronounced segregation of original insolubles and of artificial insolubles like carbon black. The separated insolubles accumulate in the upper part of the pyrolysis vessel where as a highly ordered mesophase without insolubles is found lower down.

The present work has been devoted in order to study the thermal and optical effects of hexane on pyrolysis. A detailed study has been undertaken to study the carbonising and graphitizing behavior of hexane. Differential thermal analysis (DTA) and thermogravimatric analysis (TGA) of the sample have been carried out in order to see whether it is graphitic or non graphitic. Polarized-light photomicrographs of the sample have been examined at different heat-treatment temperatures to see whether the sample is isotropic or anisotropic and ultimately to get an idea about the graphitizability of the sample.

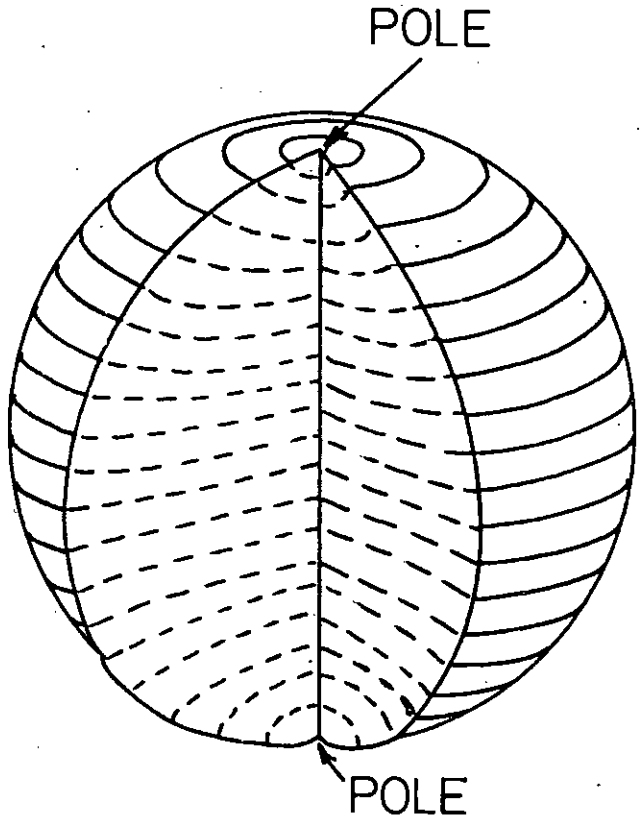

Fig 1.1. MESOPHASE SPHERE WITH SECTION INCLUDING POLAR DIAMETER

BEFORE CONTACT

JUST AFTER CONTACT

SHORT TIME AFTER CONTACT

TYPE OF COMPLEX INTERNAL STRUCTURE FORMED WHEN COMPOSITE OF TWO OR MORE SPHERES CONTRACTS TO ONE LARGE SPHERE

REARRANGEMENTS WHICH APPEAR TO OCCUR WHEN TWO SPHERES COALESCE

Fig 1.2

REFERENCES

1.1 Taylor, G.H., Fuel, 1961, 40, 465

1.2 Kipling, J.J., Sherwood, J.N., Shooter, P.V. and Thompson, N.R., Carbon, 1964, 1, 315.

1.3 Kipling, J.J., Sherwood, J.N., Shooter, P.V. and Thompson, N.R., Carbon, 1964, 1, 321.

1.4 Kipling, J.J. and Shooter, P.V., Second Conf. Ind. Carbon and Graphite, Soc. Chem. Ind., 1965, 15.

1.5 Brooks, J.D. and Taylor, G.H., Carbon, 1965, 3, 185.

1.6 Brooks, J.D. and Taylor, G.H., Nature, 1965, 206, 697.

1.7 Kipling, J.J. and Shooter, P.V., Carbon, 1966, 4, 1.

1.8 White, J.L., Guthrie, G.L. and Gardner, O., Carbon, 1967, 5, 517.

1.9 White, J.L., Dubois, J. and Souillart, C., J. Chim. Phys., Special volume, April, 1969, 33; Euratom Report 4094 e, 1969.

1.10 Honda, H., Kimura, H., Sanada, Y., Sugawara, S. and Furuta, T., Carbon, 1970, 8, 181.

1.11 Dubois, J., Agace, C. and White, J.L., Euratom Report 4627 e, 1971.

1.12 Honda, H., Kimura, H. and Sanada, Y., Carbon, 1971, 9, 695.

1.13 Marsh, H., Foster, J.M. Hermon, G. and Iley, M., Fuel, 1973, 52, 234, 243, 253.

1.14 Abramski, C. and Mackowsky, M.T., Methoden und Ergebnisse der angewandten Koksmikroskopie, Hand buch der Mikroskopie inder Technik, Ed. H. Freund; Vol. II, pt. I, p. 311, Verlag Umschau; Frankfust; 1952.

1.15 Graham, S.G., Ph.D. Thesis, 1974, Salford University.

1.16 White, J.L., In Petroleum-Derived Carbons (Edited by Grady, T.M.O. and Deviney, M.I.), Am. Chem. Soc. Symp. Ser., 1976, 21, 282.

1.17 Hossain, T., J. Bangladesh Academy of Sciences, Vol. 7, No. 1 and 2, 1983, 57.

1.18 Blayden, H.E., Gibson, J. and Riley, H.L., Inst. of Fuel, Wartime Bulletin, 1945, 125.

1.19 Franklin, E., Proc. Roy. Soc., A, 1951, 209, 196.

1.20 Walker, P.L., Carbon, 1972, 10, 369.

1.21 Dollimore, J. and Jenkins, M.J., private communication, 1966.

1.22 Chen, C.J. and Back, M.H., Pergamon Press Ltd., 1979, 17, 175.

1.23 Palmer, H.B. and Cullis, C.F., Chem. Phys. Carbon, 1965, 1, 265.

1.24 Fitzer, E., Mueller, K. and Schaefer, W., Chem. Phys. Carbon 1971, 7, 237.

1.25 Cullis, C.F. ACS Symp. Ser. 1976, 21, 348.

1.26 Lahaye, J. and Prado, G. ACS Symp. Ser. 1976, 21, 335.

1.27 Hüttinger, K.J. and Rosenblatt, U., Pergamon Press, Carbon, 1977, 15, 69.

1.28 Hüttinger, K.J. and Rosenblatt, U., Proc. 4th conference on industrial carbon and graphite, London, 1974. Society of Chem. Ind., London, 1976.

CHAPTER - II

CARBONISATION AND GRAPHITIZATION

2.1 INTRODUCTION

CARBON is the sixth element in the periodic table. In the elementary form, it occurs naturally in 'amorphous, forms as coal, lignite, gilsonite and in more limited quantities in its two allotropic crystalline forms : natural graphite and diamond.

Carbon has an atomic weight of 12.011 on the chemical scale. The electron configuration of carbon is $1S^2\ 2S^2\ 2P^2$. Out of the six electrons in a neutral atom, four are in the outer L-shell ($2S^2\ 2P^2$), and they are always available for chemical bonding. This bonding is principally carried out by the excitation of one S-state electron into a P-state, followed by orbital mixing. Several hundred thousand carbon-containing compounds are known till to-day, because of this unique atomic structure of carbon which results in its ability to react chemically with most other elements, as well as to bond with itself.

The process by which the non-carbon atoms such as oxygen, hydrogen, nitrogen or sulpher etc. are removed from the carbon-containing materials when pyrolysed to high temperatures, is known as 'carbonisation'.

At least three stages of carbonisation process can be recognised. They comprise a precarbonisation stage, an intermediate stage involving active decomposition, and a final stage in which residual traces of non-carbon elements are removed and some struc-

tural rearrangement in the solid product can occur. These stages are not of course sharply defined : they overlap and may vary according to the material concerned[35].

The carbonisation process is followed by a rearrangement of order within the remaining carbon atoms giving rise to a greater degree of order within the carbon produced which develop a three-dimensional order. Such development of a three-dimensional order gives rise to a structure very close to the well-defined structure of pure graphite which is termed as 'graphitization'. In fact, graphitization does not occur in "graphitizable carbons" untill they are annealed above 2500°C. The temperature range from 2500°C to 3000°C is called the"graphitization temperature range" which has been found to differ from material to material.

The designation "nongraphitic carbon" is used for carbonaceous materials when their powder patterns show only diffuse maxima at scattering angles corresponding to the (001) and (hK0) indices of graphite. These materials are also referred to as "amorphous carbon" or "pregraphitic carbons." A variety of materials belong to this class : cokes, chars, carbon blacks, and, in a larger sense, coals and anthracites. These materials may contain other elements, e.g., hydrogen, oxygen, and nitrogen, but the carbon atoms determine the essential features of the structure.

2.2 DIFFERENT FORMS OF CARBON

There are only two allotropic crystalline forms of carbon: (i) graphite and (ii) diamond. Both exist in nature and also can be produced artificially from many carbon containing materials. The main difference between these two allotropic forms is determined by the forces lying within crystallites.

Graphite is of a laminar structure and this structure is the anisotropic allotropic form of carbon. Each layer consists of a very large number of carbon atoms covalently linked to form what may be considered to be a huge polynuclear aromatic macromolecule. Each layer is planer, or very nearly so. The accepted ideal crystal structure which was first established by Bernal[3] (1924) is illustrated in fig. 2.1. It is a stable hexagonal lattice where the basal planes or layer planes consist of open hexagons with inter-atomic C-C distance being 1.415°A (for strongly linked), and these planes are stacked in an alternating sequence, the interplaner distance being 3.354°A (for weak bonding).

Diamond is metastable to graphite. It is a face centred cubic material with each carbon atom bonded covalently to four others in the form of a tetrahedron. The inter-atomic distance is 1.54°A. It is the hardest and most permanent of all known substances due to the rigidness of the tetrahedral covalent bond lattice of the single macromolecule that forms the perfect crystal. It has great industrial importance in cutting, shaping and polishing hard substances.

Three natural types of dimonds are available :

(i) crystalline and cleavable diamonds, more or less off grade and off color; (ii) bort, translucent to opaque, gray, or dark brown, with a radiated or confused crystalline structure (inferior grades of crystalline diamonds are also called bort); and (iii) carbonado, frequently known as a black diamond, or carbon. It occurs in an opaque, tough, crystalline aggregate without cleavage.

The graphite is converted into diamond by the assistance of catalysts as well as high temperatures and pressures. Though the structure of diamond (fig.2.7) is not the hexagonal, but Ergun and Leroy[1] have shown that a hexagonal structure for diamond is possible. Again at ordinary pressure diamond changes spontaneously to graphite above $1500^{\circ}C$[2] and at atmospheric pressure the graphite is a more stable form of carbon.

Crystallographically perfect graphite has a density of 2.266 gm/ml, while for diamond the density is 3.53 gm/ml. In the graphite structure only three of the four valence electrons of carbon form regular co-valent bonds with adjacent carbon atoms. The fourth electron is free and it resonates between the valance bond structures. The weak Van der Waals' forces exist between planes, while the strong chemical bonding forces exist in the basal planes. The bonding energy between planes is only about 2% of that within the planes[4,5].

The weak forces between layer planes account for (a) the tendency of graphite materials to fracture along planes, (b) the formation of interstitial compounds, (c) the lubricating, (d) the compressive and (e) many other properties of graphite.

For the hexagonal graphite structure, the stacking sequence of the planes is AB AB (fig. 2.1) so that the atoms in alternate planes are congruent. A rhombohedral structure has been found to exist in many graphites where the stacking sequence is ABC ABC (fig 2.2). In 1942 Lipson and Stokes[6] were able to show that this rhombohedral lattice which was proposed by Debye and Scherrer[7] in 1917 fully accounted for the extra X-ray-lines found in some powder photographs of graphites. The proportion of the rhombohedral form may be increased in graphites by grinding[8] which indicates that the change arises from the movements of the layers of carbon networks with respect to one another.

Plycrystalline carbon is the most natural graphite. Perfect single crystals greater than 10 µm are quite rare , although they can be produced with difficulty. Most synthetic graphites, made by high temperature calcination of pitch or coke blends, are polycrystalline. Single crystals of graphite of large dimension that occurs in some natural deposits can be obtained by pyrolytic deposition of carbon from carbonaceous vapours. The carbon deposition can take the form of highly oriented layers under suitable conditions. Subsequent treatment of this material can produce quite, large single crystals of pure graphite, known as "pyrolytic graphite".

There are another form of carbon known as 'amporphous carbon' apart from diamond and graphite. All amorphous carbons possess a small amount of order, although literally it means a structureless form of carbon. The first application of X-ray diffraction methods to amorphous carbons, however, led to the concept that they were also graphitic with their apparently amorphous

character which arises from the very minute size of the crystallites. These amorphous carbons can be prepared by the combustion of hydrocarbons in an incomplete supply of air, i.e. carbon blacks, charcoal and lamp blacks.

2.3 STRUCTURE OF CARBONS AS DETERMINED BY X-RAYS

There are two types of carbons - graphitizing and non-graphitizing : soft and hard.

Graphitizing carbons may be defined as those which begin to develop three-dimensional order on heating to temperatures near 1700°C. Such type of carbons are produced by two main processes : (i) the deposition from the vapour phase and (ii) the solidification from liquid or plastic state to form cokes. Substances which produce graphitizing carbons from the liquid or plastic state include vitrinites of medium volatile coking coal, high temperature coal-tar pitch, petroleum bitumen, polymers such as P.V.C and polynuclear aromatic compounds. By heating these substances, carbons which are coke like in appearance are obtained and they show complex patterns of optical anisotropy.

"Non-graphitizing carbons" are defined as the carbons in which the graphite-like layers lie in parallel groups but are not oriented like the crystalline structure of graphite, the three-dimensional structure of crystalline graphite is not present in these types of carbons. Heating to sufficiently high temperatures between 1700°C and 3000°C the graphite - like layers show a tendency to change from a 'random layer structure' towards an ordered structure of crystalline graphite which can be shown by X-ray powder

photography method. These intermediate type of structures in which the three-dimensional graphite structure is partly developed are called "graphitic carbons". Such formations have been given by Franklin[9]. Also those carbons which on heating to temperatures between 1700°C and 3000°C showed a continuous change from a non-graphitic to a graphitic structure were called "graphitizing carbons". These two types can be distinguished in terms of the relation between crystal height and crystal diameter on heat-treatment which are shown in fig. 2.3 where L is the average layer distance and M is the mean value of the number of layers per crystallite.

Graphitizing carbons are generally relatively soft and are of high apparent density. Such carbons possess little micro-porosity and are relatively rich in hydrogen or low in oxygen, sulpher and nitrogen. They were termed as 'soft carbons' by Mrozowski[10]. During the early stages of the carbonisation process Franklin[11] considered that the crystallites in the graphitizing carbons were fairly mobile and that in the region of 1000°C, a high proportion of the crystallites lay nearly parallel to each other. Weak cross-linking was supposed to exist between the crystallites. A model reproduced in fig. 2.4 was put forward by Franklin for the structure of a graphitizing carbon. X-ray data also suggested the movable nature of the whole layers or groups of layers with the rise of the heat-treatment temperature, but the most significant factor was that the neighbouring crystallites had to be nearly parallel. The layer planes were linked together for the crystallite growth.

Non-graphitizing carbons are generally hard carbons and are of low apparent density. Such type of carbons have a high

microporosity and are relatively rich in oxygen, sulpher and nitrogen or low in hydrogen. They were correspondingly called hard carbons' by Mrozowski[10]. Again Franklin[11] put forward a model which is shown in fig. 2.5 to account for their structure. In this model the parallel layer groups were oriented at all angles and were joined together at their extremities, thus accounting for the microporosity. With the increase of the pyrolysis temperatures there was some growth in the basal plane direction by incorporation of disordered carbon atoms at the edges of the crystallites and the other carbon atoms acted as linkages between crystallites.

2.4 THE CARBONISATION PROCESS

Many workers have mentioned that the early stages of carbonisation process occurs during the temperature range between 350°C and 600°C and this stage is most important in determining the ability to graphitize at high temperature. A summary of the work done by some authors is given below.

Some of the properties of carbons made from a range of polymers and one polycyclic compound were described by Kipling et al[12]. Mainly, the carbons could be divided into two groups; those which became graphitic at temperatures of 2700° or above and those which remained non-graphitic. Kipling has investigated the relationship between fusion during carbonisation process and the ability of the resultant carbon to graphitize subsequently at a higher temperature. If the organic materials passed through a fusion stage under specific conditions, they could be formed into graphitic carbon

which had been later suggested by Kipling et al [13, 14]. These specific conditions were such that the pyrolytic aromatic structures formed in the residue during carbonisation readily oriented to form graphite. It was confirmed by using polarized - light microscopy[15].

Taylor[16] undertook a detailed study of the microscopic changes exhibited by a vitrinite with the progress of carbonisation using optical methods. Observations were made on a thermally metamorphosed coal. The vitrinite, which in its unaltered state was anisotropic, became isotropic and this transition was followed under controlled conditions in the laboratory. The change from anisotropy to isotropy has been found to occur at a temperature slightly below that at which the plasticity became measurable. The change from isotropic plastic vitrinite to anisotropic semicoke was indicated by the appearance of small spherules initially of micron size, in the isotropic vitrinite, forming as a separate phase. These spheres were found to grow in size with the rise of heat-treatment temperature at the expense of the plastic vitrinite which eventually coalesced to form a mosaic structure about the resolidification temperature.

The spheres which later became units of the mosaic texture, had an interesting pattern of behaviour in singly and doubly polarized-light. A particular structure having a strain effect was brought forward to account for this behaviour. It was believed that this structure was inherently improbable as because the strain effects were infact of little importance to account for the observed optical properties and hence another model having a stress effect was put forward. Using electron diffraction and optical techniques,

the original structure was later varified by Brooks and Taylor[17, 18]. The three-dimensional structure of a simple sphere has been shown in the introductory chapter (fig. 1.1). The layers consist of condensed polycyclic aromatic compounds which are aligned perpendicular to the polar diameter but curve to meet the interface with the isotropic matrix at a high angle. The poles constitute anomalous regions, but this is not sufficiently reflected in the spherical droplet. Spheres were also found to appear on heating bitumen, pitches, PVC, naphthacene and di-benzanthrone, all of which produce graphitizing carbons. This two phase liquid state structural transformation is known as 'carbonaceous mesophase formation' or 'liquid crystal formation'.

Brooks and Taylor concluded that those materials which finally produce graphitizing carbons pass through a fluid state during the early stage of carbonisation which generally occurs in the temperature range between 350°C and 600°C. In the final stages of this fluid phase a second phase having anisotropic structure is found to develop and this structure persists into the semi-coke beyond. They also concluded that any solid-surface appeared to be a preferred site for mesophase growth and that the nucleating effect of solids increased with their available surface area. However, it is now thought that nucleation is not the principal mechanism in mesophase formation, but the growth of the anisotropic liquid crystals occur at the expense of the isotropic liquid phase[19].

White et al[20] investigated the microstructure of the coalesced mesophase formed in the carbonisation coal-tar pitch. This was done by using the polarized-light micrography. They noticed

that the structural features of the coalesced mesophase were similar to those found in electron micrographs of graphitized materials. In the polarized-light extinction contours, the prominent features were the nodes and maltese crosses which did not move when the plane of polarization of the incident light was rotated. These nodal points were found to correspond to two types of linear defects in the stacking of the aromatic layer planes.

There are four types of linear defects in the stacking of the mesophase layer planes[21]. They are (i) co-rotating node (ii) counter-rotating node (iii) co-rotating cross and (iv) counter-rotating cross. The terms co- and counter- rotating nodes and crosses indicates whether the extinction contours moved with or against the direction of rotation of the plane of polarization of the incident light.

White et al concluded that the processes of the formation, coalescence and deformation of the plastic measophase established the basic elements of the graphite microstructure, i.e. the parallel alignment of the aromatic layer planes and the re-arrangement of the complex folds in the fibrous regions.

The linear stacking discontinuities, namely the nodal and cross structures, were essential characteristics of the coalesced mesophase, and at least the nodal structures were found to persist in their basic form upto graphitization temperature. However, they did not appear to be involved in shrinkage cracking, fold sharpening, the formation of mosaic blocks and kinks which occured during pyrolysis. Later White et al[22] extended their studies to include graphitizable materials such as coal-tar pitch and petro-

leum coke feedstocks and arrived at similar conclusions. Honda and co-workers[23] supplemented the works of Brooks and Taylor by examining in much more detail, the temperature effect and resident times upon the growth and physical properties of the mesophase in pitches and also they found that temperature and heat-treatment duration were essentially complementary factors.

During the early stages of carbonisation Honda et al[24] used crossed polarizers with a gypsum plate in a polarized-light study to investigate the microstructures of the carbonaceous mesophase developed in pitches. Using this technique i.e sensitive tint technique, changes in pleochroism and in extinction contours for coalesced and for deformed mesophase were observed. This method permitted distinction between crosses and nodes and so enabled four types of linear defects in the stacking of the aromatic layer planes to be identified. These were similar to those seen by White et al[21] but were now termed as (i) Y-type co-rotating nodes; (ii) U-type counter-rotating nodes; (iii) X-type co-rotating crosses and (iv) O-type counter-rotating crosses. This notation is opposite to that of White[21] probably because of opposite direction of rotation of the plane of polarisation of the incident light. Honda also explained schematically how the crosses and nodal structures were formed by the coalescence of two simple spherules and the deformation of such coalesced mesophase. Whittaker and Grindstaff[25] found that the rates of formation, growth and coalescence of the mesophase spheres varied from feedstock to feedstock and that the type of molecular structure in the original feedstocks and the type of structures developed on pyrolysis had a significant influence

on the resulting coke structure. Carbonaceous mesophase formation, a liquid state structural transition of optical anisotropy has also been found to occur in a few aromatic organic compounds[26,27] as a prerequistite to graphitization.

2.5 PRESSURE EFFECT ON CARBONISATION

Walker et al[28, 29] and Marsh et al[30, 31] performed the extensive studies on the carbonisation of some organic compounds and coal-tar pitches under extremely high pressures (~3 Kbar). The use of low pressure seems to be logical for producing high carbon residues by favoring the formation and escape of volatiles. Any conditions which would favor molecular rearrangement or increased molecular weight may also favor a high degree of carbon-carbon cross-linking or carbon - packing density. Pressure does control solubility, viscosity, density and phase separations within the system during polymerisation and carbonisation, all of which may influence the kind and degree of cross-linking in the polymer and carry through pyrolysis and carbonisation[28]. Carbonisation of well-known organic compounds under moderate pressures has been reported by several investigators.

Fitzer and Terwiesch[32] studied the effect of a gas pressures upto 100 bar on coke yield from conventional pitches. It was observed that upto 550°C the maximum coke yields are achieved at pressures of above 100 bar. Under pressures upto 200 bar, some results on studies with conventional coal-tar and petroleum pitches [33, 34] showed that increasing pressure not only increases the coke yield but also lowers the temperature at which pyrolysis is completed.

It was also observed that increasing pressure improves pre-order and graphitizability of the residues. Increasing pressure gives rise to a pronounced segregation of natural insolubles of conventional coal-tar pitches and of artificial insolubles like carbon-black. A highly ordered mesophase without insolubles is found to be deposited in the lower part whereas the separated insolubles accumulate in the upper part of the pyrolysis vessel. Fig. 2.6 shows that the spherulite size of isotropic carbon formed under one set of carbonisation conditions decreases steadily with increasing pressure of polymerization. It was also observed that the lower-pressure polymer could lead to the production of spherules which would coalesce in part.

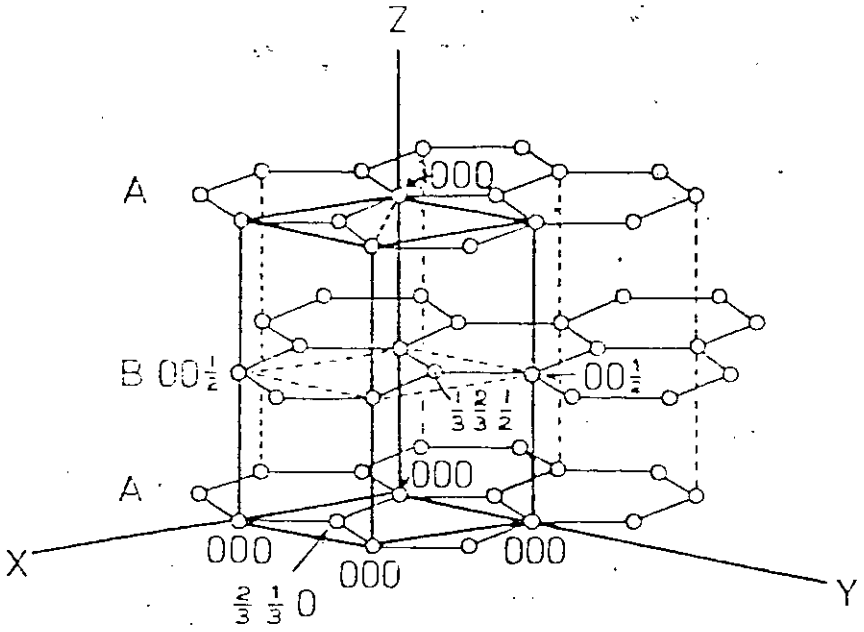

Fig. 2.1. The ideal graphite crystal structure with the hexagonal unit cell with crystal axes and lattice co-ordinates.

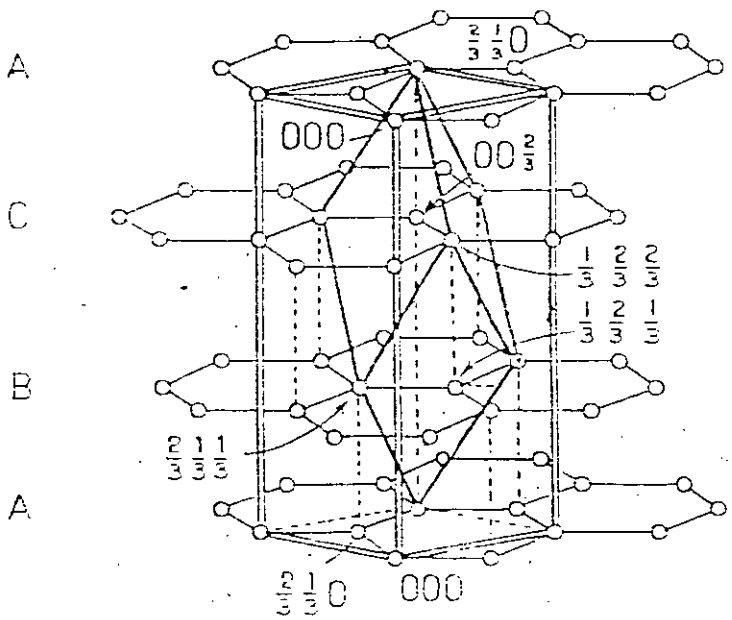

Fig. 2.2. The rhombohedral structure, showing the true unit cell and the atomic co-ordinates in the approximate hexagonal cell shown in double lines.

Fig. 2.3. Relationship between the layer diameter and the number of layers per parallel group for graphitizing (X) and non-graphitizing carbons (△).

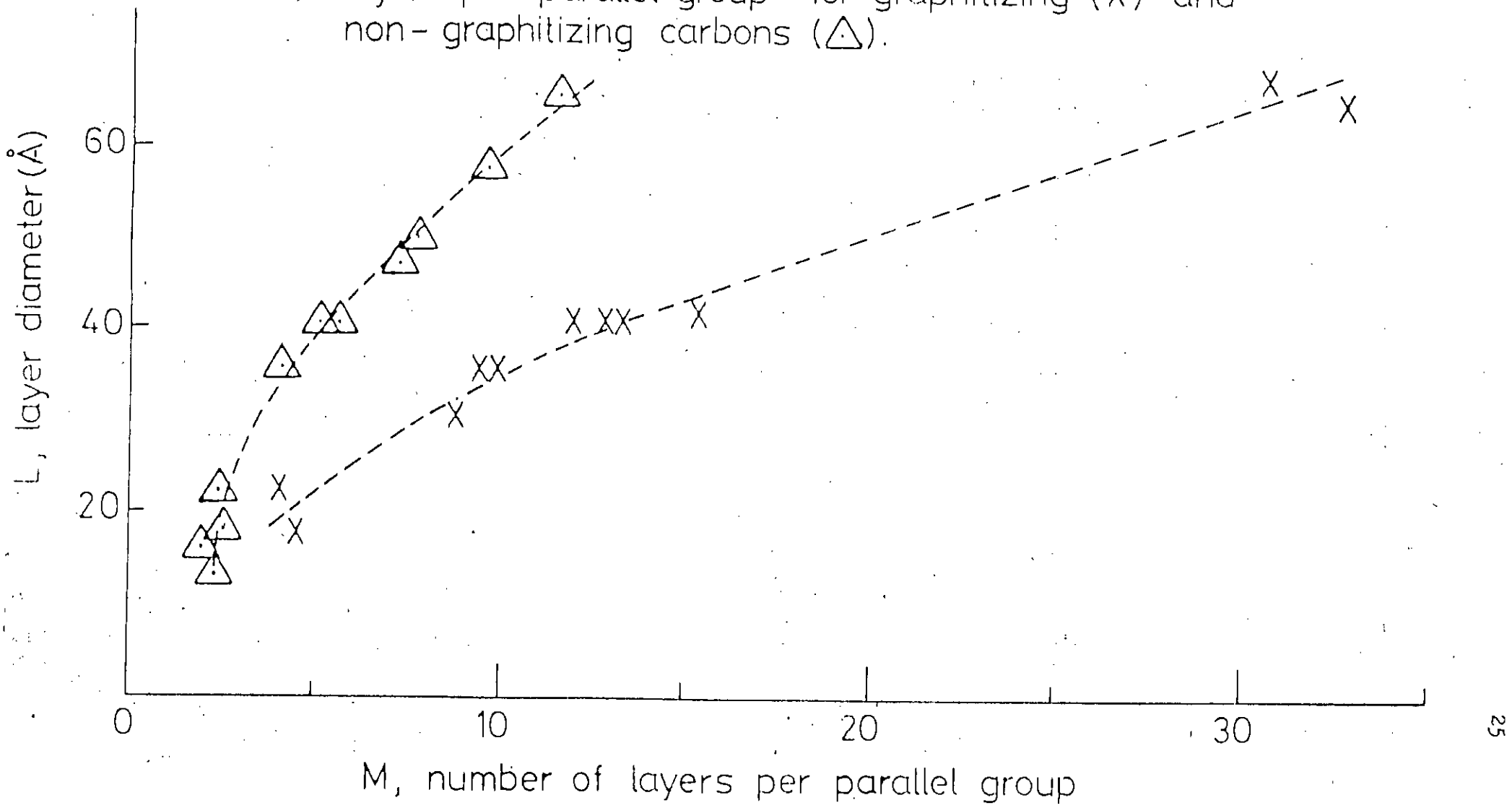

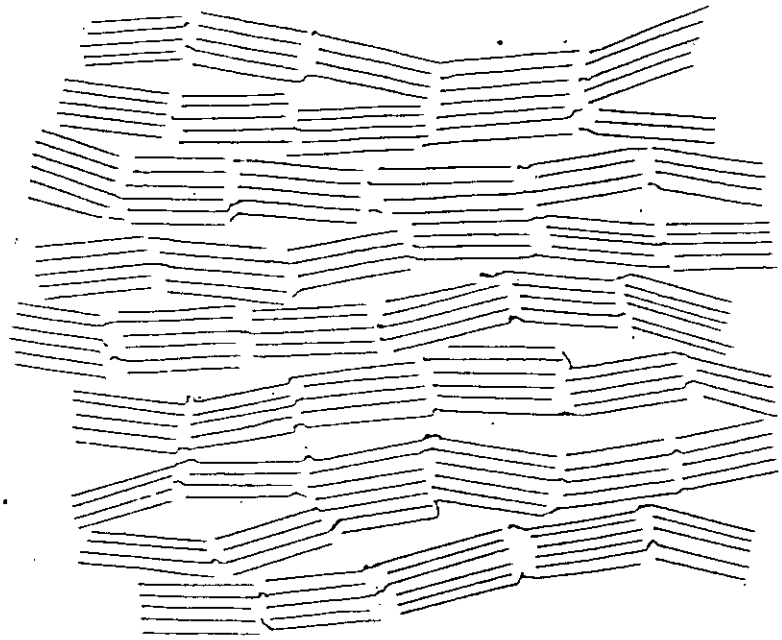

Fig. 2.4. Schematic representation of the structure of a graphitizing carbon.

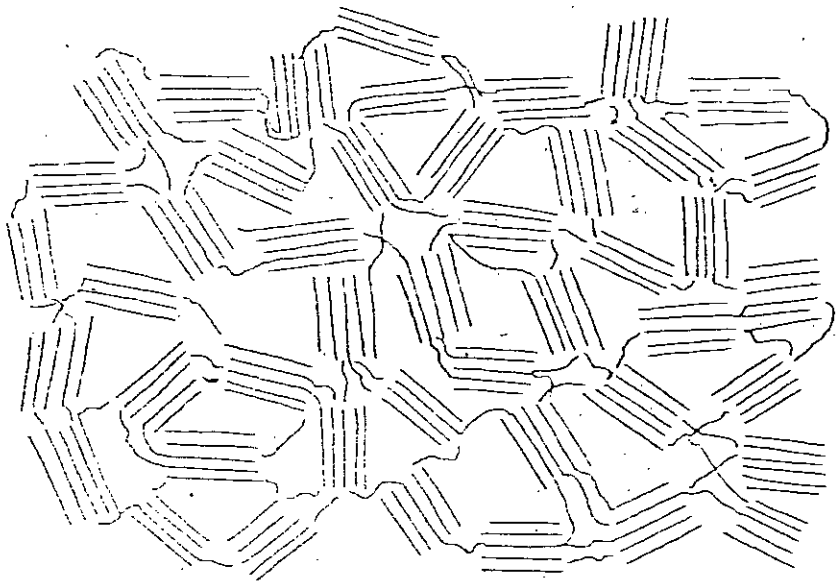

Fig. 2.5. Schematic representation of the structure of a non-graphitizing carbon.

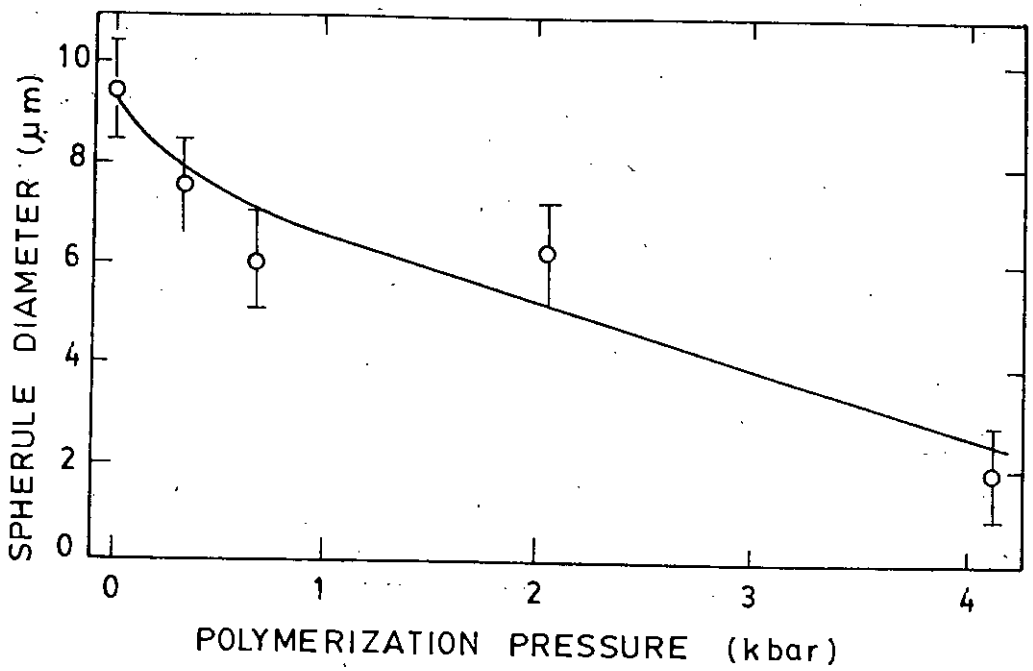

Fig. 2.6 Variation in diameter of isotropic carbon spherulites produced by carbonization under 0.69 kbar pressure at 900°C and 3h soak time following polymerization of divinylbenzene at various pressures.

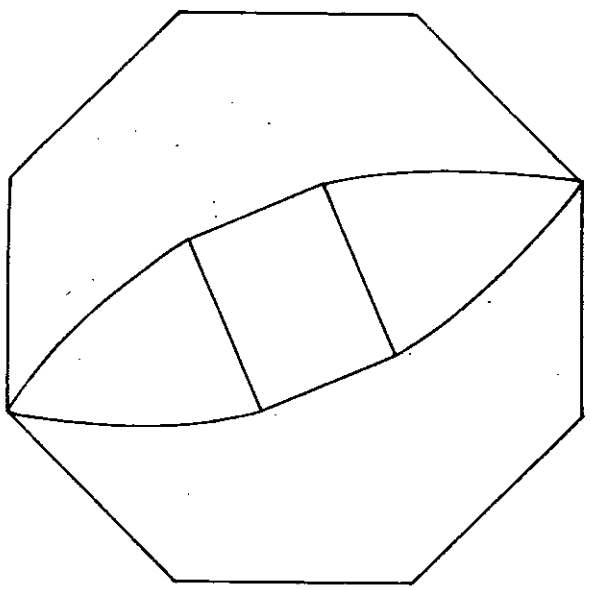

Fig. 2.7 Diamond structure

REFERENCES

2.1 Ergun, S., Leroy, E.A., Nature, 1962, 195, 765.

2.2 Seal, M., Nature, 1960, 185, 522.

2.3 Bernal, J.D., Proc. Roy. Soc. A, 1924, 106, 749.

2.4 Girifalco, L.A. and Lad, R.A., J. Chem. Phys., 1956, 25, 693.

2.5 Brennan, R.O., J. Chem. Phys., 1952, 20, 40.

2.6 Lipson, H. and Stokes, A.R., Proc. Roy. Soc. A, 1942, 181, 101.

2.7 Debye, P. and Scherrer, P., Physikal Z., 1917, 8, 291.

2.8 Bacon, G.E., Acta Cryst., 1950, 3, 320.

2.9 Franklin, R.E., Acta Cryst., 1951, 4, 253.

2.10 Mrozowski, S., Proc. First and Second Conf. on Carbon, Buffalo, 1953, 31.

2.11 Franklin, R.E., Proc. Roy. Soc. A, 1951, 209, 196.

2.12 Kipling, J.J., Sherwood, J.N., Shooter, P.V. and Thompson, N.R., Carbon, 1964, 1, 321.

2.13 Kipling, J.J., Sherwood, J.N., Shooter, P.V. and Thompson, N.R., Carbon, 1964, 1, 315.

2.14 Kipling, J.J. and Shooter, P.V., Second Conf. Ind. Carbon and Graphite, Soc. Chem. Ind., 1965, 15.

2.15 Kipling, J.J. and Shooter, P.V., Carbon, 1966, 4, 1.

2.16 Taylor, G.H., Fuel, 1961, 40, 465.

2.17 Brooks, J.D. and Taylor, G.H., Nature, 1965, 206, 697.

2.18 Brooks, J.D. and Taylor, G.H., Carbon, 1965, 3, 185; Physics and Chemistry of Carbon, 4, 243.

2.19 Walker, P.L., Carbon, 1972, 10, 369.

2.20 White, J.L., Guthrie, G.L. and Gardner, J.O., Carbon, 1967, 5, 517.

2.21 White, J.L., Dubois, J. and Scuillart, C., J. Chim. Phys., Special Volume, April, 1969, 33; Euratom Report 4094e, 1969.

2.22 Dubois, J., Agace, C. and White, J.L., Euratom Report 4627e, 1971; J. Metallography, 1970, 3, 337.

2.23 Honda, H., Kimura, H., Sanada, Y., Sugawara, S., and Furuta, T., Carbon, 1970, 8, 181.

2.24 Honda, H., Kimura, H. and Sanada, Y., Carbon, 1971, 9, 695.

2.25 Whittaker, M.P. and Grindstaff, L.I., Carbon, 1972, 10, 165.

2.26 Graham, S.G., Ph.D. Thesis, 1974, Salford University.

2.27 Hossain, T., J. Bangladesh Academy of Sciences, 1983, 7, 57.

2.28 Hirano, S., Dachille, F. and Walker, P.L., J. High Temperature-High pressures, 1973, 5, 207.

2.29 Whang, P.W., Dachille, F. and Walker, P.L., J. High Temperature-High pressures, 1974, 6, 127, 137.

2.30 Marsh, H., Dachille, F., Melvin, J. and Walker, P.L., Carbon 1971, 9, 159.

2.31 Marsh, H., Foster, J.M., Hermon, G. and Iley, M., Fuel, 1973 52, 234, 243, 253.

2.32 Fitzer, E. and Terwiesch, B., Carbon, 1973, 11, 570.

2.33 Hüttinger, K.J. and Rosenblatt, U., Proc. Fourth Conf. Ind. Carbon and Graphite, 1974, Soc. Chem. Ind., 1976, London, 50.

2.34 Hüttinger, K.J. and Rosenblatt, U., Carbon, 1977, 15, 69.

2.35 Blayden, H.E., The Carbonisation process, J. Chem., Phys., Special Vol. (April, 1969).

CHAPTER - III

THE POLARIZING MICROSCOPE

3.1 INTRODUCTION

The use of the reflected polarized-light at normal incidence in the study of the structure of metals and alloys may be divided under the following two headings:

(a) examination of the structural characteristics of a homogeneous phase and (b) indentification of inclusions and differentiation between various phases of a complex structure[3].

Both anisotropic and isotropic phase can be investigated for grain-size, incidence of twinning and general deformation, and degree of preferred orientation. For a study of anisotropic materials, sections may be polished either by suitable mechanical or electrolytic methods, but for isotropic materials it is necessary to prepare the surface in such a way that the reflection of polarized light is made dependent on the orientation of the metal.

The polarized-light technique enables us to determine quantitatively the optical properties of transparent, translucent and opaque materials by studying their influence upon reflected as well as transmitted polarized-light. This technique was initially

restricted to mineralogy; but in recent years, it is being widely applied in the field of metallurgy, chemistry, biology, crime detection, military intelligence, medicine, ceramic technology and various branches of industrial technology. Various aspects of this technique have been described in detail by a number of authors.(1-16) Hallimond has discussed the design and use of the polarizing microscope. Conn and Bradshaw[2] have described its application to metals and ores. Mott and Haines[3] have discussed its application to the examination of a number of anisotropic metals. Marshall[4] and Dale[5] have discussed optics of crystals. Hartshorne and Stuart[6] have given a good description for the microscopic examination of uniaxial and biaxial crystals under polarized-light. A review of the use of polarizing microscopy in organic chemistry and biology is also given by Vickers[7].

Recent studies by several groups on the structural conditions of graphitizability have established the fact that polarized-light microscopy has been found well-suited to the studies of carbonisation and graphitization because (a) the strong optical characteristic of the graphite crystal begins with the parallel alignment of mesophase molecules and (b) the high viscosity of the mesophase permits microstructures formed in the plastic mesophase to be cooled to room temperature with little apparent disruption. Thus the polarised-light response on a section polished at room temperature can be used to identify the orientation of the intersections of mesophase layers with the plane of the section. Most microstructures are brought out with best contrast when the polarizers are crossed. Under this condition the extinction contours define the loci of layers lying either parallel or perpendicular to the plane of

polarization of the incident light and the specific orientation can be distinguished for any particular region by the use of sensitive-tint plate.

3.2 THE POLARIZING MICROSCOPE

Generally the polarizing microscope is an ordinary compound microscope provided with calcite polarizing prisms, or more usually now, discs of 'polaroid' above and below the stage, and some convenient means of altering the orientation of the object with reference to the plane of vibration of the light incident upon it. There is a provision to insert the auxiliary lenses and compensators into the path of the light through the instrument.

The polarizing microscope has undergone many modifications because of its wide applications, but in principle all types are the same and do not differ essentially from one another. The arrangement of the main components of a typical modern polarizing microscope are described below :-

The incident light passes through the polaroid disc, the polarizer, and is thus constrained to vibrate in one plane only. The polarizer can be rotated in its own plane and the angle of rotation can be read against a fixed mark from divisions on the metal ring in which it is mounted. A second polaroid disc, the analyser, is mounted in the body tube of the instrument. The analyser can be rotated or withdrawn from the field of view to enable a sample to be viewed in unpolarized-light. When both the polarizer and analyser are in 0° - 0° position (as marked in the scale) they

are said to be in "crossed position", and they will not permit light to reach the eye-piece so long as the medium between them is entirely isotropic. This is because light emerging from the polarizer is completely extinguished by the analyser according to the principle underlying the well known Malus's experiment in optics.

The specimen under investigation, mounted in a quick-setting acrylic resin or on a glass slide, is placed on a circular stage. This specimen, which can be held in position by means of a clamp attached to the stage, is capable of movement in two directions in the plane of the stage. To permit easy return to a certain specimen point the co-ordinate positions can be read against millimeter scales. The stage can be rotated in its own plane and is provided with centering screws and 'click stops' at intervals of 45°. The angle of rotation of the stage can be measured on a degree scale. The stage is alsc provided with a clamp to arrest the motion if so desired.

Above the objective lens is a slot in the body tube of the instrument, through which the compensator or tint plate is inserted. The tint plate, which is a gypsum plate (some times called first-order red plate), is placed at an angle of 45° to the vibration planes of the polarizer and the analyser when they are in the crossed-position.

Also, there is a Bertrand lens in the microscope body which can be swung into or out of the field of the view. This Bertrand lens and the eye-piece act together to constitute a low-power microscope which can be focussed on the upper focal plane of the objective. The main purpose of this combination is, however, to

give an enlarged image of the interference figures which are formed in this plane under certain conditions. There is an iris diaphragm (sometimes called pin-hole stop) above the Bertrand lens which can be used to isolate the interference figure of the crystal occupying the centre of the field of view when several are present. The condensing lens system is situated between the rotating stage and the polariser. Its primary function is to bring the incident light to a focus in the plane of the specimen as in a compound microscope. The eye-piece lens system is fitted to the microsope body of the binocular type, having a certain magnification. This together with the different objectives produces the over all magnification.

The illumination of the microscope is provided by a low voltage 15 watt quartz-iodide bulb, the power supply of which is controlled from a regulating transformer. This lamp generally operates on 6 V, 15 watt a-c supply and contains a fixed condenser. The bulb is inserted in a well-ventilated housing with a circular opening for the emission of light.

The body tube of the microscope allows a camera adapter to be fitted after the analyser. The adaptor is supplied with a definite magnifying eye-piece. The camera used for photography is a 35 mm Kam ES - 2.

3.2.1 Modes of Observation in a Polarizing Microscope

There are two arrangements for observations in a polarizing microscope. These are the orthoscopic arrangement and the conoscopic arrangement.

The detail description of this two arrangements are described below :-

3.2.1.1 Orthoscopic arrangement

The orthoscopic arrangement is that arrangement in which the series of parallel incident rays travel along the same crystallographic direction within the crystal, and also this arrangement is similar to an ordinary compound microscope which is shown in fig. 3.1. There are three combinations of polarizer and analyser in this type of observations.

Firstly, removing both the polarizer and analyser from their positions, observations can be made on colour, crystalline form, cleavage and fracture, together with the determination of the refractive index of isotropic crystals.

Secondly, the principal refractive indices of anisotropic crystals can be determined after inserting the polarizer. Observations on pleochroism (which is the variation in colour or tint resulting from differential absorption of white light) and twinkling (which is the variation in relief when a crystal having a large double refraction is rotated in an immersion medium whose refractive index is near to one of those of the crystal) may also be made by only inserting the polarizer.

Thirdly, with the insertion of both the polarizer and the analyser in the crossed-position, distinctions can be made between isotropic and anisotropic substances and measurements can be made on extinction angles.

Most of the observations on the polarizing microscope are done with both the polarizer and analyser inserted in crossed position. Some of the effects of observation through the polarizing microscope are given below and details are explained later.

All non-opaque substances can be divided into two groups in accordance with their behavior between crossed polars, namely isotropic and anisotropic substances. The isotropic substances remain dark, like the rest of the field of the microscope whatever be their orientations. On the other hand, anisotropic substances will appear coloured on rotation in most orientations and only in certain definite positions will become dark.

The reason for this difference in behavior is that in isotropic substances light vibrates with equal ease in every direction and the wave surface seems to be same sphere. So, when such a substance is placed on the stage of the microscope between the crossed polars, it does not interfere at all in any way with the direction of light vibration, and the field remains dark as the empty stage.

On the other hand, when an anisotropic substance is placed between crossed polars, the plane polarised light emerging from the polarizer is doubly refracted on entering the crystal, the two rays vibrating in planes at right angles to one another, and travelling

with different velocities. Similarly, light reflected by a polished anisotropic surface is polarised in the two principal directions at right angles to each other and so, the two rays travel with different velocities.

The crystal will become dark at intervals of 90° from the extinction position and will become gradually illuminated being brightest at 45° from the extinction position. The section extinguishes when the traces of its vibration directions become parallel to those of one of the polars, for in such positions, the light from the polarizer is not resolved in the crystal, but passes on to the analyser uncharged as if there is no crystal on the stage, and hence darkness results.

The colours observed in the positions of illumination are known as "Polarization Colours". The polarization colours shown through the polarizing microscope depend on the optical path difference between the ordinary ray and the extra-ordinary ray e.g. the phase retardation between the two rays. The amount of retardation depends on the wave velocity difference and also on the thickness of the crystal plate. Since the wave velocities are inversely protional to their respective refractive indices, therefore, the path difference may be expressed by the following formula :

$$R = (n_1 - n_2)t ,$$

where $(n_1 - n_2)$ is the difference between the two refractive indices for the ordinary and the extra-ordinary rays, and 't' the thickness of the crystal plate.

The phase difference between the two components of velocity on emergence from the crystal is given by $\frac{2\pi R}{\lambda}$

where R — the relative retardation

and λ — the wave length of incident-light.

If in white light the sample is viewed and at the same time its thickness is varied from zero to a finite quantity, a series of different colours will be found. This is because increasing thickness introduces a phase difference between the two components of velocity and consequently constructive and destructive interference occurs at different thickness for different wave lengths. The colours are arranged in the order of Newtonian colour scale. With the increase of thickness, the colours become further and further complex because of overlapping of the extinction bands for different parts of the spectrum, Due to over lapping pale pinks and green colours merge into white.

The two reflectances belonging to the principal directions in a surface may vary independently according to the wave length of light used for bireflecting substances, where the two principal directions represent two characteristic tints in white light. Since it has analogy with pleochroism in transmitted light, so, it is sometimes called "reflection pleochroism" which depends on the absorption. The ratio of the intensity of the reflected light to that the incident beam of light (i.e. the reflectance) is determined by both the absorption and refractive index.

As the stage is rotated under polarized light illumination, the reflected light changes in tint through the admixture in varying

proportions of the two component tints and the changes obtained in this way are very characteristic. In a uniaxial crystal there are two principal colours, but in inclined sections the tints remain the same. In a biaxial crystal there are three principal colours and the effects for inclined sections are more complicated. An important aspect of these variations is that the bi-reflection for the section varies greatly with the wave length for the two principal directions. This kind of bireflection is known as "Dispersion of the bi-reflection". It causes very distinctive colour effects when the sample is examined after adjusting the two polars in crossed or near the crossed-position.

3.2.1.2 Conoscopic arrangement

Polarizing microscope in conoscopic mode is shown in fig, 3.2. An Amici-Bertrand lens, a substage condensing lens and a diaphragm are inserted in this arrangement in addition to the orthoscopic arrangement. The Amici-Bertrand lens converts the microscope into a low power telescope focussed at infinity. The substage condenser causes the object on the stage to be illuminated by a cone of light rather than by a bundle of near-parallel rays for the conscopic case. By various means, when it is possible to examine the optical character in many directions at one and the same time; an important additional information may be obtained by passing a strongly convergent beam of light through the crystal. This is done by viewing between crossed polars, not the image of the crystal, but another optical image formed in the principal focus of the objective by the strongly convergent beams of light. This optical image is called the "interference figure". Each point

in the field corresponds to a given direction through the crystal. The Bertrand lens and the eye-piece constitute a system used to examine the interference pattern in the back focal plane of the objective.

The interference figures produced in a conoscope can be classified into two broad divisions - one is for uniaxial crystals and the other is for biaxial crystals. The former pattern consists of concentric circles known as 'isochromes'. A pattern in the shape of a maltese cross is being superposed on them. The arms of the cross are known as 'isogyres'.

There are only one optic axis in a uniaxial crystal. So with the rotation of the stage, the pattern remain unchanged provided that the optic axis is centred and perpendicular to the stage. The isogyres retain a broad cross shape when the crystal section parallel to optic axis is used. Rotation of the stage causes the isogyres to move in and out going rise to a 'flash figures'. These phenomena are discussed in detail at a later section of this chapter.

In a biaxial crystal there are two optic axes, the lines bisecting the acute angle between them is called the "acute bisectrix". When a crystal section is viewed normal to the acute bisectrix, the interference figure consists of two eyes or melatopes, which mark the points of emergence of the optic axis, surrounded by white coloured bands of equal retardation. On the interference patterns are superimposed the isogyres forming a cross when the line joining both melatopes lies parallel to either polariser or analyser. The arm of the cross passing through the melatopes is

narrower than the other. Rotation of the crystal away from this position causes the cross to break up into two hyperbolic brushes which are centred on the melatopes. The isogyres revolve in a direction opposite to the movement of the stage.

3.2.2 Types of Illumination Used in Polarizing Microscope

There are three types of illumination generally used in the polarizing microscope :- these are — (i) bright field (with and without polars); (ii) dark field and (iii) phase contrast.

Bright field illumination is that one where the empty area surrounding any particular specimen being observed under the microscope appears bright. This can be observed in two different ways :-

Firstly, when both the polarizer and analyser are removed from the microscope which is the situation for the normal compound microscope. As a result the observation can be made on colour, crystalline form, cleavage and fracture together with the determination of the refractive index of isotropic crystals.

Secondly, when both the polarizer and analyser are inserted in crossed position together with a compensator or tint plate. The compensator is made of a flake of clear gypsum (or selenite ground) cleaved to a thickness such that the plate produces a path difference (i.e. retardation) of one wave length for yellow light ($\sim$ 575 nm). The plate is 0.062 mm thick and it extinguishes the yellow light so as to produce an interference colour near first-

order red in white light. The gypsum plate assists in the determination of exact extinction positions. Slight rotation from the extinction position results in a change of colours.

Dark field illumination is that one where the empty space surrounding any particular specimen, appears dark. It is obtained when both polarizer and analyser are in crossed-position with the tint plate being removed. Only those portions of the light diffracted by the specimen pass into the objective, the undiffracted rays being extinguished by the crossed polars due to the direction of illuminating rays emanating from a dark field condenser.

A method intermediate between bright field and dark field examination is provided by decentering the beam of incident light which is shown in fig. 3.3 and it results in a relatively small portion of the direct light being excepted by the objective lens.

The eye readily detects differences in amplitude by intensity changes, but it is not able to see changes in phase directly. Thus, as long as the objects on a microscope slide are opaque or absorbing, they appear in the image. If they are transparent, however, and differ only slightly from their surroundings in refractive index or in thickness, they will ordinarily not be visible. It is neverthless possible to convert the phase changes produced by such objects into amplitude changes in the final image. The so-called phase contrast microscope, devised in 1935 by Zernike, functions in this way.

Phase contrast illumination is achieved with the aid of a special objective lens containing a flat plate into which is

machined a circular groove. The difference between the thickness of the plate and the depth of the groove is of the required size to produce a phase difference of 180° between a light ray passing through plate and one passing through the groove.

Each objective lens is used in conjunction with one of the annular discs contained in the condenser so that only an annulus of light from the condenser reaches the phase plate in the upper focal plane of the objective illuminating only the groove. When a specimen is observed the diffracted rays pass through the centre of the phase plate, and interfere with the undiffracted rays passing through the annulus. Therefore, this effect changes small phase difference into large amplitude differences. This makes it possible to see the detail in a crystal which would normally be transparent in reflected as well as in transmitted light. The illumination of the field from dark to bright can be adjusted by means of an iris diaphragm contained in the objective lens close to the phase plate.

3.3 BASIC PRINCIPLE OF A TINT PLATE

The basic principle of a tint plate is shown in fig. 3.4. Sometimes tint plate is called the gypsum plate because it is usually made of a cleavage sheet of gypsum (also called selenite).

The relative retardation between the two transmitted components which is equal to one wavelength of yellow light ($\sim$ 575nm), is equal to the thickness of the plate. When it is inserted between the crossed polars, different interference colours are observed at

the end of the first order. This is also called the First-order red plate because, if it suffers a very small subtractive effect there is very marked change to orange or yellow, while if it suffers a very small additive effect the red colour is raised to indigo or blue.

The plate is sometimes made of cleavage sheet of mica or a plate of quartz ground to the right thickness. The most common compensators are quarter wave mica plate (also called the quarter undulation plate). First-order red or unit-retardation plate (some times called the gypsum plate) and the simple quartz wedge. The quarter wave mica plate is made of a sheet of muscovite mica cleaved to such a thickness that one transmitted component is retarded a quarter of a wave of yellow light behind the other, i.e. by about 145 nm. By itself between crossed polars the plate gives a pale grey interference colour.

Tint plates or compensators are often used to assist in the identification of interference colours shown between crossed polars. These are crystal plates or wedges of known optic orientation and relative retardation, suitably mounted so that they can be inserted into the microscope slot just below the analyser, intercepting the light beam. If the vibration direction of the slot through the tube is at 45^{o} to the vibration direction of the polars in their crossed position then the compensator must be mounted so that one of its vibration directions is parallel to the plate when it is inserted.

The stage of the microscope is turned so as to bring one

of the vibration directions of the specimen parallel to the slot i.e. at 45° to an extinction position. Inserting the compensator it is noted that whether the effect of this is to (a) raise or (b) lower in Newton colour scale; the original colour shown by the specimen. If the corresponding vibration direction of the specimen and compensator be parallel, then it is called the additive effect. If the vibration direction of the specimen and compensator are in opposition it is called the subtractive effect.

In general, the first-order red plate is more suitable for specimens showing a very low colour since, owing to the sensitive colour of the plate, additive and subtractive effects are sharply distinguished.

3.4 OPTICS OF CRYSTAL

To take account of anisotropy for optics of crystal we must generalise the material equations $\underline{J} = \sigma \underline{E}$; $\underline{D} = \epsilon \underline{E}$, $\underline{B} = \mu \underline{H}$.

We introduce the di-electric tensor ϵ_{KL} and the conductivity tensor σ_{Kl} for anisotropic media. Combining Maxwell's equations and the general material equations Fresnel[8] arrived at a formula for the propagation of light in crystals and also led to the concept of the O-ray and the E-ray, which travel at different speeds in the crystals. O-ray obeys the laws of refraction and E-ray does not obey the laws of refraction. A simple geometric model based on the O-ray and E-ray leads to the explanation of

many of the phenomena observed in crystals.

If we view the basal section of a uniaxial crystal in converging polarized beam of light, the rays not travelling along the optic axis are doubly refracted (fig. 3.5). At the upper surface rays O' and E' derived from a given pair of incident parallel rays EE which travel along the same path, vibrating in planes at right angles to one another. One of these rays will have been retarded behind the other by an amount which depends upon the direction of their paths through a crystal. When the retardation of one ray behind the other is exactly one wavelength or any whole multiple of one wave length, darkness results due to interference. All emergent rays so allied to one another lie on the surfaces of an infinite number of geometrically similar cones coaxial with the optic axis (fig. 3.6) and the locus of their focal points in the interference figure is a circle which gives rise to the series of concentric rings, called "isochromes" in the interference pattern (fig. 3.7).

The o-ray vibrates in the plane containing the ray and a line normal to both the ray and to the optic axis, while E-ray vibrates in the plane containing the ray and the optic axis. The directions of vibration of O- and E- rays are shown in fig. 3.8 by small double - headed arrows. The O-rays vibrate tangentially and the E-rays radially. It is obvious that the vibration planes in the polarizer and analyser are along the directions PP' and AA' respectively. The interference figures are brightly illuminated within the dark rings at extinction position. Such typical interference patterns are shown in fig. 3.7 which are in the form of a maltese cross. The arms of the maltese cross are called "isogyres".

The field in the central portions remains dark because the rays are normal to the crystal section and travel parallel to the optic axis. The interference figures are frequently very diffuse in white light. When the crystal is in the extinction position for parallel light, the hyperbolic isogyres enter into the field in the form of a broad cross in the centre and move very rapidly. During the rotation of the stage through a few degrees, the isogyres occupy the centre of the field and the impression of a momentary darkening of the whole field is seen. Such figure is called a "flash figure".

When rays of convergent light enter the section of a biaxial crystal not along the optic axis, double refraction takes place. The wave fronts of these rays travelling along the optic axis are brought to a focus in the interference figure at two points called the "Melatopes" which being extinguished by the analyser, appear dark. All other rays emerging from the crystal are made up of two components, differing in phase and vibrating in directions at right angles to one another (similar to uniaxial crystal), and therefore, resulting in interference in the analyser. Emergent rays for which the retardation is the same lie on conical surfaces surrounding each optic axis, the sections of the cones being nearly circular when the inclination to the optic axis is small, and becoming more pear-shaped as this inclination increases; at still greater inclinations the surfaces merge so as to surround both the optic axes. The relative arrangement of representative surface corresponding to retardations of λ, 2λ, 3λ etc. for a given wavelength of light is illustrated in fig. 3.9. Each surface (together with its allied parallel surfaces) produces a ring of focal points in the interference figure similar in shape to its

trace upon a horizontal plane. Such an interference figure consisting of two eyes or melatopes surrounded by coloured bands when viewed under white light is shown in fig. 3.10.

To an appreciable degree the absorption of one or more bands of wavelength of the visible spectrum, the crystals and glasses appear coloured by reflection or transmission. Absorption consists in a progressive decline in the amplitude, and as a result the intensity of light decreases as it penetrates more and more deeply in the medium and in most cases the energy lost is converted to heat. The solutions of such equations are well known for the metallic surface, but not for absorbing crystals. Born and Wolf[8] derive the expressions for the case of a partially absorbing and transmitting material. For this phenomenon the fundamental reason is that the frequency of the incident light is the same as the natural frequencies of vibration of the electron systems of the same crystal, so that a resonance effect takes place (which compensates the absorption effect).

In anisotropic crystals the absorption depends on the vibration direction of the light. Thus the two polarised components of a ray of monochromatic light are absorbed in different proportions and also white light transmission colour differs considerably; and similar for the reflection colours. This phenomenon is known as 'pleochroism'. This is one of most important optical studies by the polarizing microscope.

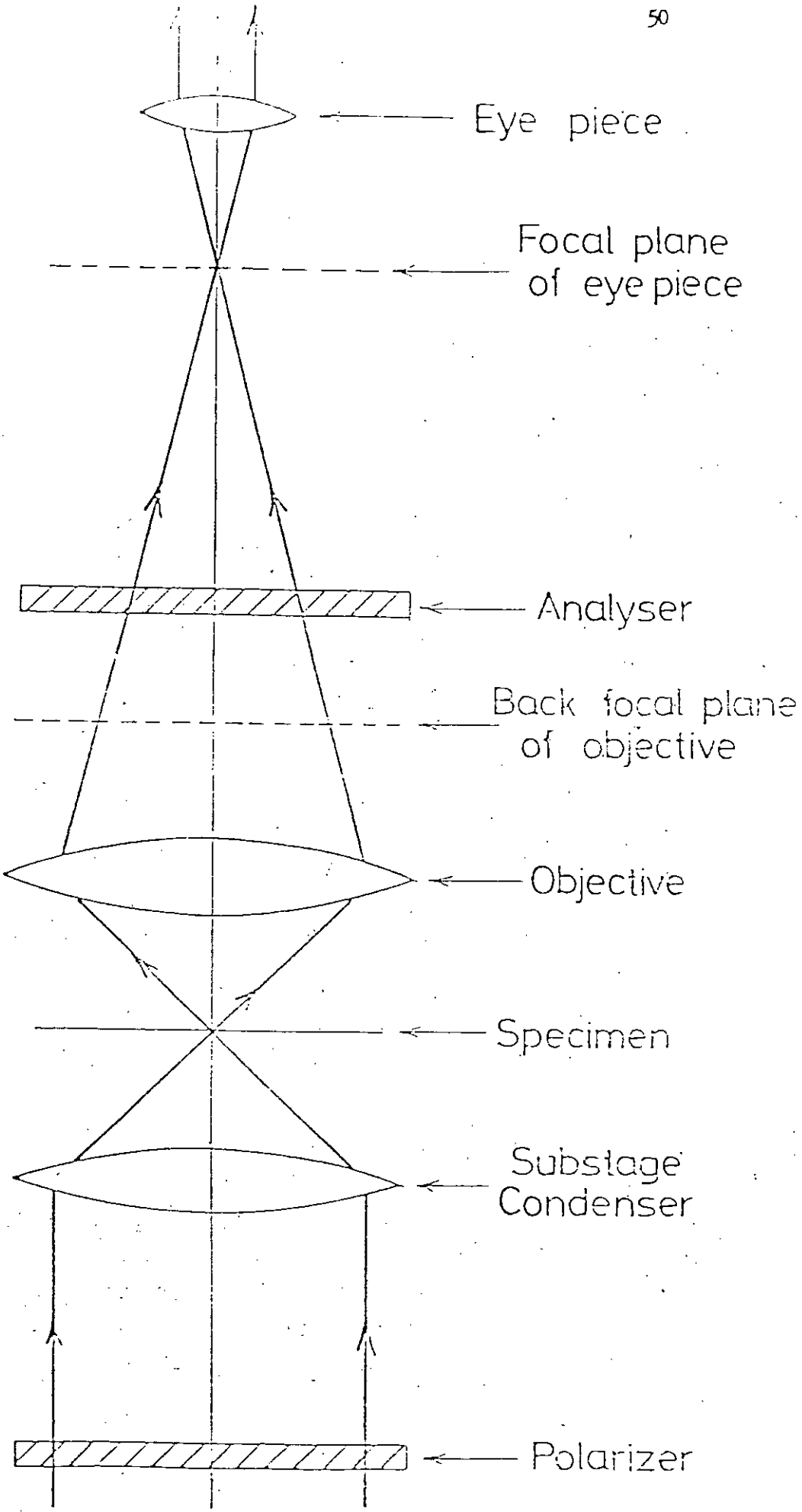

Fig. 3.1. Polarizing microscope in orthoscopic mode.

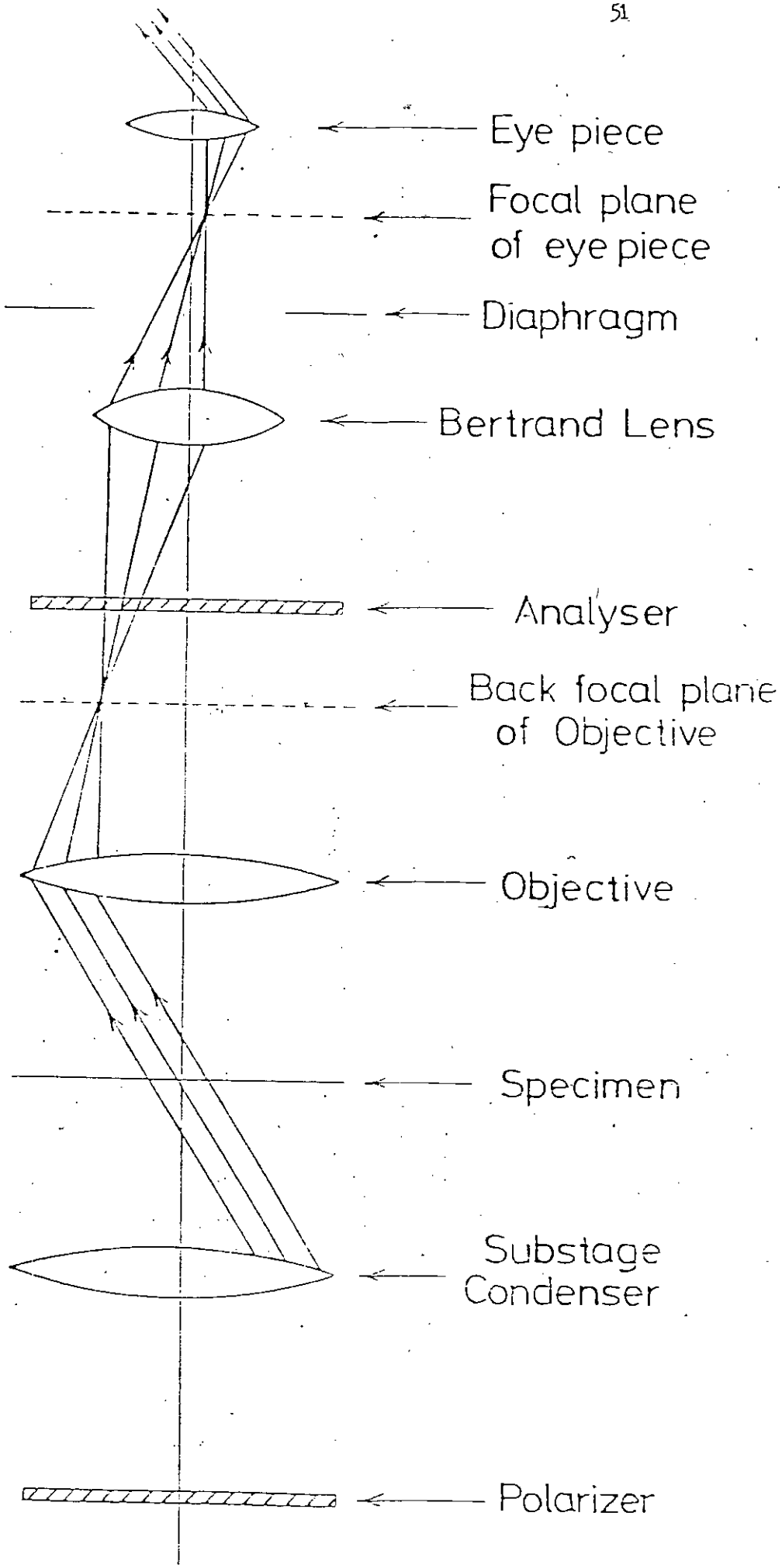

Fig. 3.2. Polarizing microscope in conoscopic mode.

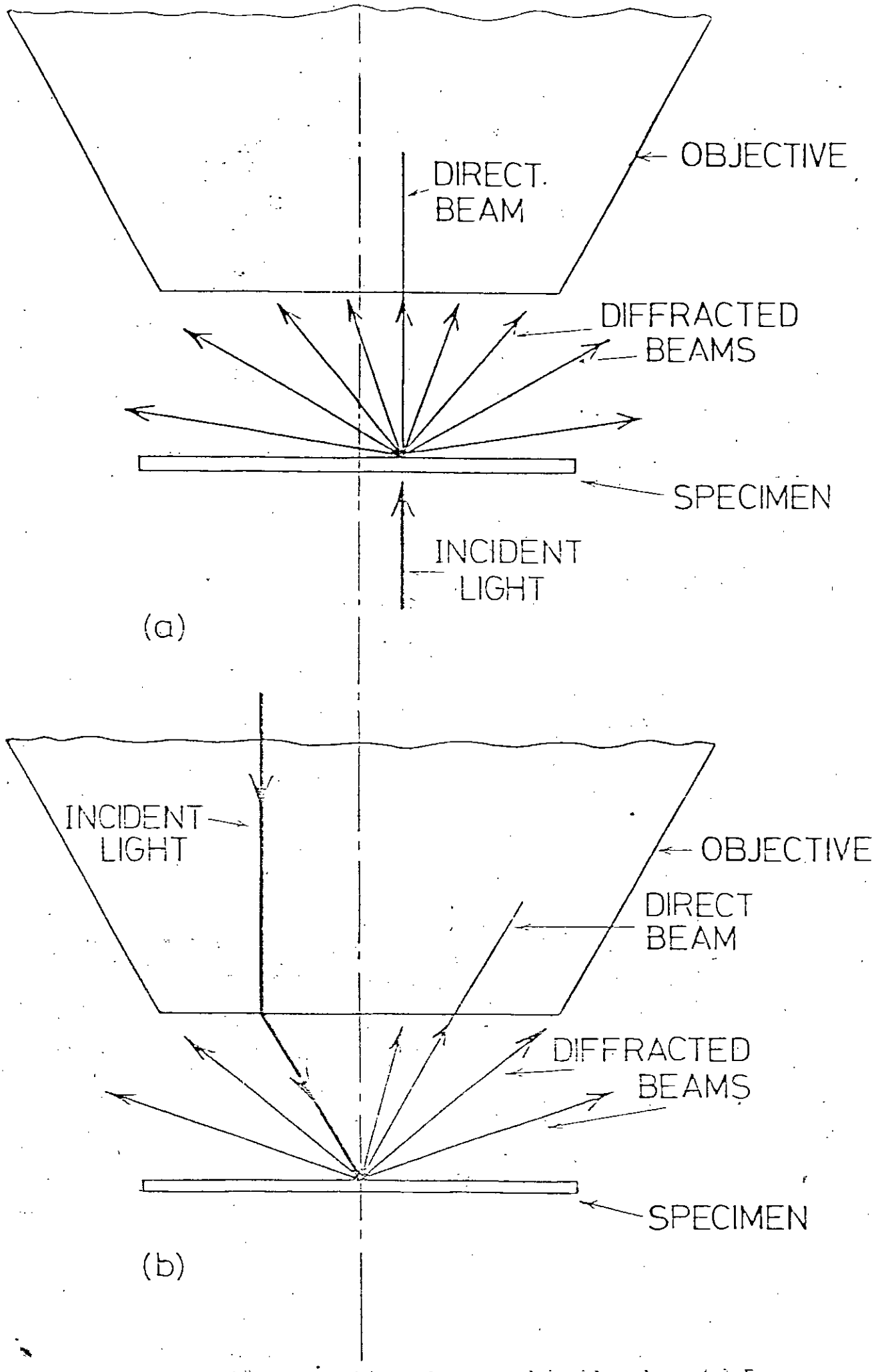

Fig. 3.3. Illumination provided by a de-centred incident beam (a) For

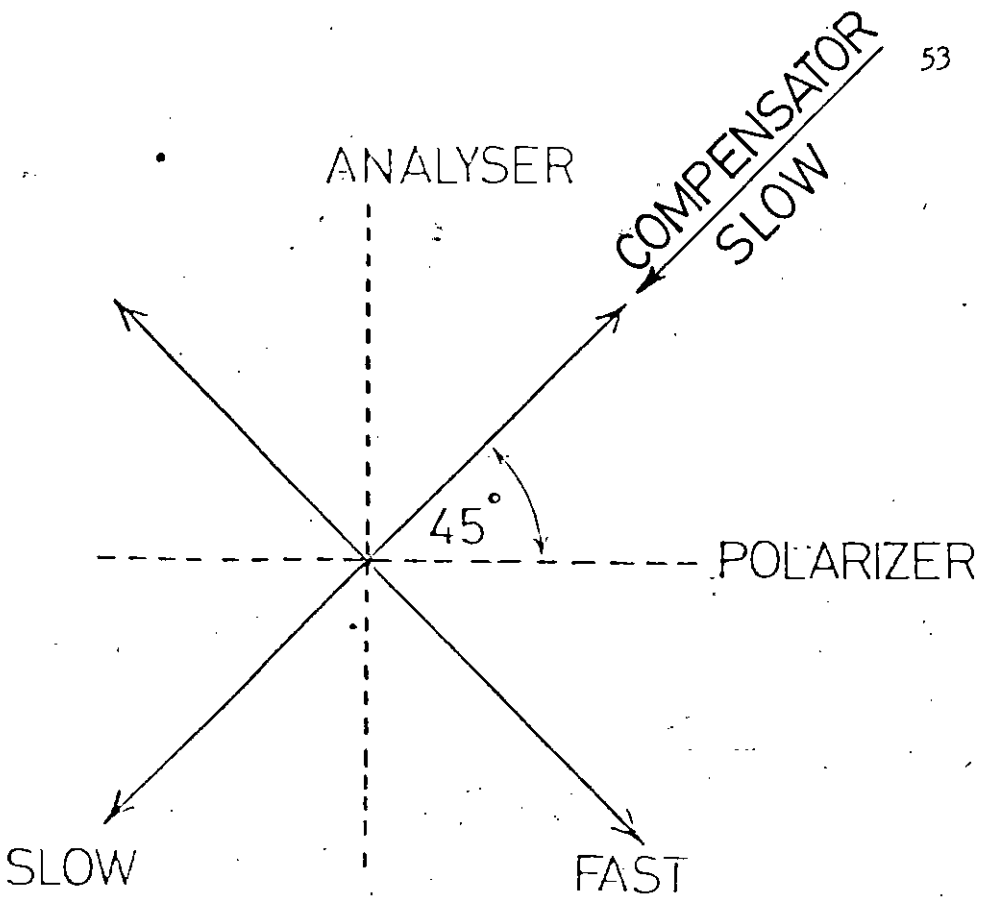

(a) Additive effect; colours raised.

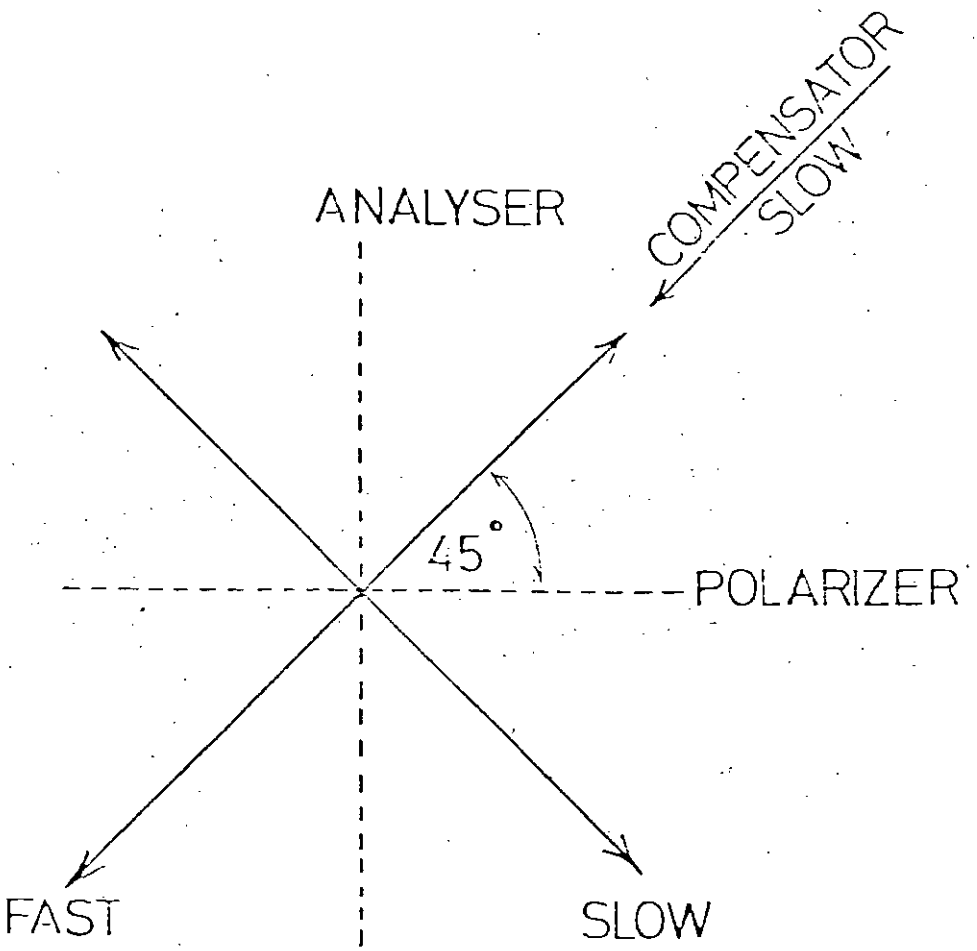

(b) Subtractive effect; colours lowered.

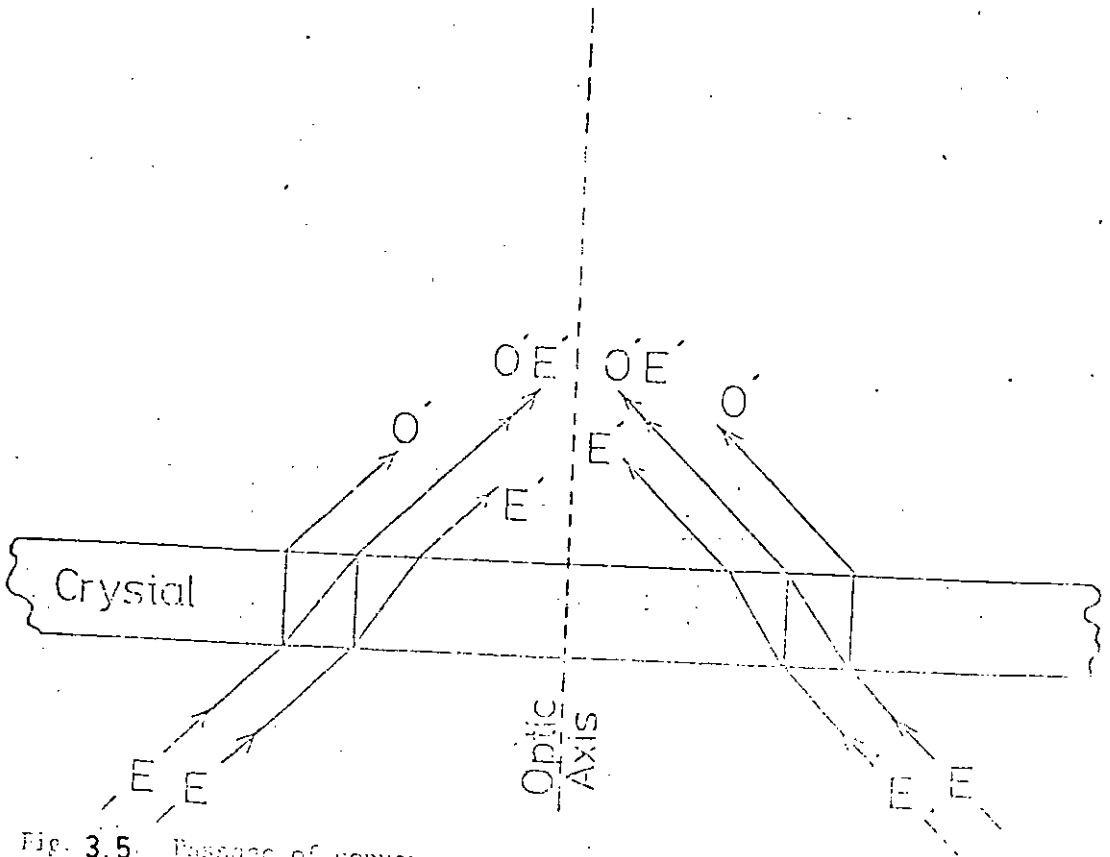

Fig. 3.5. Passage of convergent polarized light through a uniaxial crystal normal to the optic axis.

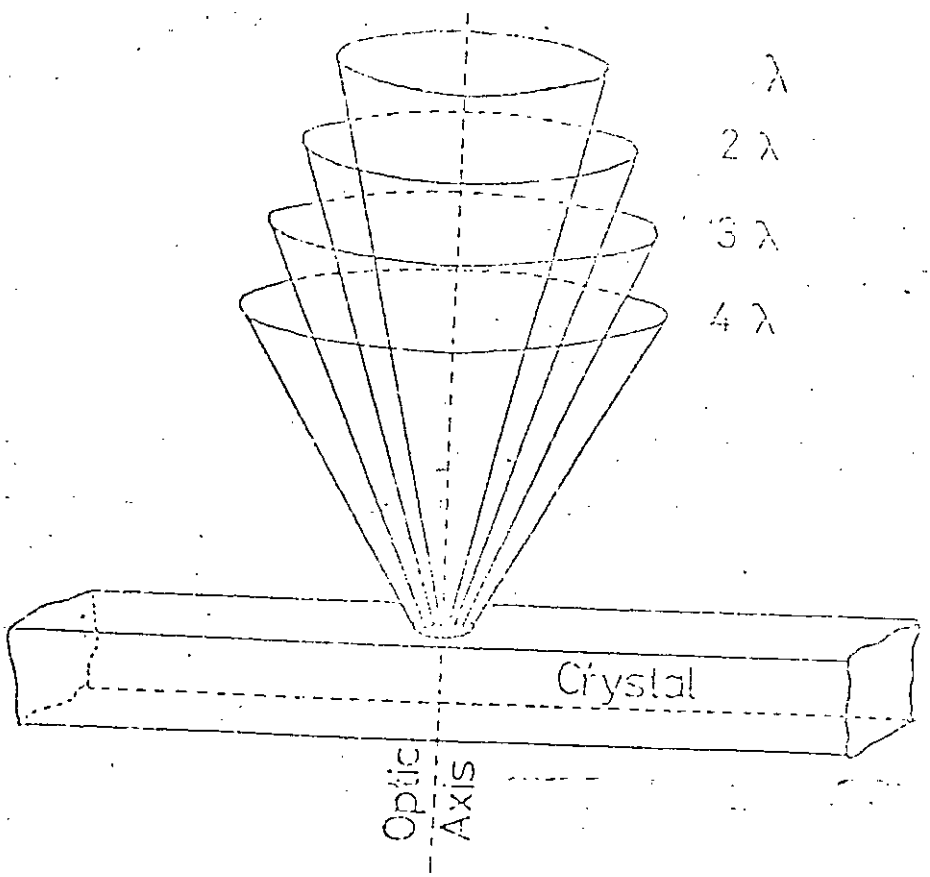

Fig. 3.6. Cones of equal retardation around the optic axis of a uniaxial crystal.

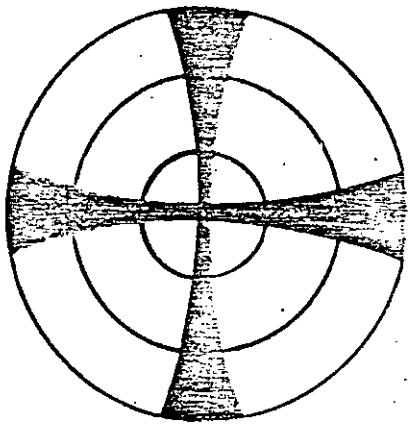

Fig 3.7 Typical interference figure for uniaxial crystal.

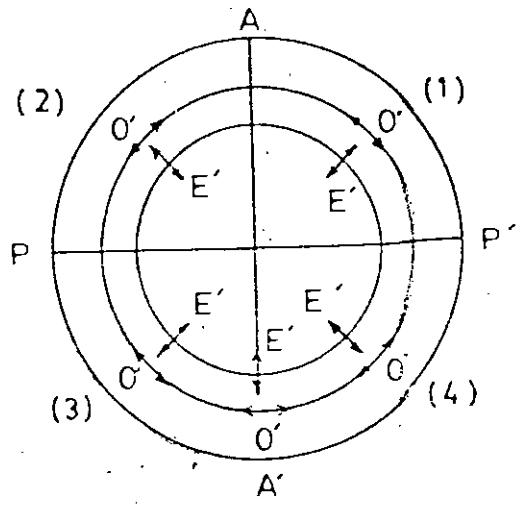

Fig.3.8A. Directions of vibration of O-and E-rays (AA'; PP' vibrational planes in polarizer and analyser).

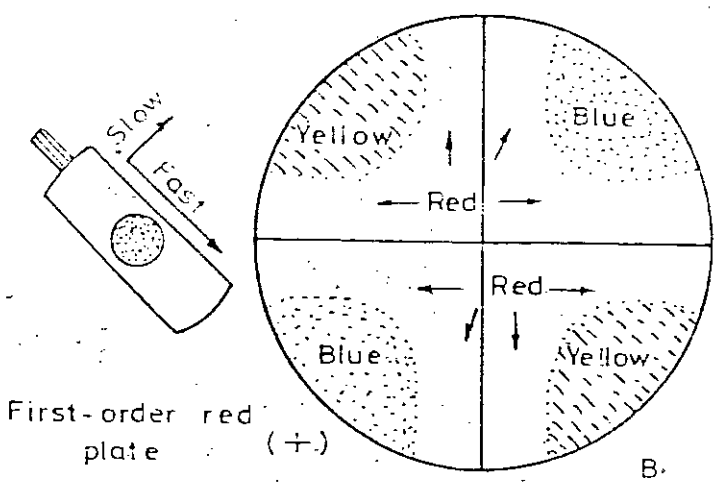

Fig. 3.8B. Effect of introducing a first order red plate over a uniaxial optic axis figure.

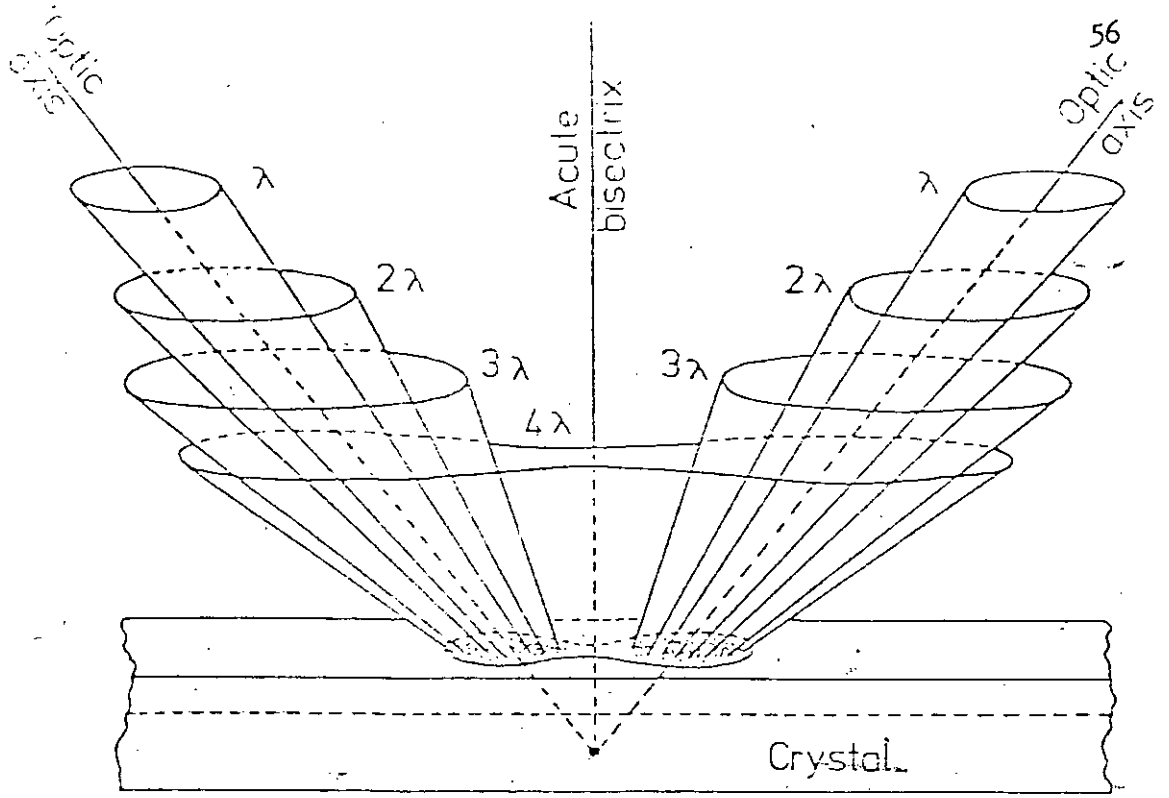

Fig. 3.9. Surfaces of equal retardation around the optic axes of a biaxial crystal.

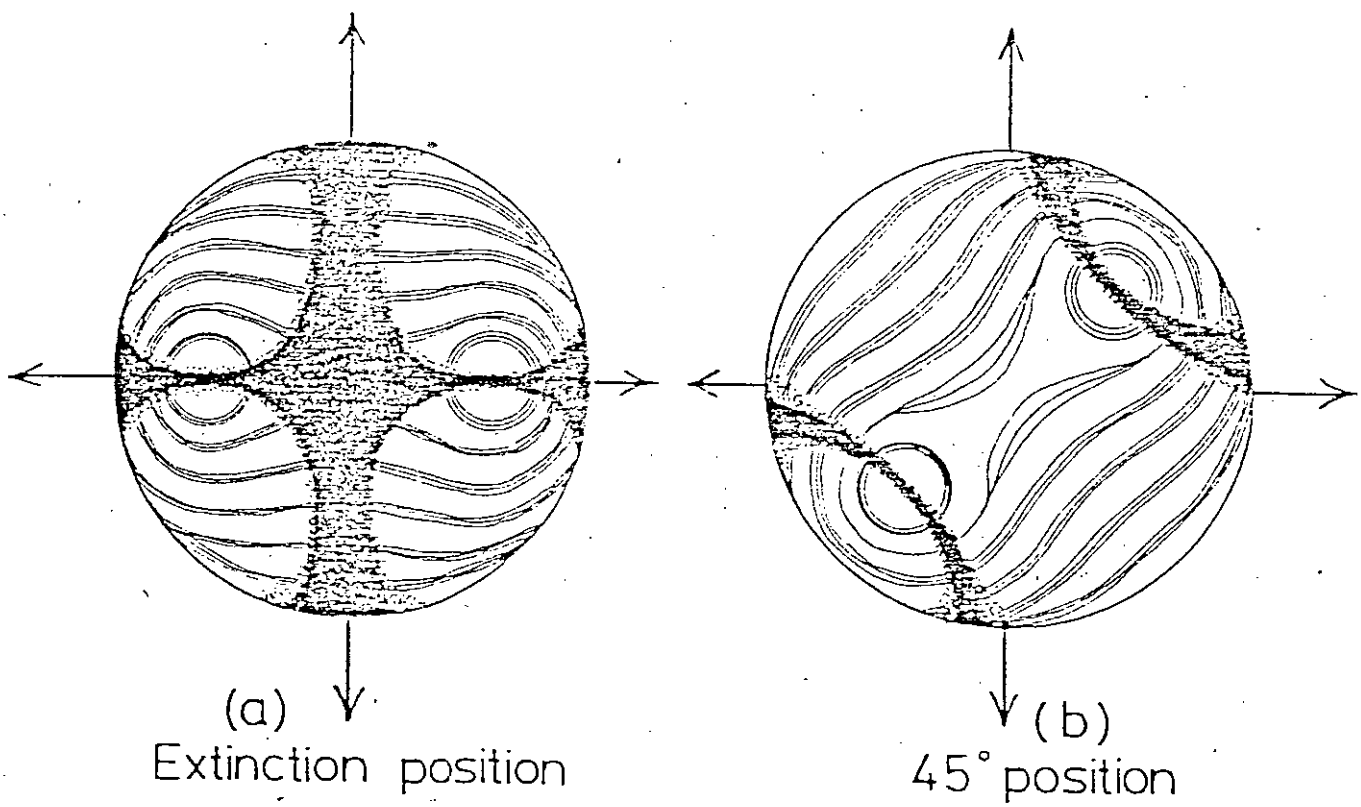

Fig. 3.10. Biaxial interference figure given by a section normal to the acute bisectrix.

REFERENCES

3.1 Hallimond, A.F., The Polarizing Microscope, Vickers Instruments, York, 1970.

3.2 Conn, G.K.T. and Bradshaw, F.J., Polarized Light in Metallography, Butterworths, London, 1952.

3.3 Mott, B.W. and Haines, H.R., J. Inst. Met., 1952, 80, 629.

3.4 Marshall, C.E., Introduction to Crystal Optics, Cooke, Troughton and Simms, York, 1953.

3.5 Dale, A.B., The form and Properties of Crystals, Cambridge University Press, London, 1932.

3.6 Hartshorne, N.H. and Stuart, A., Crystals and the Polarizing Microscope, Edward Arnold Ltd., London, 1970.

3.7 Vickers, A.E.J., 'Polarizing Microscopy in Organic Chemistry and Biology' in Modern Methods of Microscopy, Butterworths, London, 1956, 103.

3.8 Born, M. and Wolf, E., Principles of Optics, Chapter XIII, Pergamon Press, 1964.

CHAPTER - IV

OPTICS OF ISOTROPIC SUBSTANCES

4.1 INTRODUCTION

Those materials through which monochromatic light travels with the same speed, regardless of its direction of vibration are called isotropic media. Isotropic substances transmit light waves with equal velocity in all directions. In addition to glass and crystals of the isometric system, a vacuum, all gases, and most liquids are isotropic with respect to light. Within isotropic media, the vibration direction of a light ray is always perpendicular to the ray path.

The ray-velocity surface for a point source in an isotropic medium is a sphere coincident with the wavefront. Geometric constructions showing how light is reflected or refracted are based on Huygen's principle, which states that any point or particle excited by the impact of wave energy becomes a new point source of energy. Thus every point in a reflecting surface may be considered as a secondary source of radiation having its own spherical ray-velocity surface.

Both anisotropic and isotropic phases can be investigated for grain-size, incidence of twinning and general deformation, and degree of preferred orientation. For a study of anisotropic materials, sections may be polished either by suitable mechanical or electrolytic methods, but for isotropic materials it is necessary to prepare the surface in such a way that the reflection of polarized

light is made dependent on the orientation of the metal[3].

Carbons obtained under a certain range of pressure and temperature consisted of isotropic spherulitic particles upto 10 μm in diameter[9]. Carbons produced by treating the same polymer at atmospheric pressure in flowing nitrogen were also isotropic, but gave no indication of spherulitic bodies.

4.2 REFLECTION

A fundamental law of reflection states that the angles of incidence and reflection, measured from a normal to the reflecting surface, are equal and lie in the same plane. This plane is called plane of incidence. Fig. 4.1. is a Huygenian construction in the plane of incidence of incident and reflected light waves. The wave fronts are drawn exactly one wavelength (λ) apart both before and after reflection. The angle of incidence is identified as θ_1 and the angle of reflection as θ_1'.

Light energy following the rays generates spherical wavelets about point sources in the reflecting surface, and the wavefronts for the reflected light are obtained by locating planes (lines in the plane of the drawing) tangent to each family of in-phase wavelets.

In fig. 4-1 right angles abc and a'bc share a hypotenuse and are similar, and angle θ_1 is equal to angle θ_1'.

$$\therefore \quad \theta_1 = \theta_1' \qquad (4-1)$$

The extent to which light is reflected from a surface depends upon the nature of the surface. If the surface is flat and highly polished, none of the light seems to come from the surface, and the reflected object seems to lie beyond the surface. This type of reflection may be called regular (specular) reflection. If the reflecting surface is rough, it seems to be a source of light. This results in diffuse reflection. Luster depends upon the manner and quality of light reflection. That light penetrates reflecting bodies is shown by the fact that the intensity of reflected light is less than that of the incident light.

4.3 REFRACTION

In general, light waves passing from one translucent medium to another are bent or reflected. This is not true when the light falls with perpendicular incidence on a plane contact between two media or when there is total internal reflection. The power of a substance to refract light waves is sometimes described as refringence. Substance of high refractive index have high refringence; those of low refractive index have low refringence.

In fig. 4-2 it is supposed that light waves in vacuum (air) are incident, with an angle of incidence θ_1, on a plane surface of a translucent medium. These waves are reflected as in fig 4-1, but we are now more concerned with the behavior of the light waves as they penetrate the translucent medium than with the reflection of these waves.

In the translucent medium, $V_1 > V_2$ and also $\lambda_1 > \lambda_2$

$$\therefore \frac{V_1}{\lambda_1} = \frac{V_2}{\lambda_2} = f \qquad (4\text{-}2)$$

Since $V = f\lambda$

From fig. 4-2

$$a'b = bc \sin\theta_1 \qquad (4\text{-}3)$$

and $$ab = bc \sin\theta_2 \qquad (4\text{-}4)$$

In triangle a'bc,

a'b is proportional to both V_1 and λ_1

and in triangle abc

ab is proportional to V_2 and λ_2

$$\therefore \frac{a'b}{ab} = \frac{V_1}{V_2} = \frac{\lambda_1}{\lambda_2} = \frac{\sin\theta_1}{\sin\theta_2} = n \text{ (const.)} \qquad (4\text{-}5)$$

which is an expression of Snell's law. Here n is the refractive index.

The index of refraction, as defined above, applies without qualification to colorless optically isotropic substances; but, in anisotropic substances having two or three principal refractive indices, the definition should be phrased more precisely. In isotropic substances light waves transmitted along rays move in the same direction and with the same velocity as the associated wave front. However, in anisotropic substances the velocity of the wave front in the direction of its normal is not necessarily the same as the ray velocity.

4.4 TRANSMISSION OF LIGHT AND THE ISOTROPIC INDICATRIX

4.4.1 General Concept of the Indicatrix :

The optical indicatrix illustrates how the refractive index of a transparent material varies according to the vibration direction of the light wave in the material (monochromatic light assumed). Consider an infinite number of vectors radiating outward in all directions from a common point within the crystal. Each vector is drawn proportional in length to the crystal's refractive index for light vibrating parallel to that vector direction. The indicatrix is a surface connecting the tips of these vectors. The vectors themselves are omitted when this connecting surface is drawn, but in fig. 4.3 a few are shown for illustration. The indicatrix is purely a method of rationalizing optical phenomena. As such, it furnishes an orderly frame work whereby the optical phenomena associated with transparent crystals may be interpreted, remembered, and predicted. (It is particularly careful for anisotropic crystals. For isotropic media, however, indicatrix theory is not particularly advantageous, chiefly because of the simplicity of their optical behavior).

4.4.2 The Isotropic Indicatrix :

In isotropic media, by definition, the index of refraction does not change with the vibration direction of the light. Consequently, all the vectors relating refractive index to vibration direction are of equal length, and therefore, all isotropic indicatrices are perfect spheres (fig. 4-3). Transparent glasses, liquids

and isometric crystals - not under strain - are characterized by such indicatrices.

Optically isotropic translucent substances transmit light of a particular frequency with equal velocities in all directions. Examples of isotropic substances are unstrained isometric crystals, many unstrained liquids, and gases. An excellent example of an isotropic isometric crystalline substance is fluorite, CaF_2 as shown in fig. 4.4.

Consider two types of electromagnetic radiation incident on a crystal of fluorite. Relative to the dimensions of the unit cell, X radiation such as CuK radiation (wavelength 1.5418 $\mathring{A}$) has a wavelength of the same order as the inter-atomic distances and can detect the locations of individual atoms and planes of atoms. However, if Na-light (wavelength in vacuum = 5889 $\mathring{A}$) is incident on the crystal, an entirely different situation exists. The refractive index of fluorite is 1.434 for Na-light and, according to the equation

$$\mu = 1.434 = \frac{\lambda_1}{\lambda_2} = \frac{5889}{\lambda_2} \qquad (4\text{-}6)$$

The wavelength of light with the frequency of Na-light in the crystal is 4,106 A°. This ratio of this wave length to the edge of the unit cell is 4106/5.44 = 754.7. That is, the wave length of the light is many times greater than inter-atomic distances. Electromagnetic radiations with the limited range of frequencies of visible light can not resolve details of atomic or molecular structure (as do X-rays) and pass through substances as energy

pulses with widely separated maxima and minima, compared to atomic or molecular spacings. Large families of atoms or molecules are involved in the dislocations superimposed by a single energy oscillation. Because the atomic nuclei are heavy and very small and the electronic atmospheres surrounding the nuclei are relatively light and diffuse, it is assumed that most of the energy is transmitted by systematic dislocations of the electronic atmospheres surrounding the nuclei.

Light energy passing through the symmetrical fluorite crystal, accordingly, can not detect anything more than that the composite electronic atmosphere is statistically the same in all possible directions of transmission, and the light travels with the same velocity in all directions. The same is true in most liquids or gases.

In anisotropic substances such as crystals with lower symmetry than isometric crystals and in strained liquids or gases, the electromagnetic oscillations encounter statistically different dispositions of atoms and molecules in different directions, and the velocity of light differs in different directions.

The interaction between the crystal and incident transverse oscillations, according to classical electromagnetic theory, results in simple harmonic transverse oscillations within the crystal, and the velocity of transmission is strictly dependent on the direction of vibration of the transverse oscillation.

Assuming that a light wave in an isotropic substance vibrates at right angles to the direction of its propagation, the

passage of light through the medium can be related to a sphere called an isotropic indicatrix (fig. 4-5). All radii of the sphere are equal to n, the index of refraction of the medium for a particular wavelength of incident light; the radii give the refractive indices in the directions of vibration for all waves originating at a point source. The wave corresponding to a particular radius of the sphere travels at right angles to the radius with a velocity proportional to 1/n

4.5 COLOR

If the electrons in atoms or molecules have natural frequencies of oscillation of the same order as those of the superimposed electromagnetic oscillations (light waves), any or all of the component colors of white light may be effectively removed during transmission because of the phenomenon of resonance. Under conditions producing resonance, substances absorb maximum amounts of incident energy, and the electromagnetic oscillations are effectively damped. Damping is related to the kinds of atoms or molecules, and, in crystals, to the structure and the manner and kinds of bonding. A substance that is illuminated by white light and transmits only a blue color has damped out certain oscillations for other colors or, in other words, has acted as a light filter.

Color depends in a complex manner not only on the interaction of light with abundant chemical constituents but also on atomic arrangement, impurities, and structural defects in crystal structures. An example of color dependency on crystal structure is

seen in diamond and black, nearly opaque graphite, both consisting of carbon but having different arrangements and modes of bonding of the carbon atoms. Impurities disseminated through crystals in minute microscopic to submicroscopic inclusions may react with transmitted light to produce color by selective absorption, or, if the inclusions are very small, by scattering of light of certain frequencies (the Tyndall effect).

The chemical elements that are most effective in producing colors in transmitted or reflected light, whether they are integral components or are present as impurities, are the transition metals. Important and relatively abundant transition elements are titanium, vanadium, chromium, manganese, iron, nickel, copper and zinc. Differences among the transition elements are attributed to differences in the underlying shell of electrons rather than to the outer valence electrons. In transition elements a low energy photons or pulse of light energy in the visible region can dislocate an electron from one energy level to another with comparative ease, a process in which light energy of an appropriate frequency is absorbed so as to produce colored transmitted or reflected light.

Structural defects in crystals under certain conditions cause absorption of light of certain frequencies. When the defects react with white light to produce color, they are identified as color centers. The simplest type of color center is an "F" (Farben) center and is a negative ion vacancy in the crystal structure which has captured one or more electrons. It is supposed that absorption of light of one or more frequencies results from interaction between

the light and the captured electrons. "F" centers are produced by various processes including bombardment by high - energy radiation and chemical treatment.

An elegant approach to an appreciation of the nature of absorption of light energy by solids and liquids is found in modern summeries of crystal or ligand field theory.

4.6 ISOTROPISM AND ANISOTROPISM

The determination of the nature of the optical indicatrix for a particular crystal is simply performed by examining interference figures. However, on the universal stage orthoscopic procedures are relatively simple and consist of determining whether the crystal is isotropic or anisotropic and, if it is anisotropic, whether it is uniaxial or biaxial. Proof that an anisotropic crystal is not uniaxial is sufficient indication that it is biaxial.

The procedure below gives satisfactory results with most sections of crystals. If the results are inclusive for a particular crystal, search for another crystal of the same substances and try again. All operations are performed between crossed polars :

1. If the grain remains dark during rotation about A_1 (Fig. 4-6); proceed as follows :

A. Rotate section a few degrees about A_2. Then rotate about A_4. If the section remains dark, the substance is isotropic.

B. If the section becomes illuminated, return stage to rest

position, and then rotate a few degrees on A_4. If the section is still dark, return stage to rest position, rotate a few degrees on A_1 and then rotate a few degrees about A_4. If the section is anisotropic and remains dark during rotation on A_4 before and after rotation about A_1, the substance is uniaxial and is cut normal to the optic axis. If the section is illuminated after rotation on A_4 either before or after rotation on A_1, the substance is biaxial and is cut normal to an optic axis.

II. If the section is alternately extinguished and illuminated during rotation about A_1, A_3, or A_5 (M), proceed as follows, after returning stage to rest position.

A. Rotate section to extinction on A_1 and then rotate about A_4.

1. If the grain is illuminated, return A_4 to rest position and rotate section 90 degrees to next extinction position. Now rotate on A_4. If section remains at extinction, it is uniaxial. If it becomes illuminated it is biaxial.

2. If in operation 11A the section remains at extinction, return A_4 to the rest position and rotate the section through 90 degrees on A_1 to the next extinction position. Now rotate section a few degrees about A_2, and then return section to extinction by rotation about A_1. If, after this manipulation, the section remains at extinction during rotation on A_4, the substance is uniaxial. If the section is illuminated, the substance is biaxial.

4.7 OPTICS OF ISOTROPIC CRYSTALS

The theoretical back ground of the optical studies was provided largely with the aid of the mathematical treatment due to Drude[6] in 1887. This was followed by practical applications to microscopy initiated by Wright[7] in 1919. Starting from the Maxwell's equations and dealing with the special cases of normal incidence on a surface normal to an optical symmetry plane, Wright gave a summary of the theory.

When the reflected light can be represented by two plane polarized components at right angles, subject to a phase difference, such cases were dealt with more directly by Woodraw, Mott and Haines[8].

The incidence of light upon the surface of an isotropic material makes few demands on the indicatrix theory. The crystal surface in question is assumed to pass through the indicatrix centre, and the resultant intersection between surface and indicatrix is a circle of radius proportional to the crystal's refractive index for the light. In indicatrix theory such a circular section indicates that the crystal "permits" the entering light to vibrate within the crystal in the same direction (s) as it did prior to entry; that is, the light is not required to vibrate parallel to a particular direction in order to pass through the crystal. Thus, unpolarized light (Fig. 4-7A) remains unpolarized after entry into the crystal whereas polarized-light (Fig. 4-7B) maintains its same plane of polarization after entry.

Since isotropic materials can not alter the direction of polarization of the entering light, an isotropic grain, viewed

between crossed nicols, always appears extinct (that is transmits no light), even during a 360-degree rotation of the stage (The possibility of optical activity is here disregarded). This property thus serves as a test for isotropism. The following explanation will clarify:

The light from the polarizer passes through the crystal with its N-S vibration direction unchanged (Fig. 4-8A). At the analyser, however, which is usually set to transmit only E-W vibrating light, all this light is absorbed, the analyser acting as though opaque to this light. The situation is considered vectorially in fig. 4-8B. Here OP represents the amplitude and direction of the light vibrations from the polarizer that have passed through the crystal. However, vector OP has no component parallel to A' A', the direction of light vibration transmitted by the analyser. Consequently, not even the smallest component of the light energy vibrating parallel to OP is transmitted by the analyser. Rotation of the stage changes neither the polarizer's privileged direction P'P' nor the analyser's privileged direction A'A'. Thus the vectorial relationships shown in fig. 4-8B remains the same, regardless of the position of the stage.

On the other hand, if either the polarizer or analyser is rotated so as to change ϕ (Phi), the angle between P'P' and A'A' (fig. 4-8C), to a value other than 90-degrees, the isotropic grain will no longer appear extinct between the two nicols. Instead, a vector component of OP (OA in fig. 4-8C) will be transmitted by the analyser. Note that the amplitude of OA may be graphically determined from that of OP by dropping a perpendicular from point P to line A'A'; expressed mathematically the relationship is

$$OA = \cos \phi \cdot OP \qquad (4\text{-}7)$$

The greater the amplitude of vibration of the light, the brighter the light. In the case of fig. 4.8C, the light passing through the crystal (amplitude OP) is brighter than that passing through the analyser (amplitude OA). Only when the angle of above equation equals 0-degrees will OP and OA be equal and therefore represent equal brightnesses.

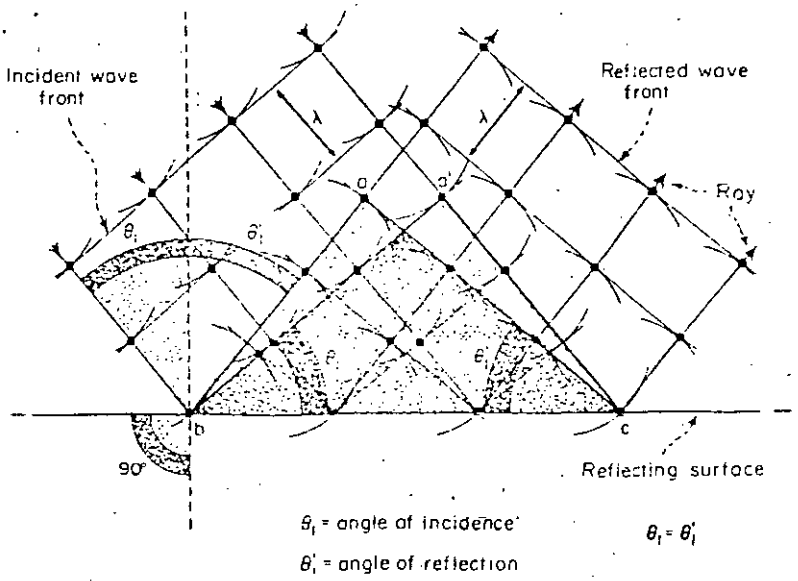

Fig. 4-1 Huygenian construction showing reflection by a plane surface.

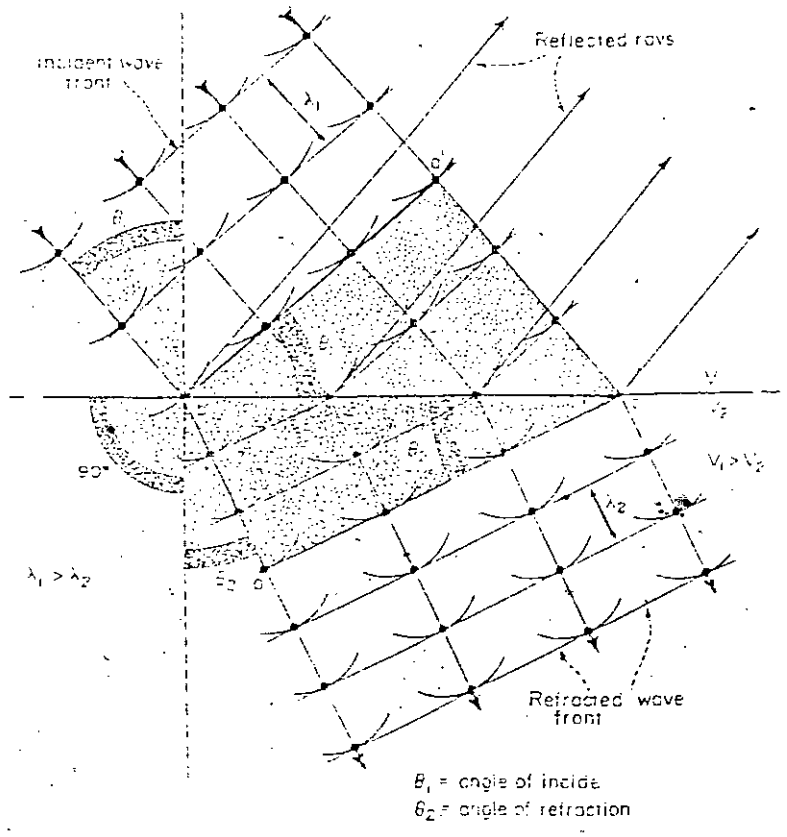

Fig. 4-2 Huygenian construction showing light waves reflected and refracted at the contact between air (or vacuum) and a translucent medium.

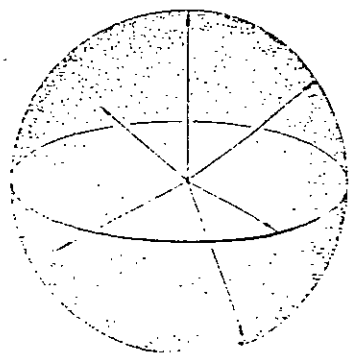

Fig. 4-3 Isotropic indicatrix of a crystal for sodium light.

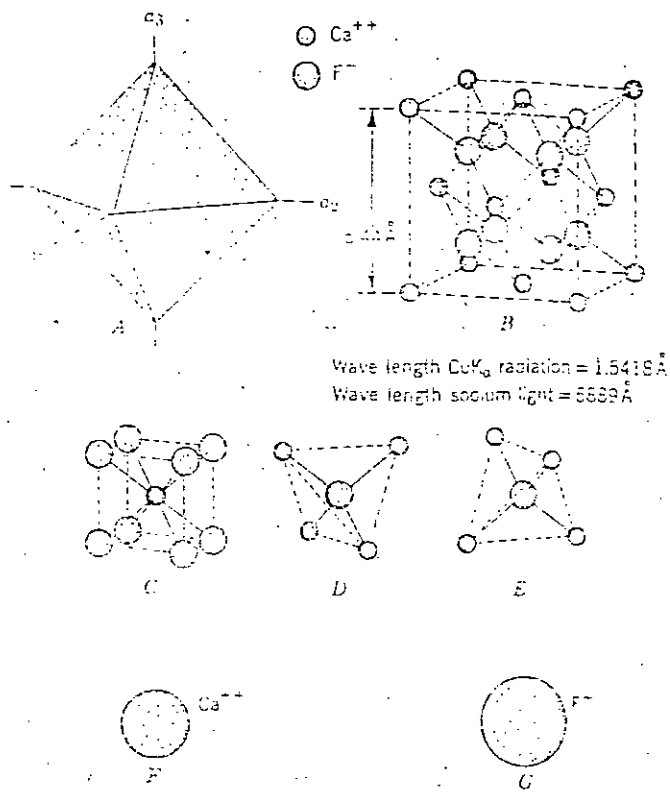

Fig. 4-4 Fluorite (CaF_2) showing structure and dimensions of unit cell.

A. Clinographic projection of an octahedral crystal.

B. Unit cell.

C, D and E. Various manners of coordination of calcium and fluorine ions in fluorite structure.

F and G. Actual dimensions of calcium and fluorine ions.

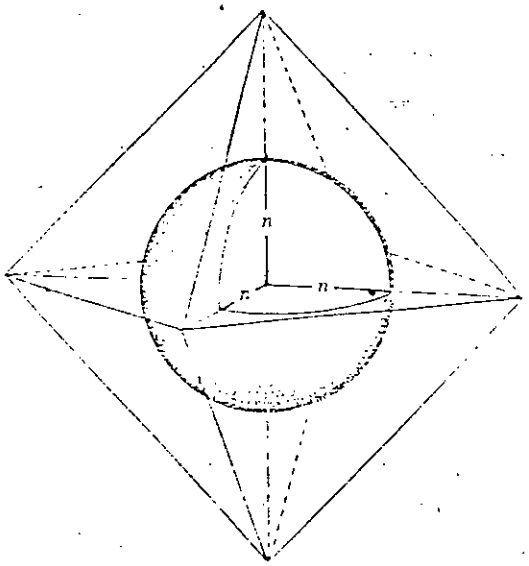

Fig. 4-5. The isotropic indicatrix.

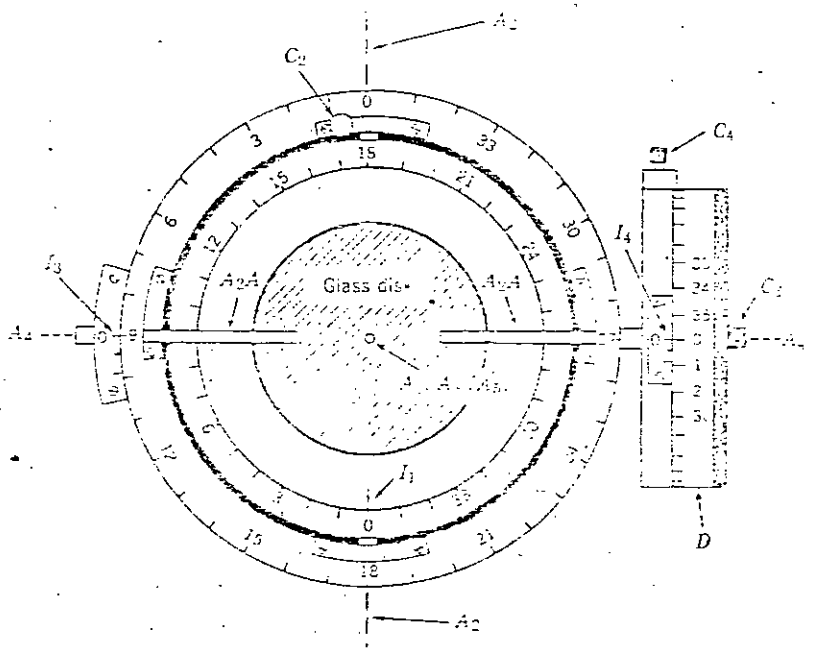

Fig. 4-6 Diagrammatic plan view of a four-axis universal stage at the rest position.

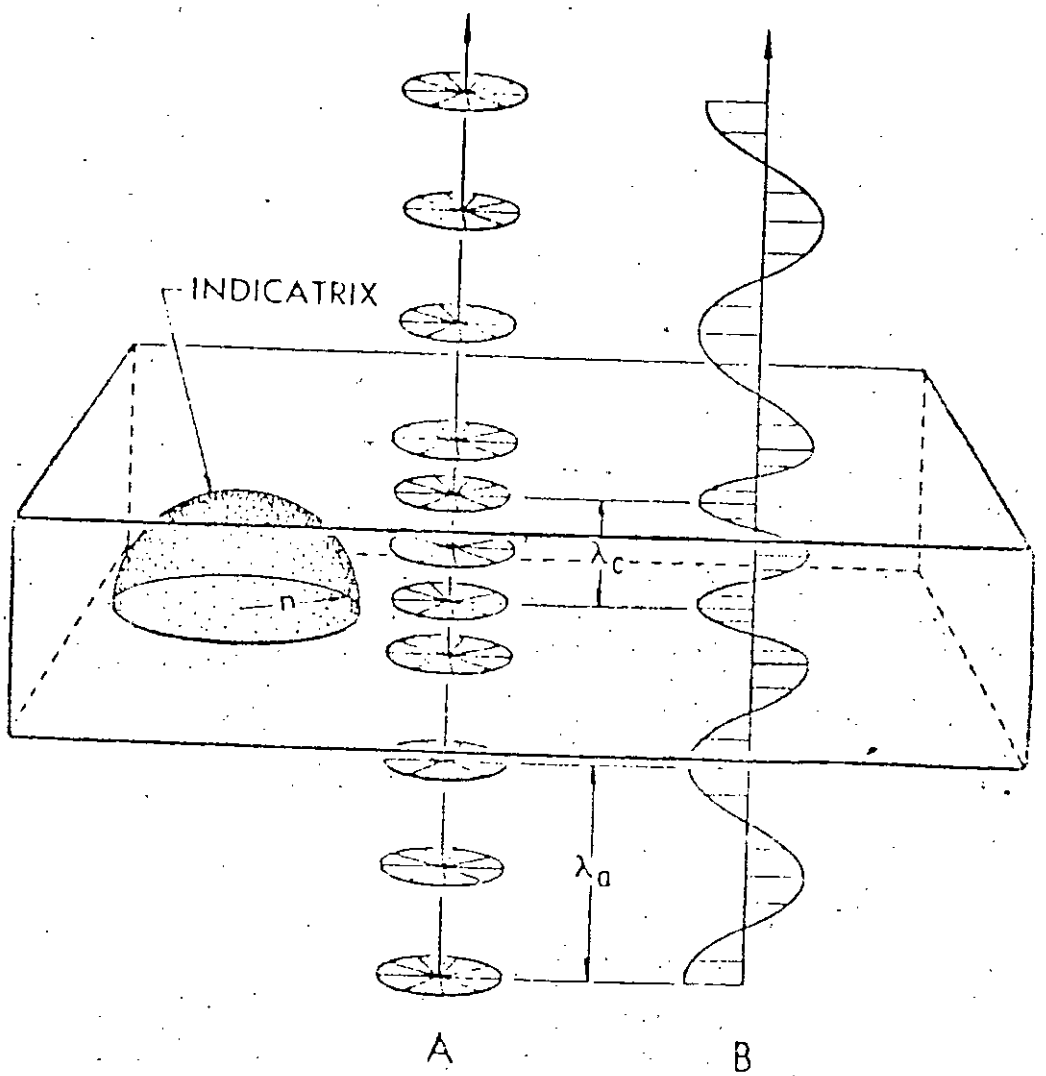

Fig. 4-7 The effect of an isotropic plate upon (A) a normally incident unpolarized ray and (B) a polarized ray.

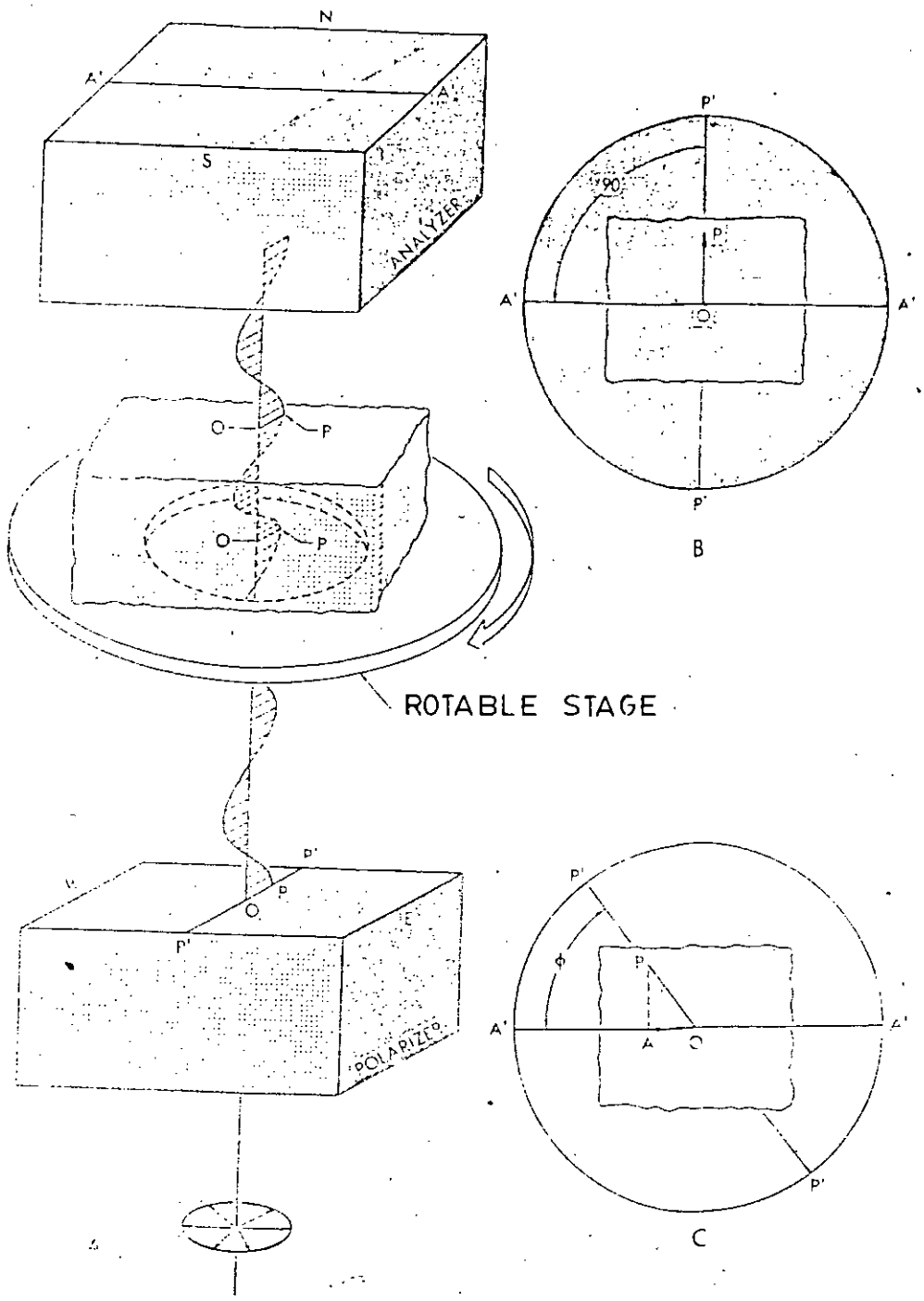

Fig. 4-8 (A) Passage of light in an isotropic plate on the stage of a polarizing microscope

(B) The grain in the field of view between crossed polars.

(C) The grain in the field of view other than cross position.

REFERENCES

4.1 Bloss, F.D., An introduction to the methods of optical crystallography, 1961.

4.2 Wahlstrom, E.E., Optical crystallography, 5th Edition, 1979.

4.3 Mott, B.W., Member, M.A. and Haines, H.R., Journal of the institute of Metals, 1951-52, 80, 629.

4.4 Rosenfeld, J.L., Determination of all principal indices of refraction of difficulty oriented minerals by direct measurement, Am. Mineralogist, 1950, 35, 902.

4.5 Wright, H.G., Determination of indicatrix orientation and 2V with the Spindle stage: a caution and a test, Am. Mineralogist, 1966, 51, 919.

4.6 Drude, P., Ann. Phys. 1887, 32, 584.

4.7 Wright, F.E., Proc. Amer. Phil. Soc., 1919, 58, 401.

4.8 Woodraw, J., Mott, B.W. and Haines, H.R., Proc. Phys. Soc., 1952, 65, 603.

4.9 Hirano, S., Dachille, F. and Walker, P.L., Jr. High Temperatures - High Pressures, 1973, 5, 207.

CHAPTER - V

DIFFERENTIAL THERMAL ANALYSIS

5.1 INTRODUCTION

Differential thermal analysis (DTA) is the technique of accurately recording the temperature difference between a thermo-couple surrounded by the sample being studied and a thermo-couple embedded in a standard inert material such as aluminium oxide while both are being heated at a uniform rate. These temperature differences arise when phase transformations or chemical reactions occur in the sample which involves evolution or absorption of heat.

The technique of differential thermal analysis (DTA) was first proposed by Le Chatelier[1] which has been a useful tool in the fields of metallurgy, ceramics, geology and chemistry. But in recent years this technique has been extensively applied to chemical problems. The study of thermal behavior of carbonising materials and its use was introduced at the fourth carbon conference by Nakamura and Atlas[2]. Smother & Chiang[3] and Mackenzie[4] described elaborately the theoretical basis and manifold applications of DTA.

In DTA, the evolution or absorption of heat by any material under heat-treatment is recorded and indicated by exothermic or endothermic peaks. The exothermic (i.e. the evolution of heat) and endothermic (i.e. the absorption of heat) reactions are generally obtained in the DTA trace as positive and negative deviations respectively from a base line. So, DTA gives a continuous thermal record of reactions occuring in a sample, although it does not

indicate what these reactions are nor does it sort out simultaneously occuring reactions. The curves obtained vary rather widely and are affected by such factors as furnace heating rate, sample particle size, furnace atmosphere, type of sample holder etc. Also due to environmental and instrumental effects, discrepancies may arise in the DTA curve which could lead to a completely false interpretation.

Generally, additional information is needed to supplement the DTA curve, namely, thermogravimetric analysis (TGA), X-ray diffraction, infrared absorption spectroscopy, visual phase examinations, mass spectrometry, gas chromatography, polarized-light micrography, etc. for correct interpretation of the thermogram peaks.

The reaction temperature and the rate of reaction together give the characteristic thermal curve for the particular material. The melting and the boiling points are obtained correct to $\pm 5^{\circ}$. The carbonaceous mesophase of a graphitizable organic compound usually appears in the temperature range of $350^{\circ}C$ to $600^{\circ}C$ with the formation of the spherules, coalescence and mosaic. The actual temperature interval in which the mesophase develops in the carbonisation of a particular organic compound may be a few degrees or it may be tens of degrees. This obviously causes practical difficulties in determining the exact temperature, interval of mesophase formation for the samples under investigation. A combination of differential thermal analysis, thermogravimetric analysis and polarised-light micrography[5, 18, 21] has proved a valuable approach to the determination of the temperature interval of meso-

phase formation.

5.2 DTA APPARATUS

The basic design of the DTA apparatus and its block diagram[6, 7] are shown in fig. 5-1a and 5-1b respectively. In these two figures a sketch of sample holder and a block diagram of controlling, detecting, amplifying and recording systems are shown.

The thermo-couple which is used in DTA apparatus consists of two matched chromel-alumel thermo-couples supported in a porcelain tube held in position in a furnace combustion tube. The sample and reference cups are nickel cylinders with a thermo-couple well extending into the centre of the cup from the bottom. With this arrangement, the thermo-couples are protected from the destructive action of the hydrocarbons during carbonisation and so the thermo-couple can be used repeatedly. The sample and the reference cups are also isolated from each other and independent of the thermo - couples. This is why weighing before and after heating can be determined easily. 100 mgm anhydrous alumina is used in the reference cup and the sample weights varies over a range of 25 mgm to 40 mgm, depending on their packed density. Normally, a heating rate is standardised at $10^{\circ}C$ per minute.

All experiments are done at atmospheric pressure in a continuous flow of a purified inert gas such as argon, nitrogen or helium. Gases are normally purzed into the furnace chamber at the lower end through a purification train in which oxygen and water are removed by heated copper wool and exhausted from the top into

a Potassium-Bromide-filled condensate trap[8] for collecting the condensable volatile products. Then the non-condensable gases pass through a sulphuric acid bubbler which seals the system and prevents back diffusion of air.

Normally the DTA thermograms on carbonisation processes are run by heating the sample continuously to 750°C at which the final product is mostly carbon. The apparatus used in this program to detect and record these small temperature differences consists of three basic units[2]:-

(i) A DTA furnace and control system,

(ii) An atmosphere control system and

(iii) Electric apparatus for amplifying and recording the temperature difference between the sample and the standard and for recording the actual temperature of the standard.

5.3 THERMAL BEHAVIOR OF CARBONISING AND GRAPHITIZING MATERIALS

During pyrolysis of any substance, the evolution or absorption of heat indicated by exothermic or endothermic peaks in the DTA trace is recorded. The temperature of reaction and the rate of reaction together give the characteristic thermal curve of that particular material.

The application of differential thermal analysis to a number of organic solids, it was found by Varma[9] that the melting and the boiling points could be determined correct to $\pm 3^{\circ}$. One of the attractive features of this method is the convenience of determining the temperatures of sublimation, decomposition, elimi-

nation of water of crystallisation, etc.; which are difficult by other methods.

Lewis and Edstrom[6, 7] used differential thermal analysis to categorise the high temperature behaviour of polynuclear aromatic as either thermally 'reactive' or thermally 'unreactive'. The thermally 'reactive' species possess sufficient reactivity in an atmospheric pressure system to undergo a condensation sequence in the liquid phase and yield a measurable quantity of polymerised carbonaceous residue at 750°C. The thermally "unreactive" entities have sufficient stability so that such condensation reactions do not occur prior to complete volatisation. Hence, the carbonisation residues are not observed at 750°C.

The DTA thermograms obtained for some aromatic hydrocarbons are shown in fig. 5-2 in which only coronene is thermally reactive and all the rest are thermally unreactive. Under the conditions of the DTA measurements, hydrocarbons with three or less condensed rings proved generally to be thermally unreactive. Such materials simply melt and distill away leaving no carbonaceous residue in open system. In general, the thermograms of such compounds exhibit only two endothermic peaks corresponding to the melting and boiling processes. For solid compounds two major endothermic peaks corresponding to the melting and the boiling processes are generally obtained. For liquid compounds a simple major endotherm representative of the distillation process is always found to be present.

Additionally, no carbonaceous residues are obtained in

DTA sample cups at 750°C and no products besides starting materials are observed in the condensed distillates. For such materials DTA offers a convenient method of measuring the melting and the boiling points. Depending on the physical characteristics of the apparatus, either the initial inflection point of the endotherm, the endo - thermic minima, or the endothermic minima minus the temperature difference between the reference and the sample couples, may give the appropriate result.

However, the initial inflexion point of the melting endotherm has been found to be the most reliable method for determining the melting points for respective substances. On the other hand, the boiling endotherms are usually broader and have no specifically defined inflexion temperature. In nearly every instance new chemical compounds in addition to the starting material are obtained in the condensed distillate. The thermograms of thermally reactive aromatics which undergo thermal condensation leading to some carbonaceous residues at 750°C, differ quite markedly from those of the unreactive category. The boiling endotherms are observed to be either completely absent or largely diminished in those thermograms, but the major melting endotherms are clearly observed.

In the case of an organic compound under heat-treatment two competing reactions are often found to occur : cross linking producing an exothermic reaction, and chain stripping and associated reaction which produce endothermic peaks. The second type often allows the planer distributions of the aromatic substances which give rise to graphitising carbon. It should be noted that the exothermic reactions may be preceded by some reactions of secondary

importance, such as loss of absorbed water or other volatile impurities. Bearing these facts in mind, the appearance of an exothermic reaction, some where in the initial polymer decomposition region ensures that the resulting carbon has non-graphitizing properties. Table 5-1 shows the DTA results of some polymers under nitrogen flow, which were reported by Dollimore and Heal[12].

The main qualitative and quantitative characteristics of the carbonisation process of graphitizable and non-graphitizable materials were obtained by Lapina and Ostrovskii[14]. From their investigations it was found that for graphitizable materials endothermal processes of transformation are typical with the values of the effective activation energy exceeding 60 Kcal/mole, while for non-graphitizable one exothermal processes of cross-linking are observed with low values of the activation energy of about 20 Kcal/mole. The DTA curves obtained by Lapina and Ostrovskii for some organic polymers are shown in fig. 5-3.

DTA data alone have led to interesting speculations on the connections between the dehydrogenation endotherm and graphite layer development, and on the correlation of multiple exothermic peaks with polymerisation and condensation mechanisms.

In 1974, Graham[5] determined the temperature interval of carbonaceous mesophase formation by using the differential thermal analysis technique. The mixtures of acenapthylene and sulpher in different ratios have been heat-treated in an atmosphere of dry nitrogen in the Stanton differential thermal analyser and their respective thermograms obtained. The pattern of the thermograms

is reproduced in fig. 5-4. Graham concluded that the temperature at which all the fluctuations terminate was nothing but the temperature of complete coalescence in the case of carbonaceous mesophase and he also added that the fluctuations in the DTA trace was due to the formation of gases within the sample during pyrolysis. These endothermal curves indicates that the sample is graphitizable. He employed also polarized-light micrography to determine the temperature intervals of carbonaceous mesophase. In the case of a few graphitizable aromatic organic compounds such as napthalene, anthracene, phananthrene and chrysene, the temperature intervals of mesophase formation are located by Hossain and Dollimore [17, 18] The selected samples which did not pass through the carbonaceous mesophase transformation due to heating at 400°C for a duration of several hours have been heat-treated in the Stanton-differential thermal analyser and their respective thermograms obtained (fig. 5-5.). These curves are all accompanied with endothermal peaks in the initial portions as in almost all graphitizable organic compounds. The DTA was determined on a Dupont-unit, with pen recording. They also used polarized-light technique to determine the temperature intervals of mesophase.[21]

Differential thermal analysis has also been employed by Hossain and Jahan[19] to ascertain the temperature interval of carbonaceous mesophase and mosaic formation. Selected sample, withdrawn during the initial thermal treatment and which has not yet passed through the carbonaceous mesophase transformation due to heating at 450°C for several hours, have been heat-treated in a pyrex tube into which is dipped a chromet-Alumel thermo-couple to measure the reaction temperatures including the temperatures of

phase transformations in the different stages of pyrolysis. The couple is connected to a sensitive potentiometer capable of reading down to millivolt. The temperature of one of the junctions is maintained at $0^{o}C$ by placing it in melting ice. The temperature of the other junction is gradually increased by heating the pyrex tube containing the sample and the e.m.fs of the couple at suitable intervals were recorded. The temperatures at different phase transformations and reactions were obtained from the e.m.f. temperature chart. The thermal curves so obtained for Benzene(fig. 5-6)[20] clearly indicate that endothermal processes of transformation in the initial portion of the curves are typical in the sample and hence it is also graphitizable. This has also been varified by polarized-light microscopy.

An investigation of the carbonisation and graphitization processes for partially carbonised anthracene-sulphur mixtures has been made by Jiban Podder[22] with the aid of differential thermal analysis of the decomposing material. The carbons resulting from this system have been examined by polarized-light microscopy. As increasing amounts of sulphur are added to anthracene, the graphitizability of the carbons produced by pyrolysis is gradually reduced. The function of the sulphur is to cause both cross-linking and dehydrogenation and the high degree of cross-linking developed in the decomposing material resulted in a non-graphitic carbon. As the amount of sulphur added is increased, the temperature range of fusion and so the mesophase interval becomes shorter and at the same time the decomposing liquid becomes more viscous. The higher the viscosity, the more difficult becomes the reorientation process which must occur at this mesophase period of all graphitic

carbon. Examination of the carbons by polarized-light microscopy during the temperature interval of mesophase shows the gradual decrease in the extent of orientation with increasing amounts of sulphur. The DTA for the investigated anthracene-sulphur mixture (Fig. 5.7) shows this effect very clearly. The narrowing of the initial large endotherm with the increase of S/H ratio indicates that the latent heat of fusion of the mixture gradually decreases. The decrease of latent heat of fusion means the consequent decrease of activation energy[23] and hence the graphitizing power. Thus, if there is any particulate matter, such as S, Al, etc. mixed with the precursor, its graphitizability is reduced. This has also been varified by polarized-light microscopy.

TABLE - 5.1

Polymer	DTA Peak first part of decomposition	Carbon Property
Polyvinyl chloride	Mainly endothermic	Graphitising
Chlorinated polyvinyl chloride	Mainly endothermic	Non-graphitising
Chlorinated rubber	Endothermic	Non-graphitising
Polyvinyl alcohol	Endothermic	Graphitising
Polyvinyl acetate	Endothermic	Graphitising
Polyvinyl buty rate	Endothermic	Graphitising
Polyvinyl ethyl ether	Endothermic	Graphitising
Polyvinyl pyrrolidone	Exothermic	Non-graphitising
Poly acrylonitrile	Exothermic	Non-graphitising
Poly acrylamide	Apparently two exothermic regions	Non-graphitising
Poly furfuryl alcohol	Exothermic	Non-graphitising
Cellulose	Partly exothermic	Non-graphitising
Cellulose acetate	Exothermic	Non-graphitising
Polyvinylidene Chloride	Exothermic	Non-graphitising
Polyphenol formaldehyde	Broadly exothermic	Non-graphitising

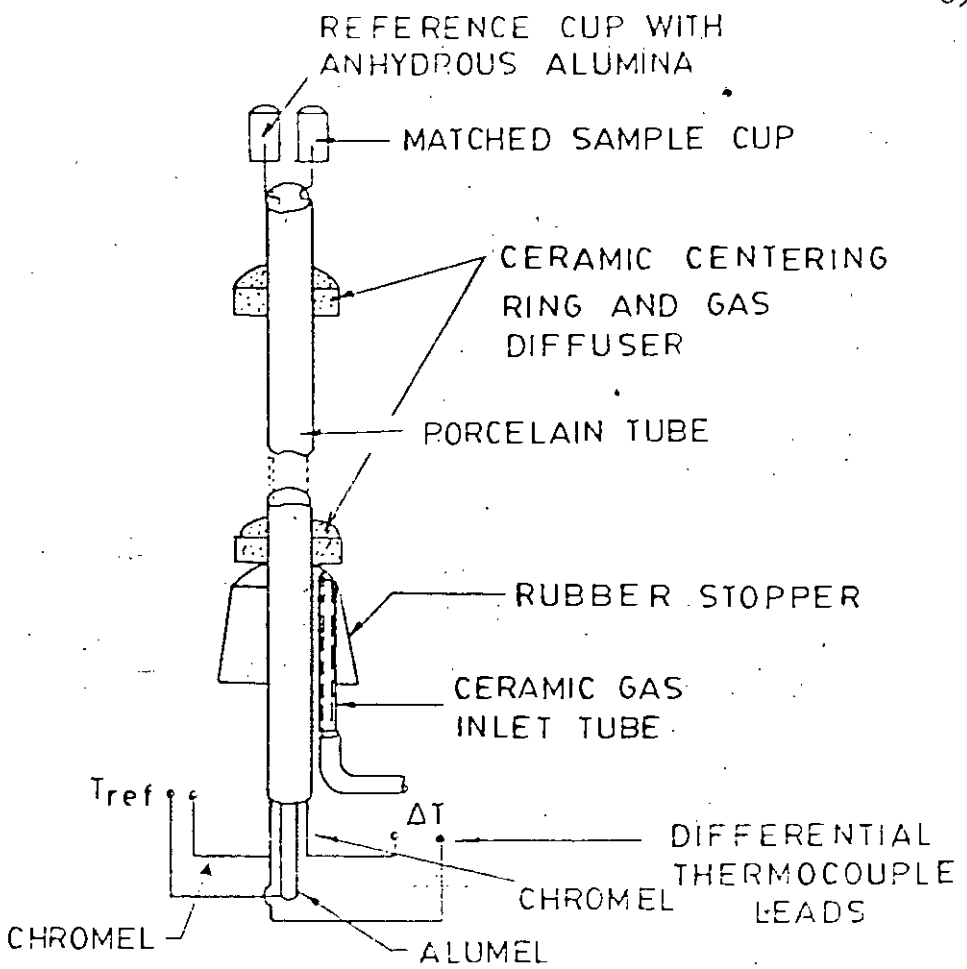

Fig. 5.1A DTA thermocouple assembly.

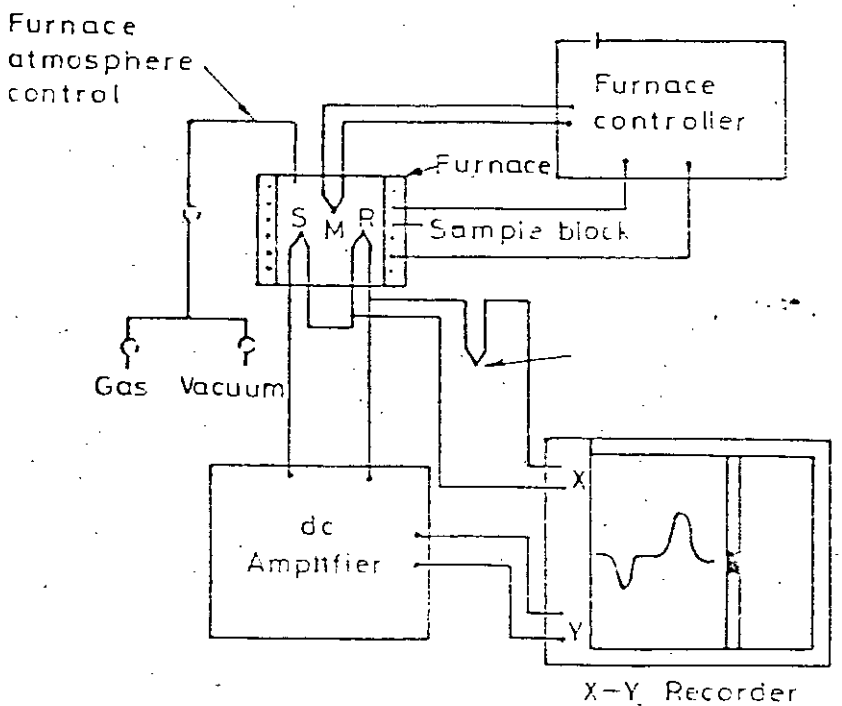

Fig. 5.1B Block diagram of a differential thermal analysis equipment, (S) sample thermocouple, (R) reference thermocouple, (M) monitor thermocouple

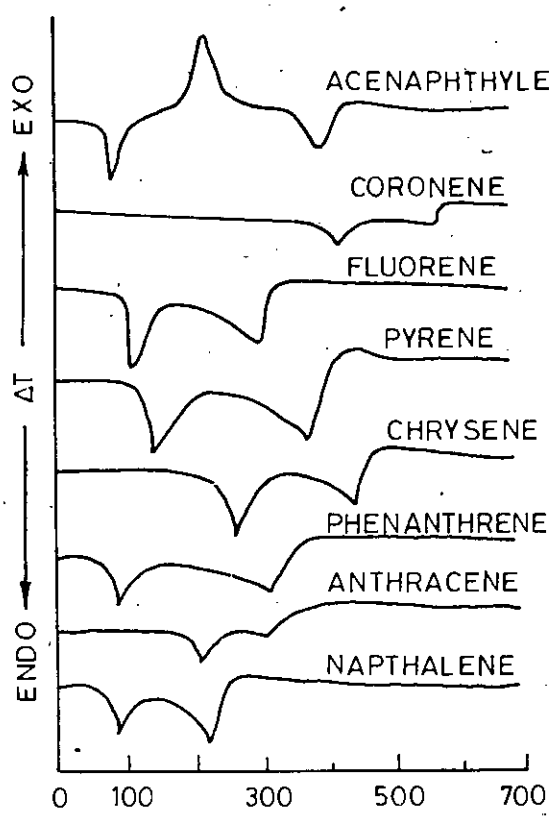

Fig. 5.2 Thermograms of some graphitizable organic materials.

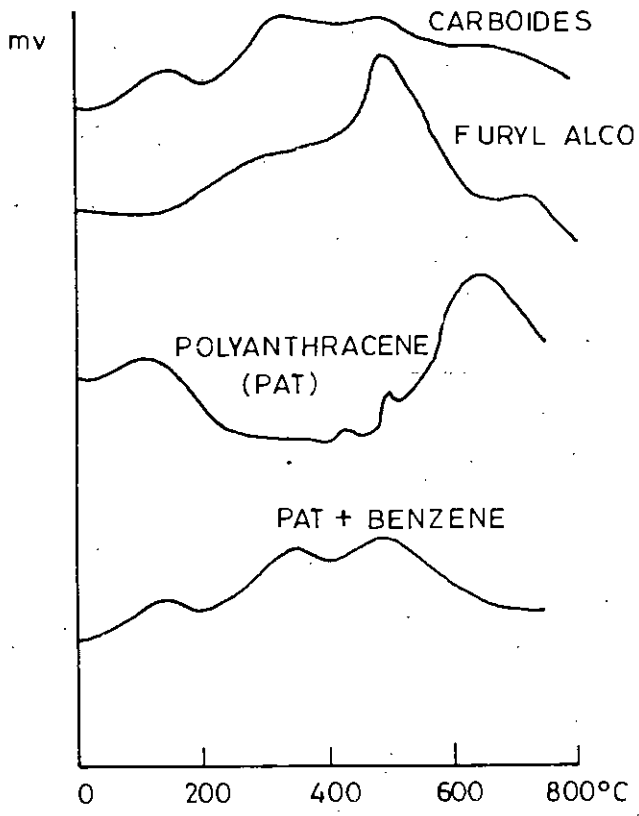

Fig. 5.3 Thermograms of some Non-graphitizable organic materials.

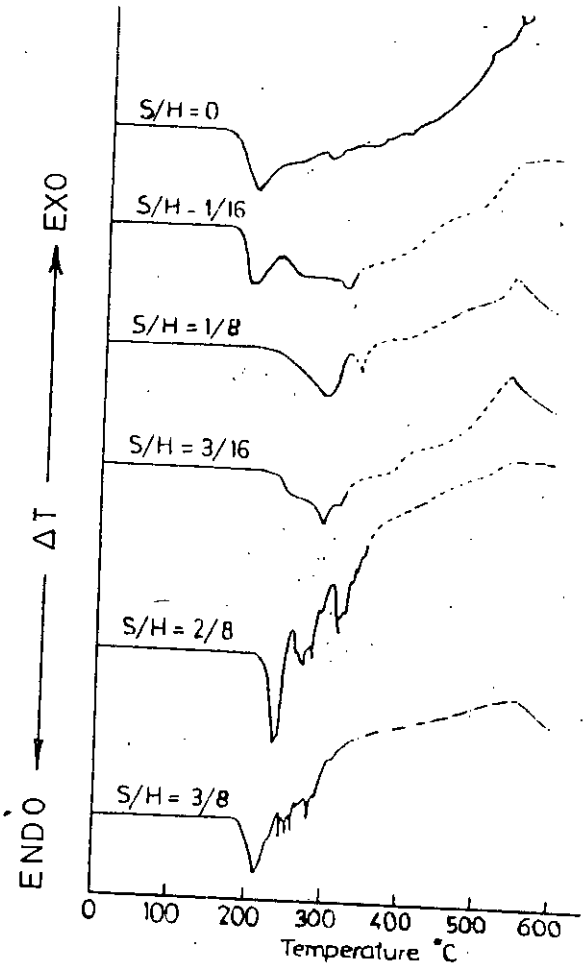

Fig. 5.4 Differential thermal analysis traces partially refluxed acenaphthalene sulphur mixtures.

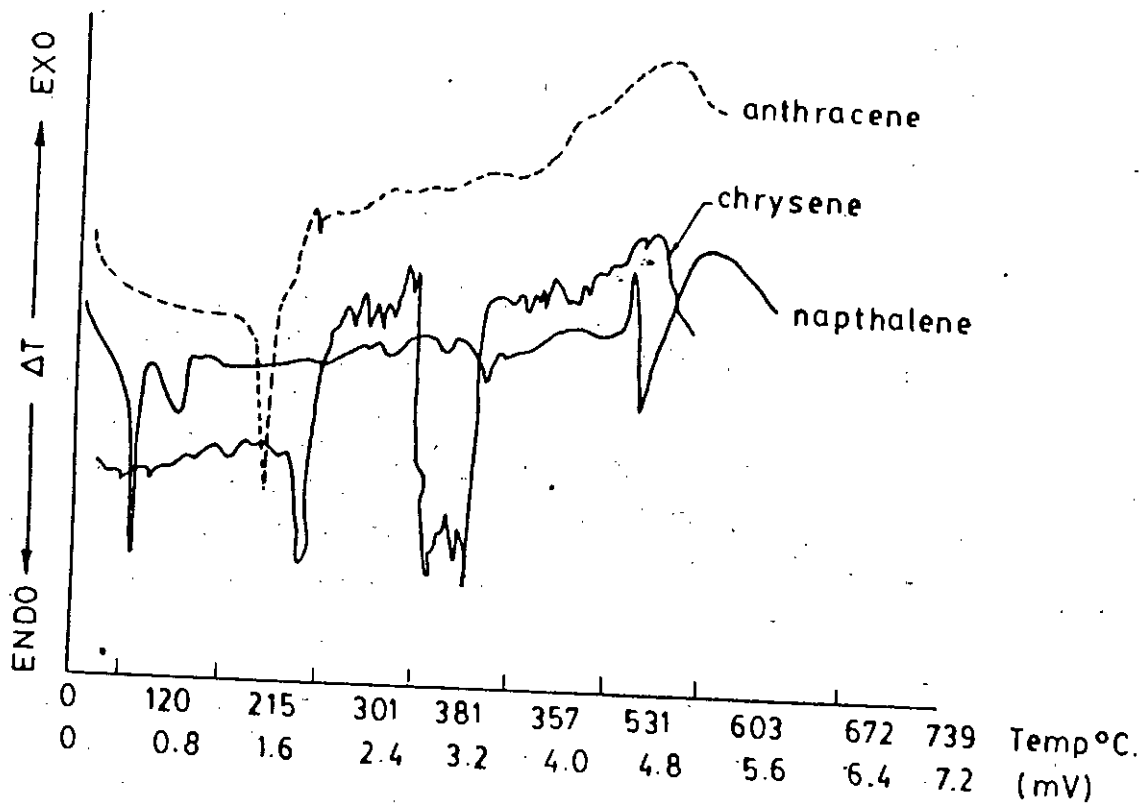

Fig. 5.5 DTA Trace of partially carbonised aromatic organic compounds[17]

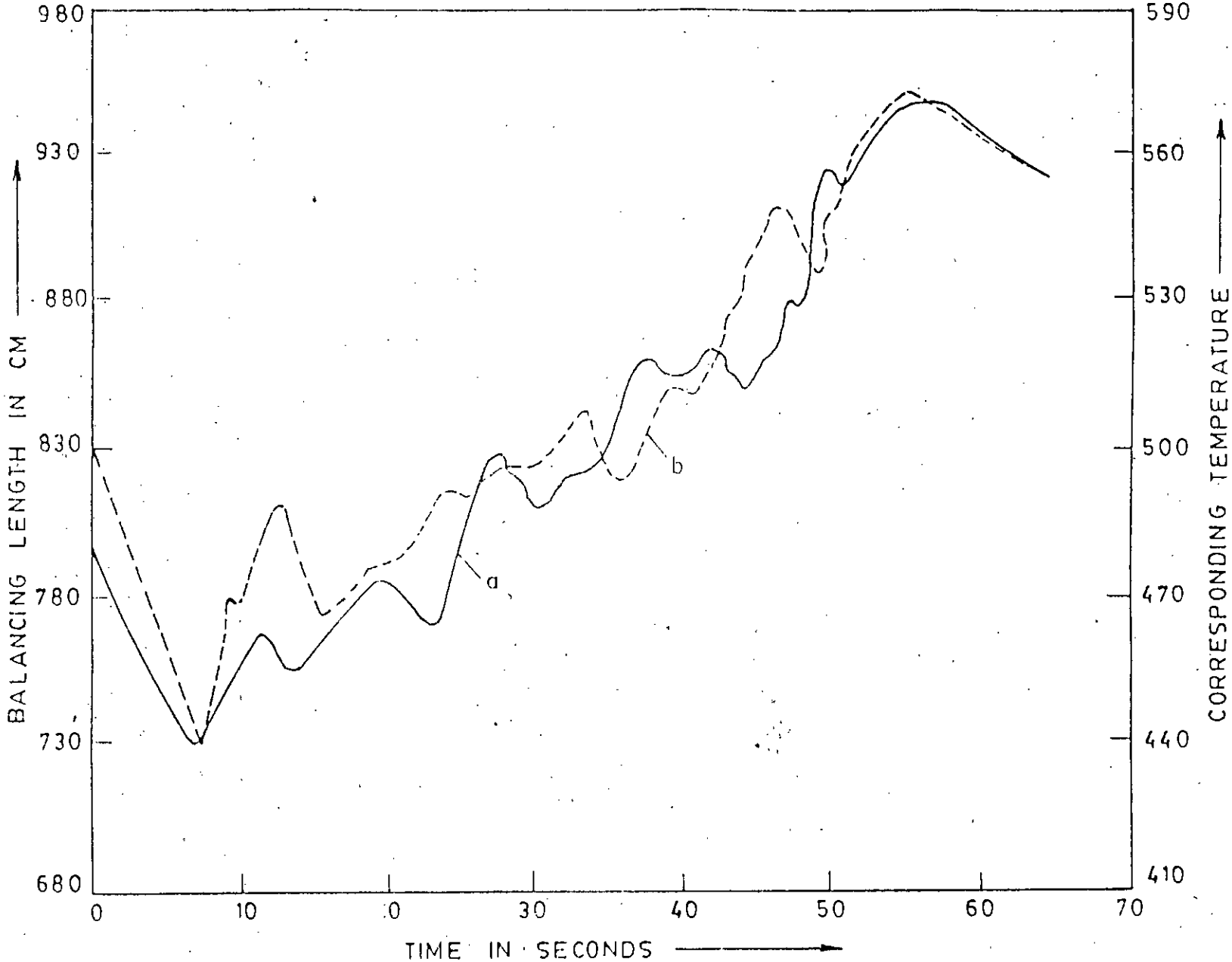

Fig. 5.6 Thermal analysis curve of partially carbonised benzene (C_6H_6) on heat-treatment at 450°C (a) for a duration of 8 hours and (b) for a duration of 12 hours.

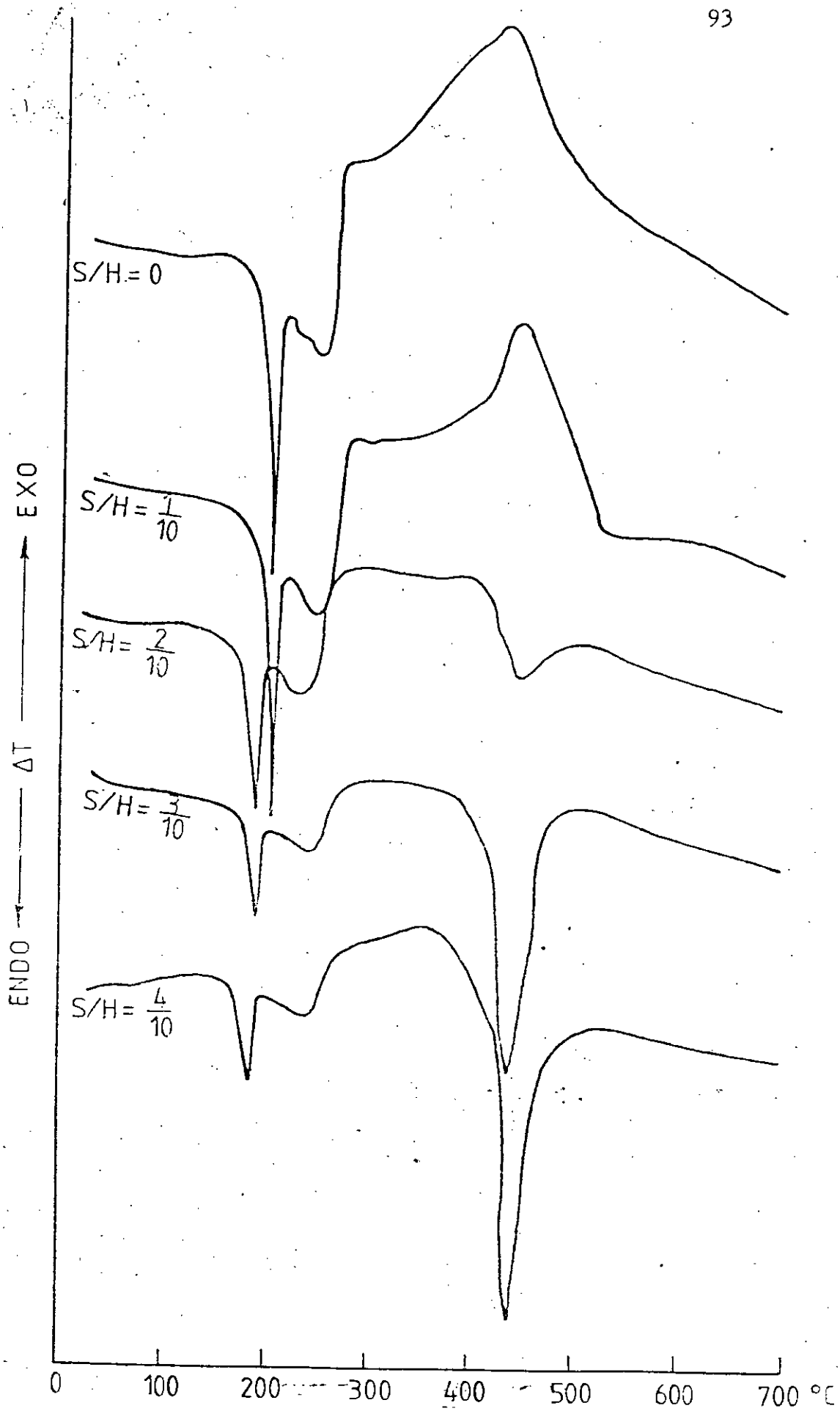

Fig. 5.7 D.T.A traces of Anthracene-sulphur mixtures in different S/H ratios.

REFERENCES

5.1 Chatelier, H. Le., Bull. Soc. franc. mineral, 1887, 10, 204.

5.2 Nakamura, H.H. and Atlas, L.M., Proc. fourth carbon conf., Pergamon Press, London, 1960, 625.

5.3 Smothers, W.J. and Chiang, Y., Differential Thermal Analysis, Theory and Practice, Chemical Publishing Company, New York, 1966.

5.4 Mackenzie, R.C. (Ed.), The Differential Thermal Investigations of Clays, Mineralogical Soc., London, 1957.

5.5 Graham, S.G., Ph.D. Thesis, Salford University, England, 1974, 235.

5.6 Lewis, I.C. and Edstrom, T., Proc. Fifth Carbon Conf., Pergamon Press, London, 1962, 413.

5.7 Lewis, I.C. and Edstrom, T., J. Org. Chem., 1963, 28, 2050.

5.8 Leggon, H., Anal. Chem., 1961, 33, 1295.

5.9 Varma, M.C.P., J. App. Chem., 1958, 8, 117.

5.10 The Coal Tar Data Book, The Coal Tar Research Association, Leeds, England, 1965.

5.11 Bulletin 606, U.S. Bureau of Mines, 1963, Anderson, H.C. and Wu, W.R.K., Properties of Compounds in Coal-Carbonisation products.

5.12 Dollimore, D. and Heal, G.R., Carbon, 1967, 5, 65.

5.13 Glass, H.D. Fuel, 1955, 34, 253.

5.14 Lapina, N.A. and Ostrovskii, V.S., Thermal Analysis, 2, Proc. Fourth ICTA Budapest, 1974, 407.

5.15 Smothers, W.J. and Yao Chiang DTA, Theory and Practice, Chemical Publishing Co. (1958).

5.16 Diamond, R. Proc. Third Carbon Cont. Pergamon Press, 1959, 367.

5.17 Hossain, T. and Dollimore, J., Chemical Engineering Research Bulletin, 5, 1981, 25.

5.18 Hossain, T., Ph.D. Thesis, Salford University, 1981, 91.

5.19 Hossain, T. and Jahan, S.T., Presursor states for the graphitization of Benzene, Xth Science Conference of Bangladesh Association for the Advancement of Science, 1985.

5.20 Hossain, T., Jahan, S.T., Podder, J., Rashid, M.A.,"Thermal properties of carbonising and graphitizing materials" 11th Science conference of Bangladesh Association for the Advancement of Science, 1986.

5.21 Hossain, T. and Dollimore, J., Thermochimica Acta, 1986, 108, 211.

5.22 Podder, J. M. Phil, Thesis, BUET, 1987, 204.

5.23 Vaughan, F., Clay Minerals Bull., 1955, 2, 265.

CHAPTER - VI

PYROLYSIS OF PURE HYDROCARBONS

6.1 INTRODUCTION

Hydrocarbons are generally stable substances which can be distilled without decomposition; but if they are subjected to high temperature in the absence of air (oxygen), their molecules disintegrate or 'crack' into smaller fragments. This process is known as pyrolysis. Thus propane when pyrolysed to 600°C gives rise to methane, ethylene, propylene and hydrogen :

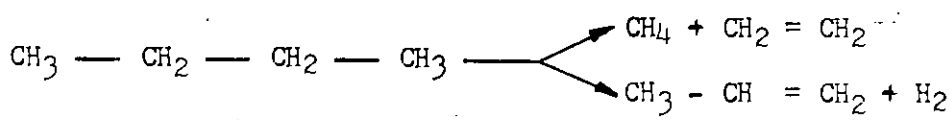

Similarly methane at high temperature yields carbon black and hydrogen. Higher hydrocarbon yields hydrocarbons of lower molecular weights.

The mechanism whereby hydrocarbons undergo pyrolysis to form elemental carbon is a complex process involving gas-phase decomposition reactions, nucleation of liquid microdroplets, diffusional transport of the nuclei to the surface and dyhydrogenation to form carbon[1,2].

Organic compounds are the main and almost exclusive raw materials for the production of artificial carbons and graphite. By pyrolysis, these carbon compounds are converted to solid carbon as the main product and to different volatile compounds as by-products. Such thermal decompositions below 1000°C are carried out

by a great variety of technical processes where the pyrolysis is controlled by a few reaction parameters, such as temperature, heating rate,heat-treatment duration and the total gas pressure.

The low-temperature stage of pyrolysis below 700°C, has the greatest influence on both the carbon yield and carbon properties.

In all such technical cases, the primary importance is to achieve a high carbon yield which is also determined by the mechanism of the pyrolysis. The pyrolysis must be directed towards the formation of carbon - free volatile by-products and towards avoiding the formation of stable volatile carbon compounds. Thus, the carbon yield can be influenced by the choice of the compound to be pyrolysed, by its thermal and chemical pre-treatment, as well as by the reaction conditions prevailing during the pyrolysis.

As to the pyrolysis technique, five different methods are used alternately :

(1) Pyrolysis in a sealed tube, starting the heating under increasing pressure caused by the pyrolysis gases.

(2) Pyrolysis in autoclaves, where the pressure can be regulated during the whole reaction time.

(3) Liquid pyrolysis in an open crucible with continuous removal of the gaseous by-products; this is mostly used for reactions carried out under normal pressure.

(4) Gas cracking in a steady-state tubular flow reactor with

relatively fast heating of the evaporated starting material and in most cases with quenching of the volatile products.

(5) The hot wire method as a special arrangement of the flow system.

In the first three cases mentioned above low temperatures and prolonged heat-treatment duration are used, where as in the last two cases the shortest contact times and the highest temperatures are generally applied. Here, the influence of evaporation and physical condensation phenomena on these chemical reactions are also considered.

In those cases where the organic materials vaporises on pyrolysis it becomes necessary to heat the samples in sealed tubes in order to obtain appreciable carbon yields[3]. This is because increased gas pressures of evaporated hydrocarbons lead to high carbon yields. Again, as the vapour pressure of the compound being carbonised inside the sealed-tube is not known, it is always preferred to take a heavy-walled pyrex tube or quartz tube so that the tube can stand the increased pressure of the pyrolysis gases. Even then the tube may burst. So, some safety enclosure round the tube should be taken as a precautionary measure against any blow or blast.

Due to heavy pressure inside, it can not be opened ordinarily by cutting with a diamond edge or by tungsten blade without adopting any safety measure against the blow or blast if any. It is, therefore, advised to open the tube inside a strong safety box. Alternately, the tube can be opened without the aid of a safety

box provided it is immersed in a Dewar containing liquid nitrogen for at least an hour before opening. Since the second process involves a thermal shock, it should be avoided.

In the sealed tube technique of pyrolysis mentioned before, heating of the sample is first carried out under normal pressure and then under increasing pressure caused by the pyrolysis gases.

The possibilities for pyrolytic reactions of hydrocarbons are based on thermodynamic considerations as well as on the experience gained during pyrolysis. Pure hydrocarbon compounds must be pyrolysed as model substances. Results will be organised according to the compounds or molecular groups to be pyrolysed, with emphasis on the intermediate products which could be isolated.

6.2 ALIPHATIC HYDROCARBONS

Alkanes are the simplest class of organic compounds which contain only carbon and hydrogen; and they contain two types of bonds : (C - H) and (C - C) single covalent bonds. They are divided into three large classes : (a) aliphatic (b) alicyclic and (c) aromatic. Aliphatic hydrocarbons are open-chain compounds or a cyclic, while alicyclic and aromatic are closed-chain compounds.

Aliphatic hydrocarbons are further divided into (i) saturated and (ii) unsaturated hydrocarbons. Saturated hydrocarbons are those in which linked atoms are bonded with one pair of electrons, called single bond (σ - bond). In unsaturated hydrocarbons having two or three pairs of electrons i.e. having double or triple

bonds as illustrated below [7]

Saturated hydrocarbon

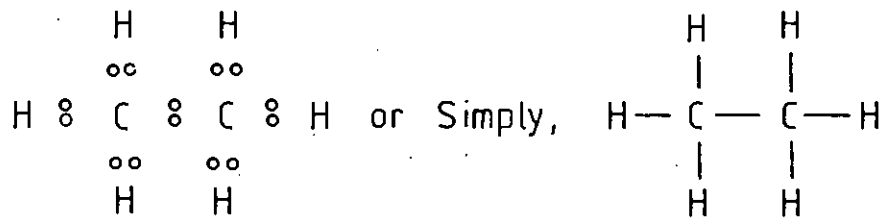

Ethane

Unsaturated hydrocarbon

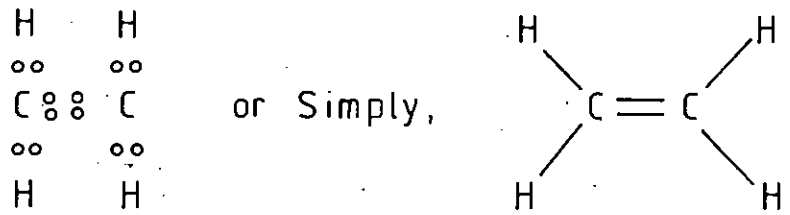

Ethylene

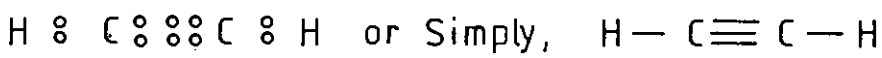

Acetylene

Saturated hydrocarbons are the homologues of methane. They are also known as paraffins due to their inactivity. They are widely distributed in nature. The lower members occur in natural gas. Hydrocarbons of medium and higher molecular weights are found in abundance in petroleum — a mineral oil. Names and properties of some common saturated hydrocarbons are given in table 6-1. They form a homologous series with the general formula $C_n H_{2n+2}$[4], where n is the number of carbon atoms in the molecule. The first number is Methane CH_4 (n = 1); second number is C_2H_6 (n = 2) Ethane, etc.

At ordinary temperature and pressure, the first four members of the series (C_1 - C_4) are gases (C_5 - C_{17}) are colourless liquids and less dense than water; C_{18} and above are all wax like solids.

In general, the boiling point, melting point, viscosity and specific gravity of alkanes increase with an increase of the molecular weights. Isomeric hydrocarbons have different physical properties. The boiling points of n-alkanes increase in a smooth manner with increasing molecular weight(fig. 6-1) where as the melting points do not increase in such a regular fashion (fig. 6-2). Except for a very few alkanes, the boiling point rises by 20°C to 30°C for each carbon that is added to the chain.

For alkane which exists in isomeric forms, the branched chain isomer will have a lower boiling point than the corresponding n-isomer. With branching the shape of the molecule tends to approach that of a sphere and thus the surface area decreases. As a result of the decrease of surface area, the intermolecular forces become weaker and can be neglected at a lower temperature. The density of alkanes also increases with the size of the molecule and tends to approach a constant value of nearly 0.8 with octa-decane. Thus all alkanes are lighter than water.

6.3 POSSIBLE REACTION MECHANISMS OF HYDROCARBON PYROLYSIS

The possible pyrolysis reactions of hydrocarbons can be divided into Degradation reactions and Synthesis reactions.

Degradation Reactions : All degradation reactions are characterised by the mutual effects of cracking and dehydrogenation phenomena. In cracking reactions, paraffins decompose to one paraffin and one olefin, the sum of the carbon and the hydrogen atoms contained in the paraffin and olefin formed being equal to the number of carbon and hydrogen atoms of the starting material.

$$2R_1 - CH_2 - CH_2 - CH_2 - R_2 \begin{cases} \rightarrow R_1 - CH_2 - CH_3 + R_2 - CH = CH_2 \\ \rightarrow R_1 - CH = CH_2 + R_2 - CH_2 - CH_3 \end{cases}$$

In dehydrogenation reactions, hydrogen is split off, causing the formation of a double bond without changing the chain length of the original paraffin.

$$CH_3 - CH_2 - CH_2 - CH_3 \longrightarrow CH_3 - CH = CH - CH_3 + H_2$$

The pyrolytic cracking of a C - C or C - H bond can take place by way of radical or ion formation. This is commonly called homolytic or heterolytic decomposition, respectively as shown below for a compound AB :

$A : B \longrightarrow A^{\cdot} + B^{\cdot}$ Radical mechanism (Homolytic decomposition).

$$\left.\begin{array}{l} A : B \longrightarrow A^- + B^+ \\ A : B \longrightarrow A^+ + B^- \end{array}\right\}$$ Ionic mechanism (Heterolytic decomposition).

The homolytic decomposition leading to the formation of

the radials A• and B• is energetically favoured in comparison to the heterolytic decomposition leading to carbonium cations and carbonium anions. The heterolytic decomposition requires approximately three times as much energy as the homolytic radical reactions.

Therefore, the thermal pyrolysis will proceed primarily according to the redical mechanism, where as catalytic reactions, e.g., the cracking over oxide catalysts, will favour the heterolytic path. In this treatment the catalytic cracking is unimportant. Once formed, the radicals can proceed to react in various ways since such chain reactions require only a very small activation energy of 5 to 10 Kcal/mole.

Propane can also decompose by way of a radical chain mechanism, leading to the formation of four different reaction products.

$$CH_3 + CH_3 - CH_3 \longrightarrow CH_4 + CH_3 - CH_2^{\bullet}$$

$$CH_3 - CH_2\cdot \longrightarrow CH_2 = CH_2 + H\cdot$$

$$H\cdot + CH_3 - CH_3 \longrightarrow H_2 + CH_3 - CH_2\cdot$$

Higher alkanes crack to hydrogen and a mixture of alkanes and alkanes with a varying number of carbon atoms.

During recent years the radical mechanism has also been confirmed for the pyrolysis of cyclic compounds in the liquid phase.

The synthesis of hydrocarbon molecules having a greater number of carbon atoms than the starting material requires reactive species such as are formed by the degradation reactions. It is for

this reason, the degradation reactions and synthesis reactions are commonly called primary and secondary pyrolysis reaction respectively.

6.4 HEXANE

n-Hexane, having molecular formula C_6H_{14} (n = 6) is a colourless mobile and highly refractive liquid with a sharp smell. Its melting point is — 94.3°C and boiling point is 69°C. Its density is 0.66 gm/cc. It is highly inflammable and burns with a smoky luminous flame. Practically it is insoluble in water but soluble in many organic liquids such as Benzene. The orbital structure of hexane is shown below :

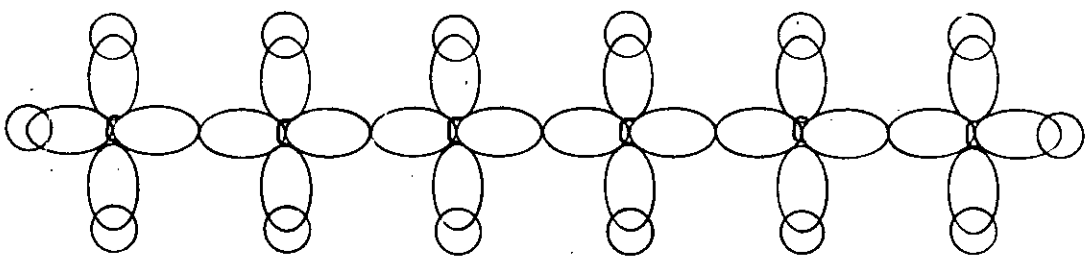

n-Hexane yields benzene, when heated to 300° - 400°C in presence of a catalyst.

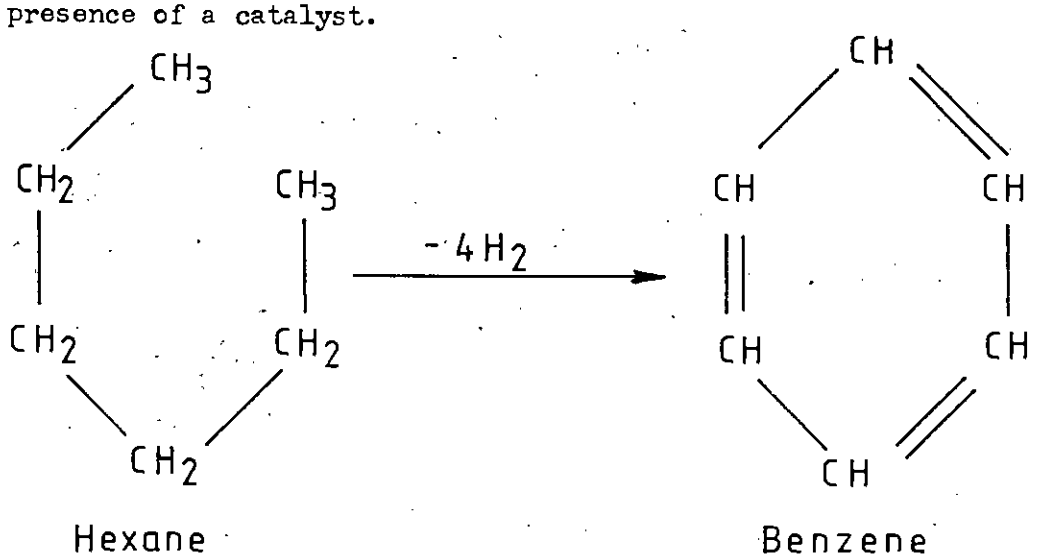

The catalysts used for such aromatization are generally oxides of chromium, vanadium, molybdenium on alumina. Platinum or palladium on charcoal is also used as the catalyst.

6.5 PYROLYSIS OF BENZENE

The pyrolysis of benzene, first described by Berthelot,[9] leads to biphenyl, which is produced today in a large industrial scale. During pyrolysis of Benzene, terphenyls and polyphenyls appears as by-products. The mechanism with formation of phenyl radicals as intermediates is shown in fig. 6-3.

In a sealed tube, biphenyl formation has been observed as beginning below 300°C. The dependence of the bi-phenyl yield on temperature and experimental arrangement[9] is presented in table 6-2[10].

TABLE - 6-1

Some saturated hydrocarbons

Name	Formula	M.P. °C.	B.P. °C.	Density
Methane	CH_4	-184.	-161.4	0.414
Ethane	C_2H_6	-172.	- 88.3	0.546
Propane	C_3H_8	-189.9	- 44.5	0.585
Butane	C_4H_{10}	-135.	- 0.55	0.578
Isobutane	C_4H_{10}	-145.	- 10.2	0.557
Pentane	C_5H_{12}	-131.4	36.2	0.626
Isopentane	C_5H_{12}	-159.	28.	0.621
Neopentane	C_5H_{12}	- 20.	9.5	0.590
Hexane	C_6H_{14}	- 94.3	69.	0.660
2-Methylpentane	C_6H_{14}	-154.	60.	0.654
3-Methylpentane	C_6H_{14}	-118.	64.	0.668
2,2-Dimethylpentane	C_6H_{14}	- 98.3	49.7	0.649
2,3-Dimethylbutane	C_6H_{14}	-135.1	58.1	0.666
Heptane	C_7H_{16}	- 90.	98.4	0.684
Octane	C_8H_{18}	- 56.5	124.6	0.703
Nonane	C_9H_{20}	- 51.	150.6	0.718
Decane	$C_{10}H_{22}$	- 32.	174.	0.730
Undecane	$C_{11}H_{24}$	- 26.5	197.	0.741
Dodecane	$C_{12}H_{26}$	- 12.	216.	0.749
Tridecane	$C_{13}H_{28}$	- 6.2	234.	0.757
Tetradecane	$C_{14}H_{30}$	5.5	252.5	0.765
Pentadecane	$C_{15}H_{32}$	10.	270.5	0.772
Hexadecane	$C_{16}H_{34}$	20.2	287.5	0.775
Heptadecane	$C_{17}H_{36}$	22.5	303.	0.778
Octadecane	$C_{18}H_{38}$	28.	317.	0.782
Nonadecane	$C_{19}H_{40}$	32.	330.	0.777
Eicosane	$C_{20}H_{42}$	38.	205.	0.778
Pentacosane	$C_{25}H_{52}$	54.	259.	0.779
Tricontane	$C_{30}H_{62}$	64.7	304.	0.779
Tetracontane	$C_{40}H_{82}$	81.3	150.	0.778

TABLE - 6.2

Formation of Biphenyl from Benzene[10]

T	F, liters/hr.	Yield of biphenyl, wt%
685°C	0.846	14.6
	0.423	22.4
	0.282	26.2
	0.212	27.8
	0.141	29.2
	0.121	29.4
	0.106	29.4
	0.0282	29.4
	0.0141	29.4
760°C	2.75	13.7

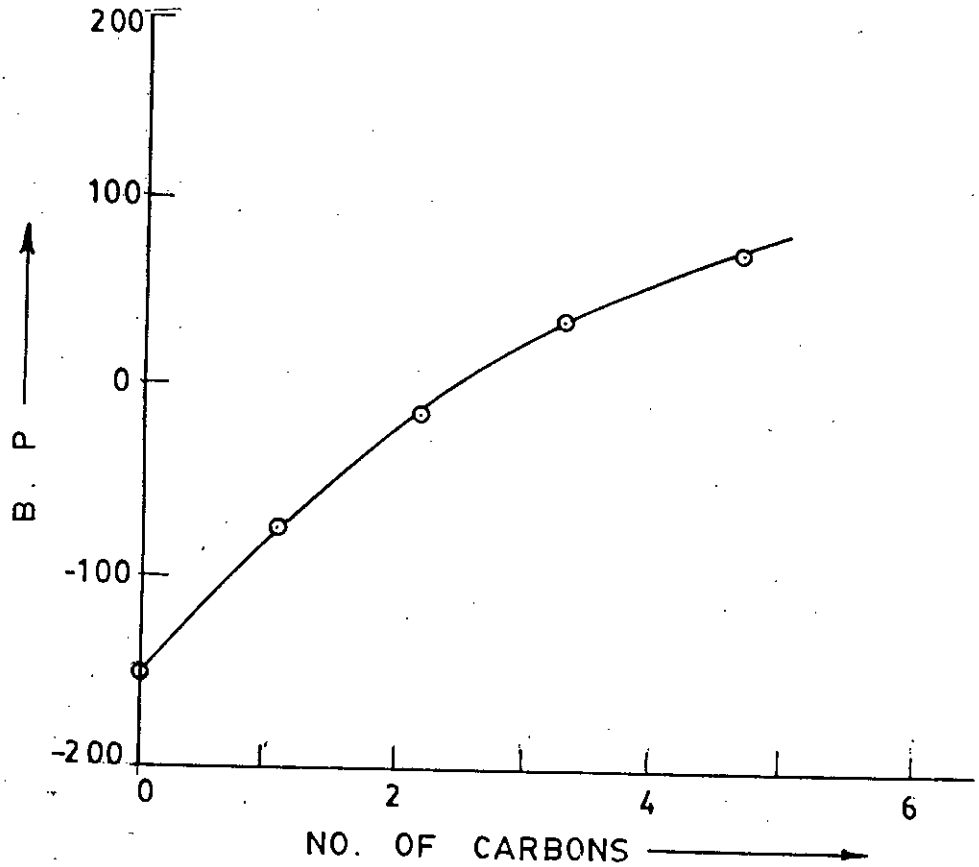

Fig. 6.1 B. P. of n-alkanes.

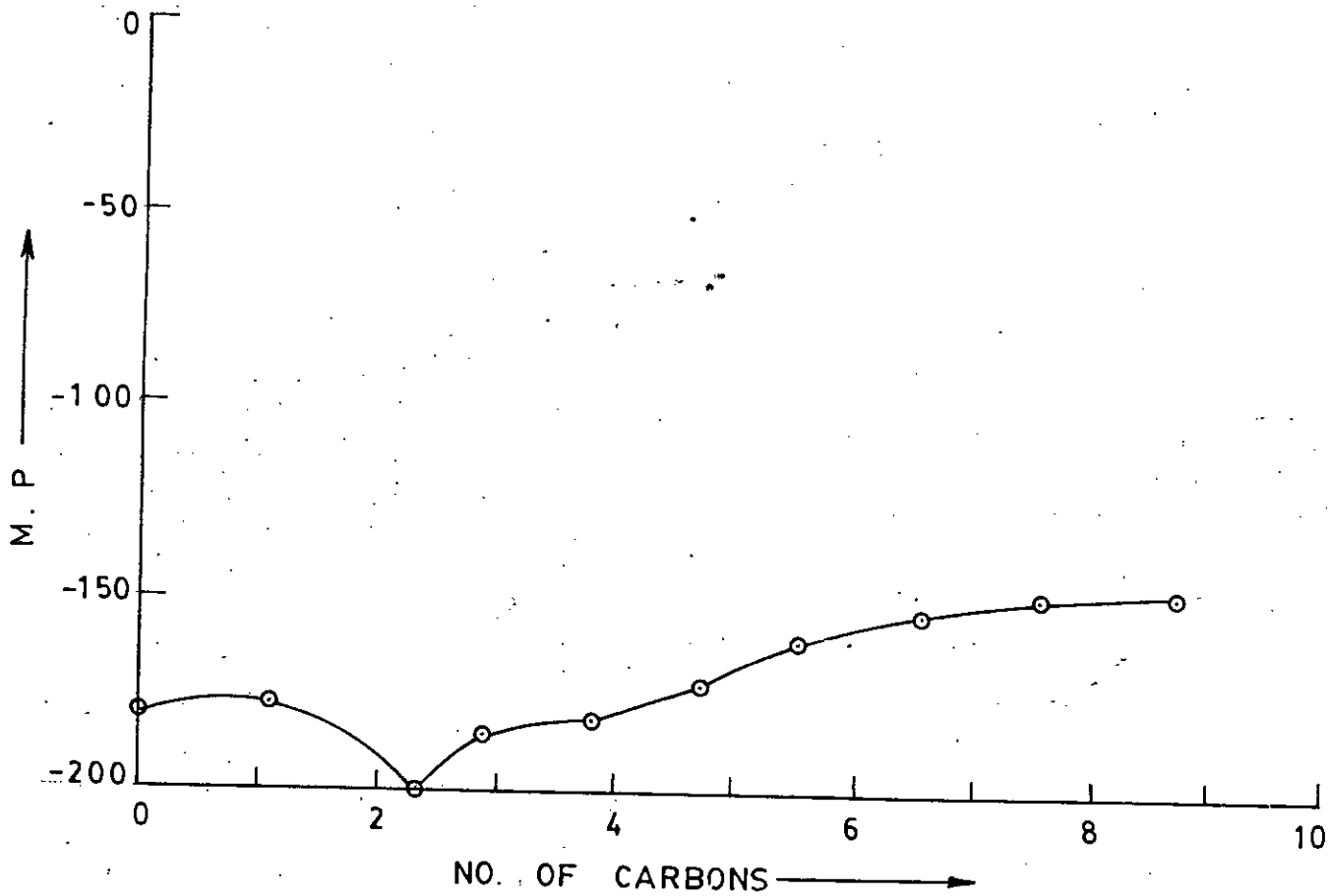

Fig. 6.2 B. P. of n-alkanes.

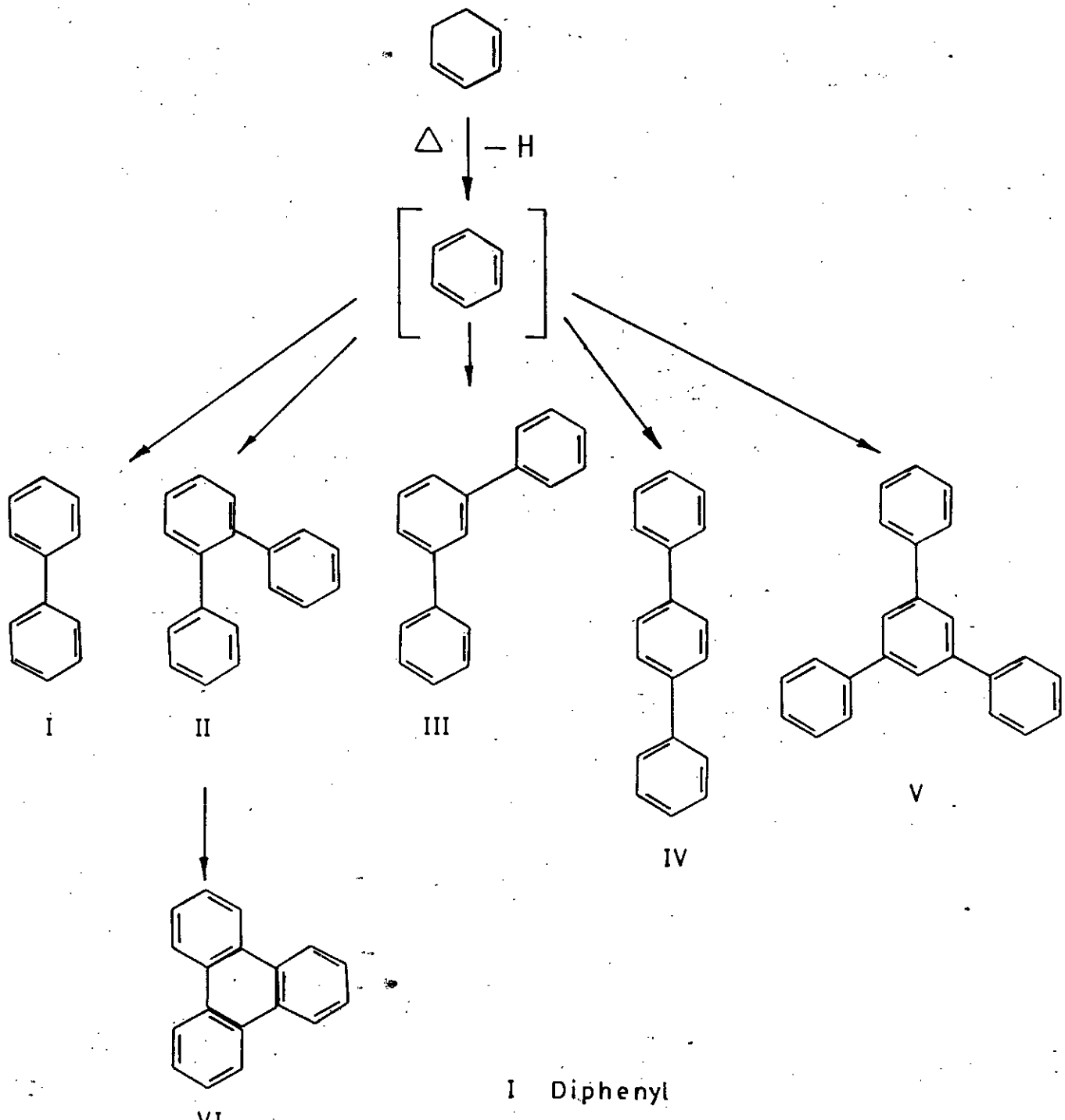

I Diphenyl
II 1, 2 Diphenylbenzene
III 1, 3 "
IV 1, 4 "
V 1, 3, 5 Triphenylbenzene
VI Triphenylene

Fig. 6.3 Pyrolysis of benzene.

REFERENCES

6.1 Fitzer, E., Mueller, K. and Schaefer, W., Chem. Phys. Carbon, 1971, 7, 237.

6.2 Chen, J. and Back, M.H., Pergamon Press, Carbon 1979, 17, 175.

6.3 Fitzer, E., Mueller, K. and Schaefer, W., Chem. Phys. Carbon, 7, 255.

6.4 Hückel, Z. Electrochem., 1937, 43, 752, 827.

6.5 Finar, I.L., Organic Chemistry, 1976, 1, 577, Longmann, London and New York.

6.6 Wheland, G.W., Resonance in Organic Chemistry, 1955, John Wiley, New York.

6.7 Ahmed, M. and Mian, A.J., A text book of organic chemistry.

6.8 Brooks, B.T., The Chemistry of Petroleum Hydrocarbons, 1955, 2, 114, Reinhold Publishing Corporation, New York.

6.9 Hougen, O.H. and Watson, K.M., Chemical process principles, Vol. III, Wiley, New York, 1900, p847.

6.10 Fitzer, E., Mueller, K. and Schaefer, W., Chemistry and Physics of Carbon, 4, 278.

CHAPTER - VII

EXPERIMENTAL RESULTS, DISCUSSIONS AND CONCLUSIONS

7.1 INTRODUCTION

Scientists have shown considerable interest in the mechanism of carbonisation of organic materials. Pyrolysis conditions such as heating rate, temperature, pressure and geometry of the surface certainly affect the properties of carbonisation, but these parameters are usually maintained within relatively narrow ranges.

On heating, the hexane residues undergo appreciable physico-chemical changes in the temperature range of 300 - 600°C. Reactive molecules break along with the weakest bonds forming various free radicals which subsequently recombine with other radicals or molecules to form more highly condensed species and volatile compounds. The carbons formed on heating materials or compounds which do not pass through a fused state have usually isotropic structures and do not graphitize readily.

Most carbon rich materials fall into one of the following three categories :

(1) Pyrolytic carbons, grading into pyrolytic graphite, formed typically from the cracking of hydrocarbon gases at comparatively high temperatures,

(2) Cokes from the carbonisation of material which passes through a mesophase stage[1]

(3) Carbons with highly disordered structures formed in

different ways - for example, by carbonisation of some carbonaceous materials which do not fuse or do not pass through a mesophase stage, by evaporation of carbon, and by combustion of some carbonaceous materials in an insufficient supply of oxygen. Isotropic carbon i.e. the non-graphitizing carbon which has relatively high atomic ratios of hydrogen to non-carbon elements in part resembling carbon black was present in the sample.

The effect of high gas pressure during pyrolysis can be discussed on the basis of

(a) evaporation of carbohydrade compounds and

(b) chemical reactions during the formation of non-volatile polyaromatics.

In the present study the carbonisation of hexane has been examined and polarized-light photomicrography of the sample during carbonisation has been taken in order to study the nucleation, growth and coalescence process if any at different heat-treatment temperatures. Thermal analysis of the partially carbonised sample has been carried out to get the information about the graphitizing or nongraphitizing properties of the material.

The pressure pyrolysis experiments were performed in the laboratory (in furnace) upto maximum temperature of 600°C. Here also thermogravimatric analysis was carried out in order to see the carbonising properties of the material under study.

7.2 EXPERIMENTAL

7.2.1 Sample

n-Hexane, the aliphatic hydrocarbon manufactured by BDH chemicals Ltd.,Poole,England, was used in this study. It had a purity more than 99.99%.

Sample	Formula	Melting Point of Solidified Hexane °C	Boiling Point °C
Hexane	C_6H_{14}	-94.5°C	70°C

7.2.2 The safety device for opening sealed tubes containing heat-treated organic sample.

A heavy pressure is developed when an aliphatic organic compound is heat-treated inside a sealed tube because of the presence of H_2 gas and other hydrocarbon gases which are generally evolved during pyrolysis.

The safety box consists of a mechanical devise for cutting the sealed tube inside it with a diamond edge, having no risk of explosion. The external wall of the safety box is made of 16 SWG aluminium sheet and its design plan is illustrated in fig. 7.1. The portion of a 16 SWG aluminium hinged lead carrying a makralon viewing panel constitute the roof of the box. A spring loaded plunger carrying the diamond edge or tungsten blade is fitted at the lid. The plunger thus slides up and down when pressed and released and its circular motion is restricted by screw in slot. The sealed tube containing the heat-treated sample is placed inside

the safety box in a horizontal position and after cutting it in its central position with the diamond edge a strong push is made on the cutting area from below, as a result of which the tube is found to open very easily.

The above easy method is secured in the following way : The tube is allowed to rest on two 1" Tufnol rollers fitted with two 3/16" M.S. spindles which are in turn fitted to a 10 SWG aluminium frame work clamped firmly on the floor of the box. The ends of the tube passes into rubber caps provided at the ends of two other spring loaded plungers, placed in the same height at the two opposite side walls of the box. These plungers carrying the sealed tube in horizontal position is capable of clockwise or anti-clockwise rotation.

By pressing the lid plunger down and holding it in such a position that the diamond tip/blade is in touch with the tube, a complete rotation is given to the tube by rotating the side plungers placed at the two opposite walls. The sealed tube will thus be found to be cut at the centre. A strong push is then applied on the cutting area by means of a rigid rod having a sharp edge and the tube will be found to open very easily without any blow or blast because of the heavy pressure of the pyrolysis gases inside. To see the tube from outside, the makralon portion of the hinged lid having the size 11" x $4\frac{3}{4}$" x 3 mm is slanted to make an angle of 30° with the vertical wall. A 3" exhanst with a gauze is fitted at one corner of the safety box for clearance of the onrushing gas.

7.2.3 Increasing pressure developed inside pyrolysed sealed tube accelerates carbonisation process

A number of workers[2,3] studied the influence of very high pressures on the carbonisation of pure organic compounds, pitches and coal. They concluded that increasing pressure not only increases the coke yield but also lowers the temperature at which pyrolysis is completed.

Little information seems to be available in the open literature as to the amount of pressure that is developed on pyrolysis of a certain amount of vaporising pure organic sample inside a sealed tube. In such technique of pyrolysis, heating of the sample is first carried out under normal pressure and then under increasing pressure caused by the pyrolysis gas. It is this increasing pressure which accelerates the carbonisation process with a high percentage of carbon yield. In view of the above fact, the sealed tube method was adopted in the case of Hexane.

7.2.4 Differential thermal analysis (DTA)

The formation of the growth of carbonisation accompanied by temporary liquefaction or plasticizing of the materials has earlier been stated to occur generally in the temperature range 350°C to 600°C. DTA has been found to be an important aid in detecting non-graphitizable and graphitizable organic compounds and if graphitizable, DTA trace can be used to ascertain the temperature interval of mesophase formation.

A small amount (about 1.32 gm) of the sample was taken

in a heavy - walled pyrex tube of 2.7 mm thickness and of 12.8 mm internal diameter. The tube along with the sample inside was sealed at both the ends and again placed inside a steel bomb fitted with screw caps at both the ends. The sample was then heat-treated inside a solenoidal furnace (plate - 7.1) at a fixed power input to the bomb upto 500°C, at which temperature the sample was kept for a long duration.

During heating, the pressure inside the sealed tube increased primarily because of the presence of H_2-gas and other hydrocarbon gases which were evolved. After allowing the tube to cool to room temperature, the sealed-tube was opened inside a specially designed safety box to avoid blow or blast, if any due to heavy pressure inside. After opening, the heat-treated sample was removed from inside the tube, dried and then ground in a pestle and mortor.

The sample, withdrawn during the initial thermal treatment after prolonged heating at 500°C, have been heat-treated in the Stanton differential thermal analyser. The sample (40 mgm) was heated in the inconel head to 700°C with dry alumina being employed as the inert material in the reference cell. The DTA traces so obtained (Figs. 7.2 and 7.3) for hexane, were used to study whether it forms isotropic or anisotropic carbons e.g. whether it is non-graphitizable or graphitizable.

7.2.5 Micrographic preparation of samples

The micrographic preparation of the samples comprises the steps of impregnation and mounting, grinding, rough polishing and then final polishing. The procedures were developed from those employed in the micrographic preparation of conventional carbons and graphite[4,5], and differ appreciably only in the final steps. Samples for observation by reflected polarized-light were obtained by heating the original sample (1.32 g) individually in sealed tube inside the solenoidal furnace as before to the desired temperature in which investigation was necessary.

A heating rate of 10°C/min was adopted by the temperature controller. The sample was heated to carbonise at a fixed temperature for a fixed duration. The heated sample was then allowed to cool and on reaching the room temperature the sealed tube was opened inside the safety box as before. The sample was then removed from inside the tube, dried and then embedded in a cold setting mounting resin in the manner described as follows :

A $1\frac{1}{2}$" length of $1\frac{1}{4}$" O.D. x 10 SWG brass tube with one end accurately machined to a flat finish was taken. A piece of metal plate was also taken and its surface was smeared lightly with vaseline. The inside wall of the tube was coated with veseline to prevent adhesion to the mount. The heat-treated sample was then placed on the plate facing downwards and the tube was placed over the sample. The plastic powder was then poured on the tube and it was saturated with the liquid methyl methacrylate. The slurry was kept stirred gently at the beginning to prevent air bubbles

adhering to the sample. After 20 - 25 minutes, the mould was lifted off the plate and the mount was tapped through with a rod and hammer.

The mounted sample was then ground by water proof silicon carbide papers, using tap water as lubricant and progressing from 320 to 600 grit to expose the carbonised residue in the way described as follows :

The silicon carbide paper in the form of a disc was fixed on the top of a rotator and the sample was allowed to be rubbed by the silicon paper when the disc was kept on rotation. Light but steady pressures were applied on the sample while it was rubbed by the carbide paper. During each stage, the direction of polish was maintained constant except for reversals made at regular intervals by lifting and rotating the sample by 180° in hand, accordingly the sample was not moved about the wheel but was only moved laterally between the centre and the periphery. The sample was washed with tap water before using with another comparatively finer grade of carbide paper.

The best results were found to be achieved by using fresh paper for each sample and by grinding somewhat further than what was necessary at each grit level to remove the scratches from the preceding paper. After the final grinding on 600 - grit paper, the surface of the sample appeared bright independent of the level of heat-treatment.

Subsequent polishing was done with diamond lapping compounds ($6\,\mu$ size followed by $0.5\,\mu$ size) on a wet polishing silk

cloth supplied by Buehler Limited, U.S.A. in the way described as follows :

The coarse grade diamond compound was spread over the polishing silk cloth fixed on one of the rotating discs of the Shimadzu polisher and the sample was kept on rubbing for about five minutes and then thoroughly washed with tap water. The finer grade diamond compound was then spread over another polishing silk cloth fixed on the other rotating disc of the polisher and the sample was again kept on rubbing for another five minutes.

Final polishing of the sample was carried out by high purity Alpha Alumina Powder. The powder was first wetted with distilled water and the sample was then rubbed gently by it with hand in the same direction for about ten minutes. The final polishing resulted in a highly polished surface which proved suitable for observation by polarized-light microscopy.

7.2.6 Polarized-light microscopy

Samples prepared in the above manner were observed and photographed with a Reichert "METAVERT" polarizing microscope (Plate - 7.2) using reflected polarized-light. Black and White photographs of the carbon phases and of subsequent heat-treated samples were obtained using FUJI NEOPAN SS Black and White 135 mm 36 exp. film. The analyser and the polarizer remained parallel to each other, when the analyser and polarizer remained cross with respect to each other with the gypsum plate at an angle of 45° with the analyser, extinction occurs giving dark background. This

is the so called sensitive tint technique. The light source of the microscope was 6V, 15 W low-voltage halogen bulb. An exposure time of 10 minutes per photograph was used.

7.3 RESULTS AND DISCUSSIONS

7.3.1 Appearance of carbons obtained by sealed - tube pyrolysis of Hexane

The pyrolysis of hexane within sealed-tube at different heat-treatment temperatures and durations gives carbon. The deposit of carbon is a closely adhering films of silver grey colour (i.e. black carbon). The physical appearance of each product of carbon was nearly same and such type of carbons are shown in plates 7.3 and 7.4 respectively.

7.3.2 Differential thermal analysis (DTA)

Differential thermal analysis traces of three hexane samples of different heat-treatment duration are presented in figs. 7.2 and 7.3. Characteristic of these curves is the presence of an initial large exotherm which is then followed by small fluctuations in the trace before a smooth trace returns. The fluctuations are characteristic of all the different hexane samples. The maximum point of the extreme right in the curves represents the temperature at which the fluctuations terminate and the curve changes direction sharply. The extreme right hand side turning point in the thermal curves of hexane indicates that the carbonisation is almost complete.

Similar observations were observed for hexane heat-treated to a different duration.

The DTA traces obtained for the hexanes under study clearly indicate that exothermal processes of transformation in the initial portions of the curves are typical in all the samples and so they all seem to be non-graphitizable[9]. However, optical analysis is required to confirm non-graphitizable property of the sample.

The actual fluctuations in the curves may arise through the formation of gases within the sample. This may result in the sample being lifted away from the thermocouple momentarily thus causing a small peak to occur in the curve. This process may then repeat itself, till the sample is decomposed to produce carbon residues.

The deflections in the DTA trace are also due to chemical reactions and devolatization. The deflections downward in the DTA trace are caused primarily by devolatization. The exothermic reaction is sometimes superimposed on an endothermic reaction resulting in a nearly feat portion in the curve[10].

7.3.3 Carbonisation is enhanced by temperature, duration of heating and pressure

The conversion of hexane to carbon is catalyzed by the presence of contact surfaces, especially coke or carbon. No doubt the hydrocarbons are absorbed on such surfaces, and undergo dehydrogenation, forming bi-radicals or even other complex condensation

products. The biradicals are eventually converted to carbon. The gradual increase of temperature and duration, more and more carbons are produced and the vaporising pressure is consequently reduced. When the vapour pressure of the product becomes negligible at high temperatures it is thus classified as carbon. The increase of carbon-yield with the increase of temperature and heat-treatment duration during carbonisation is illustrated in Table 7.1 as well as in fig. 7.6. Variation of carbon percentage with the rise of temperature at a different heat-treatment duration during the initial pyrolysis of hexane is illustrated in fig. 7.7.

The variation of pressure inside the sealed-tube with temperature at different heat-treatment duration during carbonisation is well documented in table 7.2 as well as in fig. 7.8. The increasing pressure inside the sealed tube thus enhances the carbonisation process. It is well known[8] that pressure increases the viscosity of liquids. Thus the effect of pressure will not only reduce considerably any tendency of bubble formation, but also reduce disorder produced by convection currents within the system (because of enhanced viscosity).

Increasing pressure enhances molecular condensation reactions as well as the viscosity of the system. The enhanced viscosity affect both diffusion and coalescence rates. As the temperature is further increased, the isotropic liquid phase should entirely be removed, but in this sample it did not do so and therefore, the sample is isotropic.

7.3.4 Polarized-light photomicrograph

The polarized-light photomicrographs of hexane at different heat-treatment temperature and duration presented in plates 7.6 to 7.11. clearly indicate that they are optically isotropic and so nongraphitic in character because of the following two main observations :

(i) The well - defined maltese cross-patterns of optical anisotropy, the important criterion of graphitizable organic compounds are absent in the case of hexane when pyrolyzed between usual mesophase interval (300° - $600^{\circ}C$), where nucleation, growth and coalescence processes should generally occur in the case of graphitizable organic compounds.

(ii) The structure of the carbonised sample when viewed under cross-polars with the gypsum plate at an angle of 45° with one of the polars (sensitive tint method) did not display nodes and crosses having any change of colour with the rotation of the stage along with the sample. This confirms the fact that hexane gives rise to non-graphitic carbon of optically isotropic in nature. The DTA and TGA curves also confirmed the isotropic and non-graphitizing nature of hexane.

7.4 CONCLUSIONS

It was presumed that hexane when decomposed on pyrolysis should give rise to benzene which is graphitizable in character. The DTA curve (fig. 7.4) and the polarized-light photomicrograph

(plate 7.5) of benzene confirmed its graphitizing character from long before. The thermal and optical studies confirm that hexane on pyrolysis produce non-graphitizing carbon of optical isotropy. This is because the benzene yield obtained by the decomposition of Hexane is very poor and a small mass of anisotropic matrix(benzene) is suspended in a big mass of isotropic matrix(Hexane).It is therefore, expected that isotropic characters should become prominent and this has exactly occurred in the present case of investigation pyrolysis of hexane might have produced simultaneously two reactions, one of which is exothermic and the other endothermic.

The DTA curve of hexane is flat in some portions and is initially exothermic, possibly this is because of superimposition of exothermic peak on endothermic peak. The prominent one will be observed in the DTA trace and this has rightly occured in this case. So our expectation that hexane should produce graphitizing carbon is not correct. In this present study hexane produced non-graphitizing carbon which is isotropic in nature.

In the case of an organic compound under heat-treatment the exothermic reaction because of cross linking somewhere in the initial portion of the DTA trace indicates non-graphitizing nature of the sample. This is why, hexane is said to produce non-graphitizing carbon, isotropic in character.

TABLE - 7.1

Conversion of Hexane to carbon in % on pyrolysis

No. of Observation	Temperature in ^{o}C	Duration in hours	Amount of the sample taken in gm.	Wt.of the Carbonised sample + HC gas along with tube in gm.	Wt. of the tube after breaking in gm.	Wt. of the Carbon in gm.	% of Carbon obtained
1	515	10	1.32	66.12	66.002	.118	8.94
2	515	12	1.32	66.20	66.068	.132	10.00
3	520	10	1.32	66.25	66.078	.172	13.03
4	520	12	1.32	66.30	66.102	.198	15.00
5	525	8	1.32	66.32	66.129	.191	14.47
6	525	10	1.32	66.30	66.069	.231	17.50
7	525	12	1.32	66.32	66.056	.264	20.00
8	530	8	1.32	66.40	66.156	.244	18.48
9	530	10	1.32	66.42	66.143	.277	21.00
10	530	12	1.32	66.43	66.10	.330	25.00
11	535	8	1.32	66.51	66.22	.290	21.97

Contd.

(Contd.)

Conversion of Hexane to carbon in % on pyrolysis

No. of Observation	Temperature in °C	Duration in hours	Amount of the sample taken in gm.	Wt. of the Carbonised sample + HC gas along with tube in gm.	Wt. of the tube after breaking in gm.	Wt. of the Carbon in gm.	% of Carbon obtained
12	535	10	1.32	66.53	66.20	.330	25.00
13	535	12	1.32	66.51	66.127	.383	29.02
14	540	8	1.32	66.52	66.19	.330	25.00
15	540	10	1.32	66.55	66.167	.383	29.02
16	540	12	1.32	66.57	66.148	.422	31.97
17	545	8	1.32	66.58	66.21	.370	28.03
18	545	10	1.32	66.55	66.134	.416	31.52
19	545	12	1.32	66.53	66.068	.462	35.00
20	550	8	1.32	66.52	66.124	.396	30.00
21	550	10	1.32	66.55	66.101	.449	34.02
22	550	12	1.32	66.53	66.042	.488	36.97

TABLE - 7.2

Variation of pressure with temperature at different heat-treatment duration during the initial carbonisation of hexane in sealed tube

No. of Observation	Temperature in ^{o}C	Duration in hours	Wt. of the sample taken in gm.	Wt. of carbon obtained in gm.	Wt. of HC in gm.	Pressure developed in the sealed tube in atm.
1	515	10	1.32	.118	1.202	533.87
2	515	12	1.32	.132	1.188	529.83
3	520	10	1.32	.172	1.148	515.12
4	520	12	1.32	.198	1.122	507.69
5	525	8	1.32	.191	1.129	506.48
6	525	10	1.32	.231	1.089	495.17
7	525	12	1.32	.264	1.056	485.72
8	530	8	1.32	.244	1.076	488.45
9	530	10	1.32	.277	1.043	479.16
10	530	12	1.32	.330	0.990	464.23
11	535	8	1.32	.290	1.030	472.53

Contd.

(Contd.)

Variation of pressure with temperature at different heat-treatment duration during the initial carbonisation of hexane in sealed tube

No. of Observation	Temperature in ^{o}C	Duration in hours	Wt. of the sample taken in gm.	Wt.of carbon obtained in gm.	Wt. of HC in gm.	Pressure developed in the sealed tube in atm.
12	535	10	1.32	.330	0.990	461.36
13	535	12	1.32	.383	0.937	446.52
14	540	8	1.32	.330	0.990	458.52
15	540	10	1.32	.383	0.937	443.71
16	540	12	1.32	.422	0.898	432.94
17	545	8	1.32	.370	0.950	444.69
18	545	10	1.32	.416	0.904	431.97
19	545	12	1.32	.462	0.858	419.26
20	550	8	1.32	.396	0.924	434.83
21	550	10	1.32	.449	0.871	420.27
22	550	12	1.32	.488	0.832	409.56

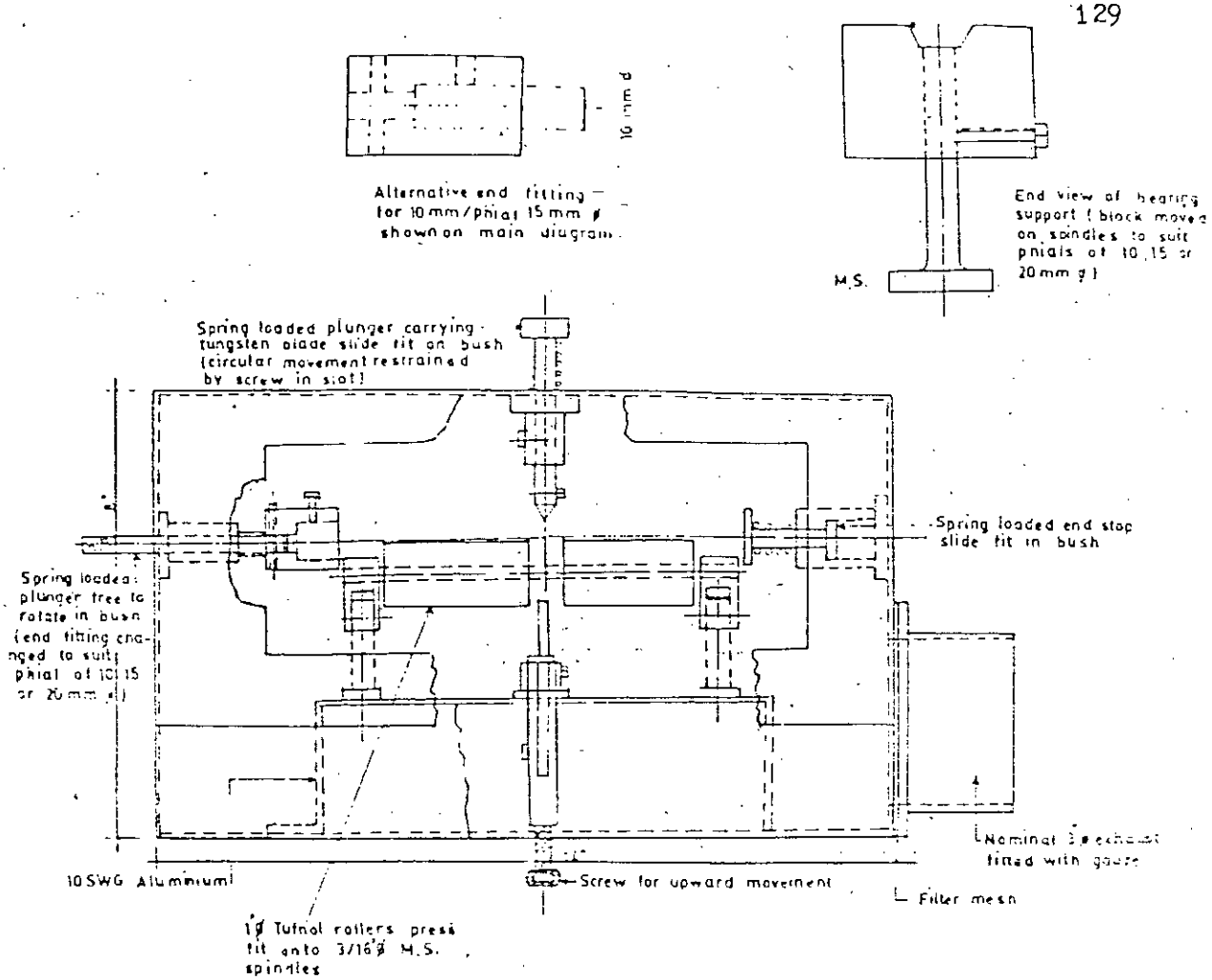

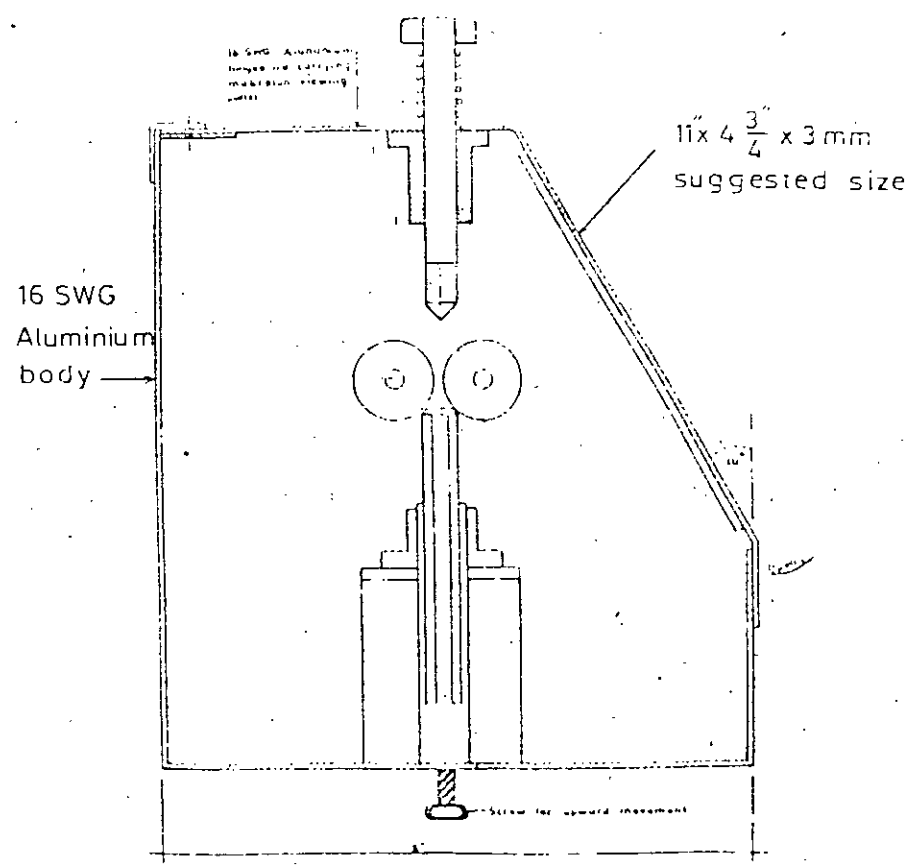

Fig. 7.1 Design plan of the Safety Box

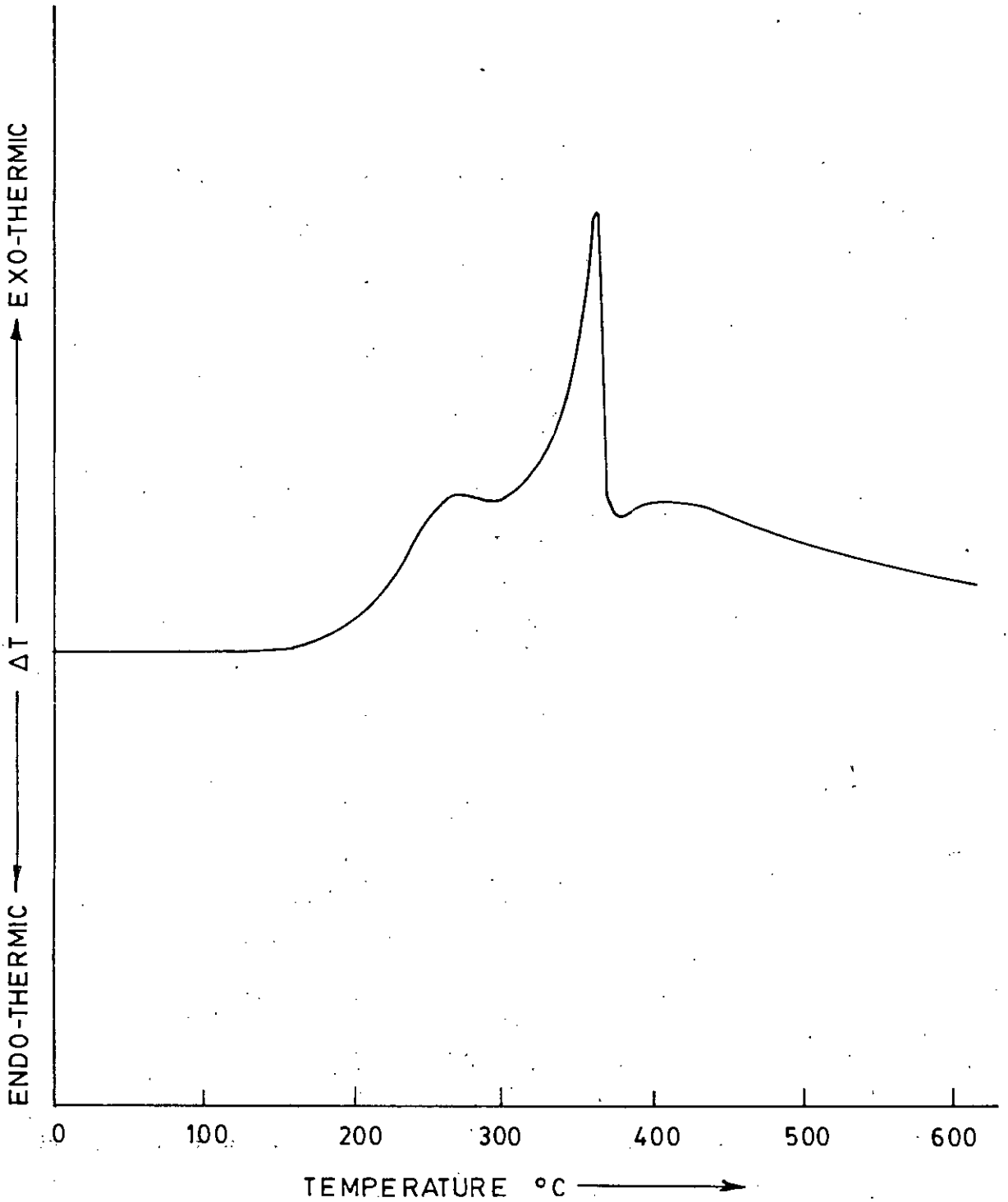

Fig. 7.2. Thermal analysis curve of partially carbonised hexane ($C_6 H_{14}$) on heat-treatment at 500°C for a duration of 8 hours.

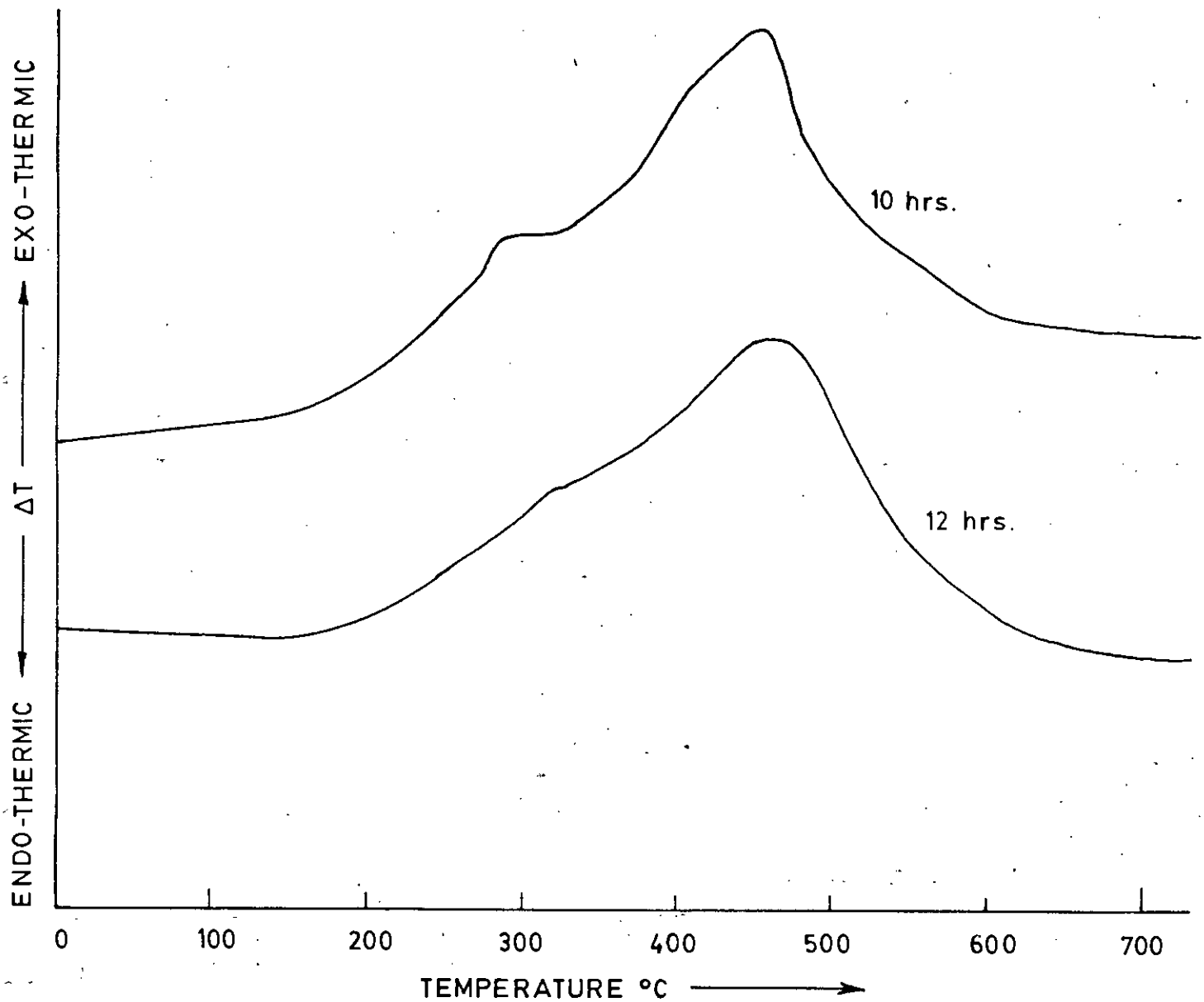

Fig. 7.3 Thermal analysis curve of partially carbonised hexane ($C_6 H_{14}$) on heat-treatment at 500°C for a duration of 10 hours and 12 hours respectively

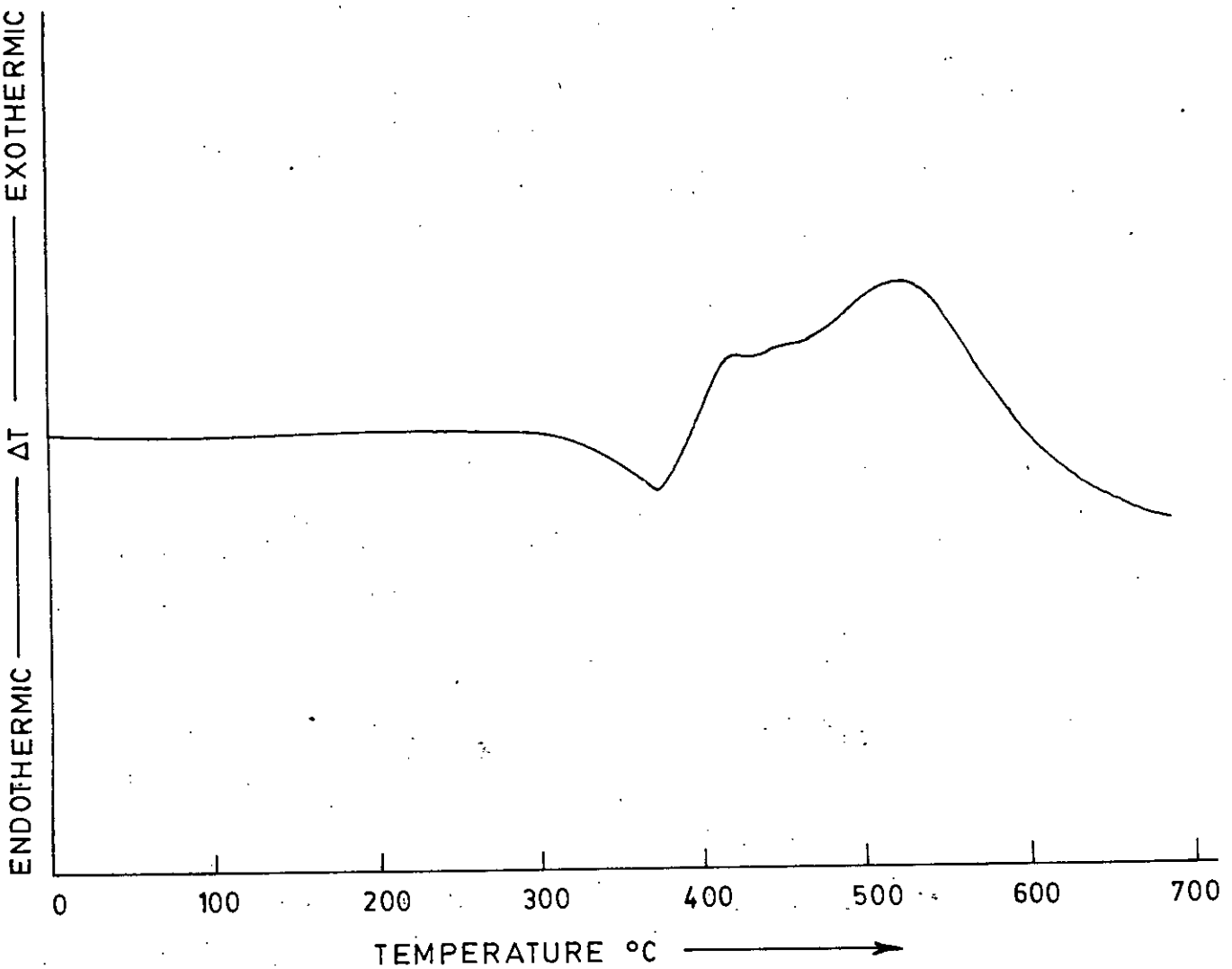

FIG. 7.4 Thermal analysis curve of partially carbonised benzene (C_6H_6) on heat-treatment at 500°C for a duration of 12 hours.

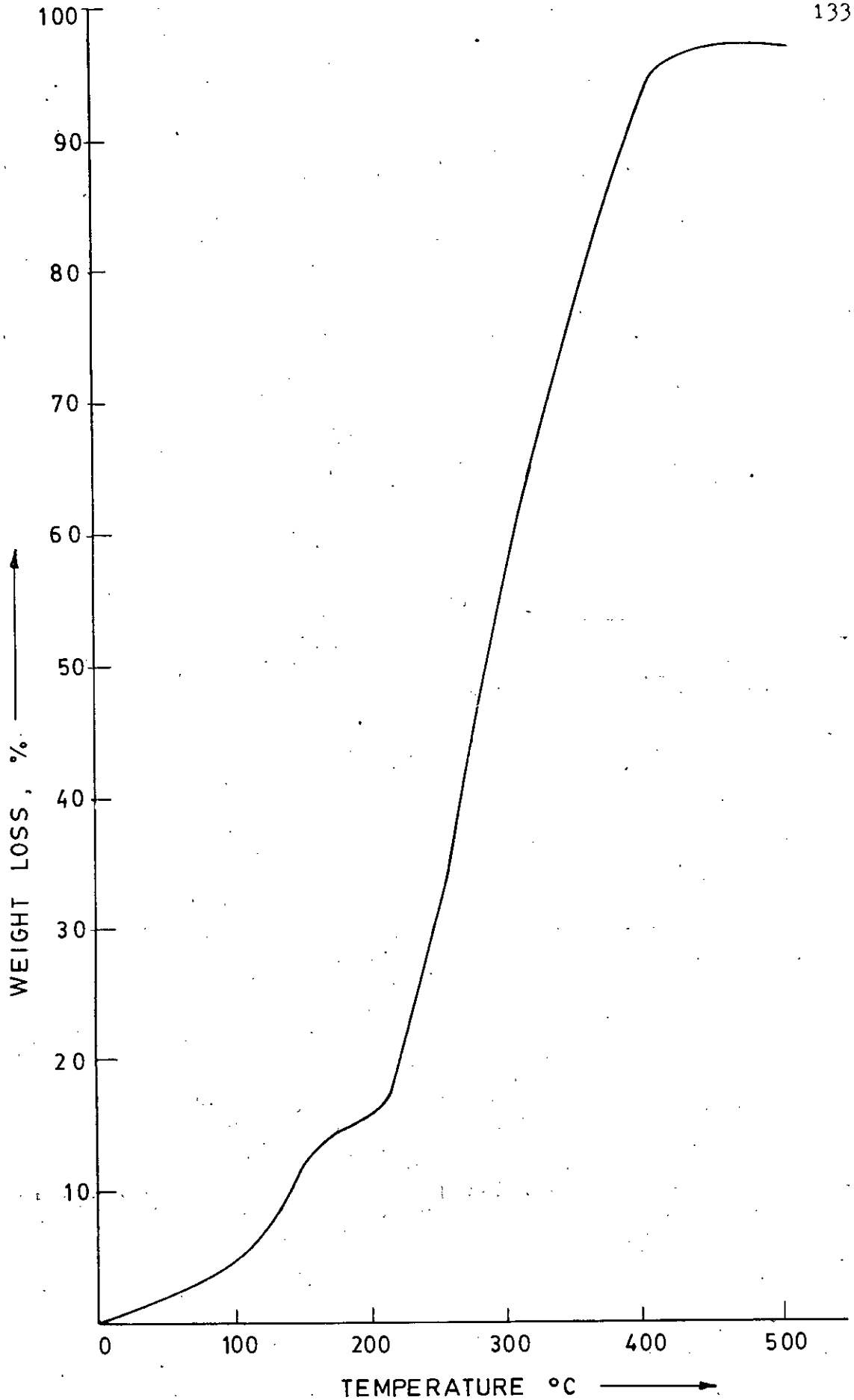

Fig. 7.5 TGA trace of partially carbonised hexane (C_6H_{14}) on heat-treatment at 500°C for a duration of 12 hours.

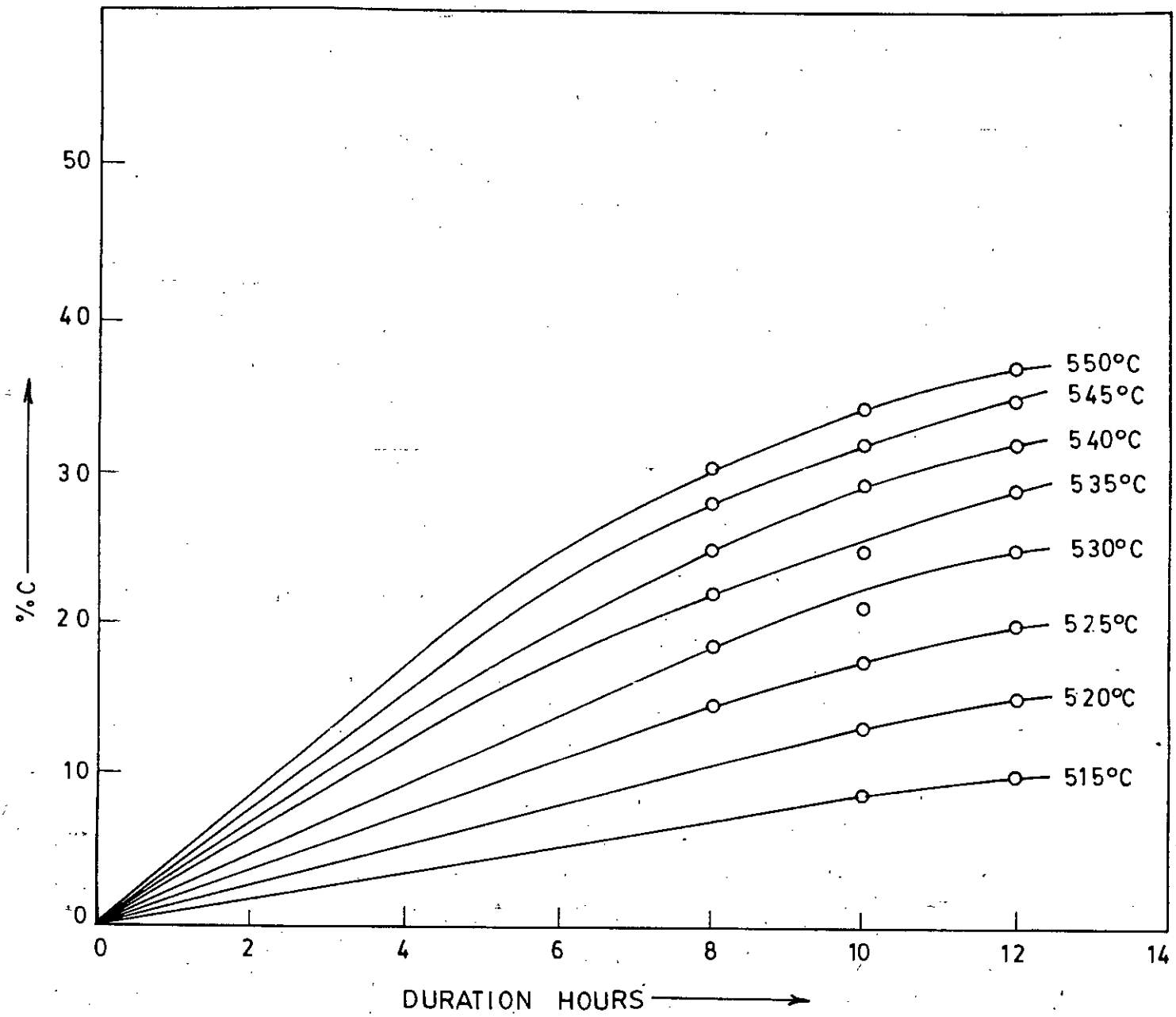

Fig. 7.6 Conversion of Hexane to carbon during pyrolysis of Hexane.

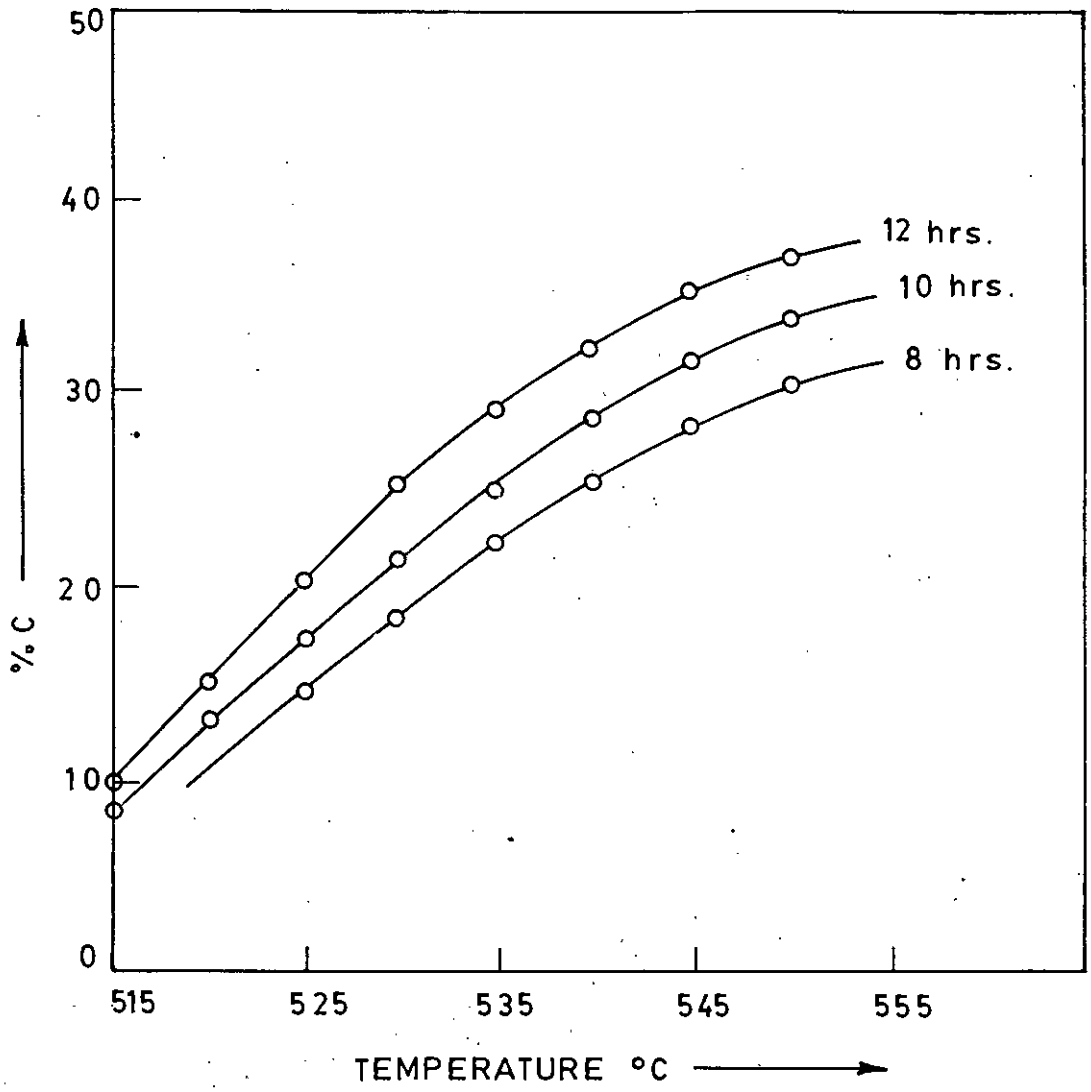

Fig. 7.7 Variation of % C with the rise of temperature at a different heat-treatment duration during the initial pyrolysis of Hexane.

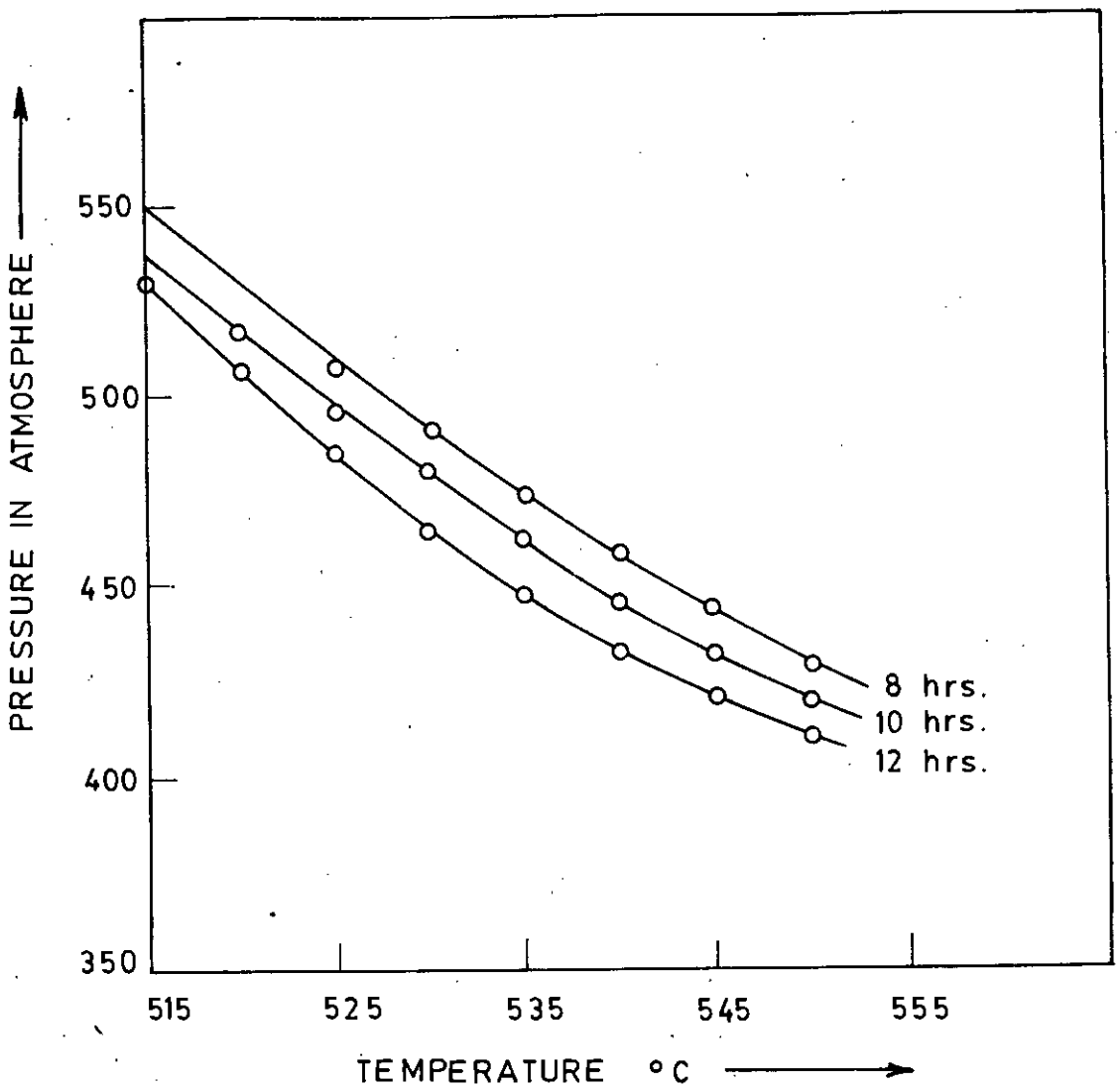

Fig. 7.8 Variation of pressure with temperature at different heat treatment duration during pyrolysis of Hexane.

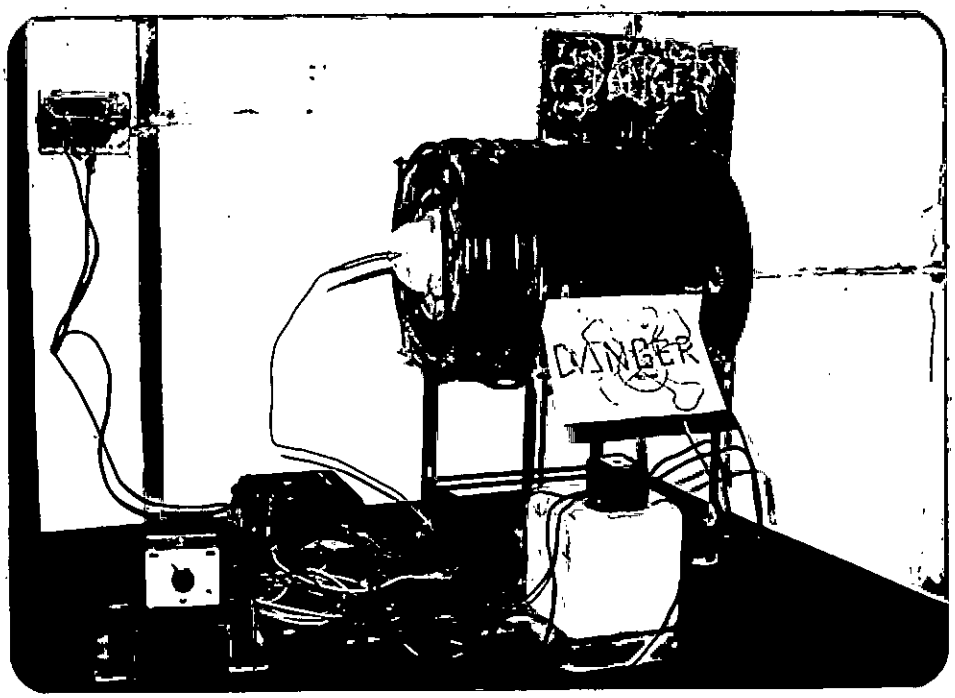

Plate 7.1 : A locally manufactured solenoidal electric furnace having temperature range upto 800°C.

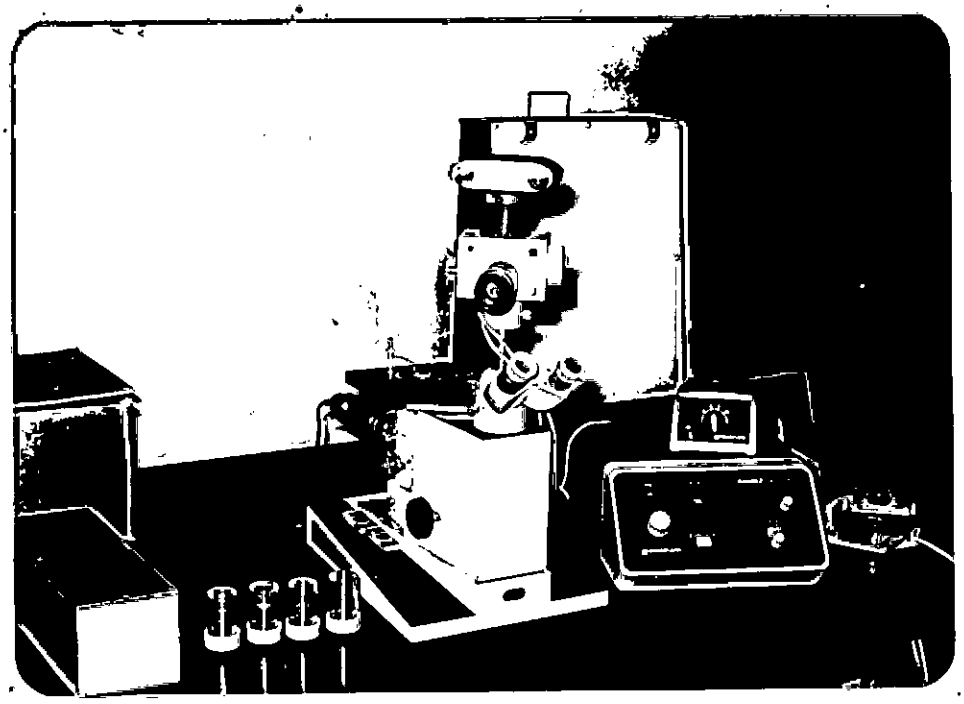

Plate 7.2 : REICHERT METAVERT Polarizing Microscope equipped with 35 mm kam ES2 Camera.

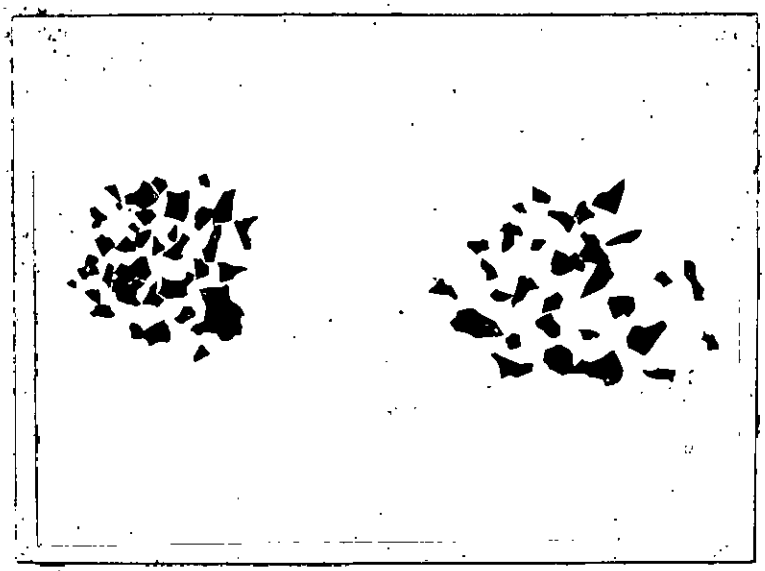

7.3 : Physical appearance of carbon prepared from Hexane.

7.4 : Physical appearance of carbon prepared from Hexane.

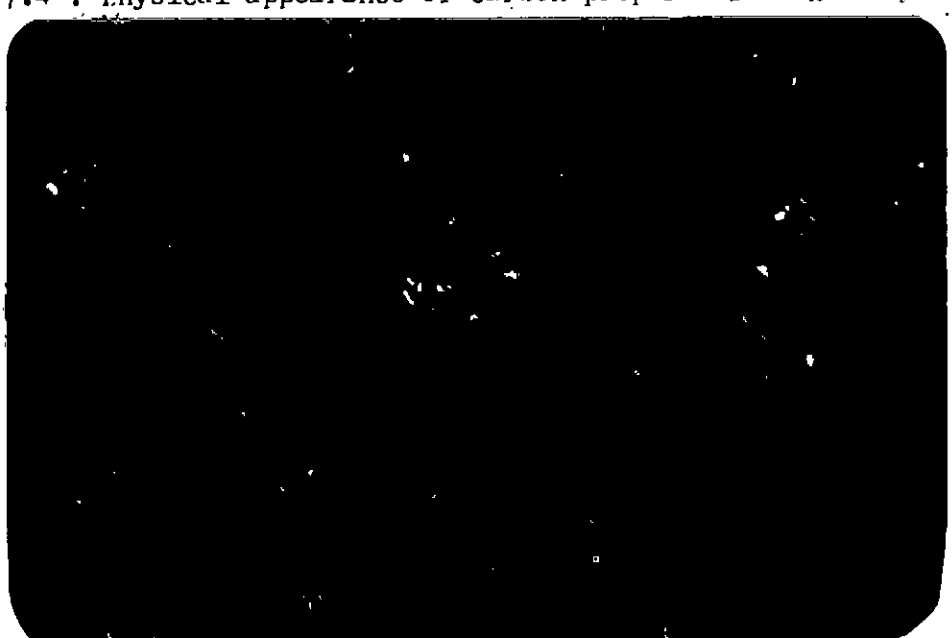

7.5 : Mesophase spherules in benzene heat-treated to 540°C for a duration of 10 hours.

Plate 7.6 : Polarized-light photomicrograph of Hexane on heat-treatment at 540°C for 10 hours.

Plate 7.7 : Polarized-light photomicrograph of Hexane on heat-treatment at 540°C for 12 hours.

Plate 7.8 : Polarized-light photomicrograph of Hexane on heat-treatment at 545°C for 10 hours

Plate 7.9 : Polarized-light photomicrograph of Hexane on heat-treatment at 545°C for 12 hours.

Plate 7.10 : Polarized-light photomicrograph of Hexane on heat-treatment at 550°C for 10 hours.

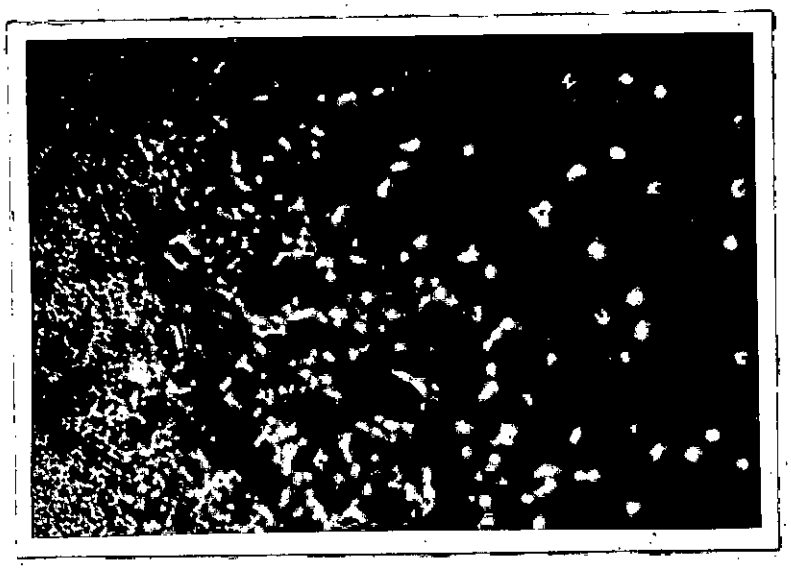

Plate 7.11 : Polarized-light photomicrograph of Hexane on heat-treatment at 550°C for 12 hours.

REFERENCES

7.1 Brooks, J.D. and Taylor, G.H., Nature, 1965, 206, 697.

7.2 Whang, P.W., Dachille, F. and Walker, P.L., J. High Temperatures - High Pressures, 1974, 6, 127.

7.3 Hüttinger, K.J. and Rosenblatt, U., Carbon, 1977, 15, 69.

7.4 Pincus, I. and Gendron, N.J., Proc. Fourth Conf. on Carbon, 1960, 687.

7.5 Clark, T.J., USAEC Report HW-68182, Part 1 (1961).

7.6 Gray, G.W., Molecular Structure and the Properties of Liquid Crystals, Academic Press, 1962.

7.7 Graham, S.G., Ph.D. Thesis, Salford University England, 1974, 235.

7.8 Kinney, C.R. and Delbel, E., Ind. Eng. Chem., 1954, 46 (3) 548.

7.9 Dollimore, D. and Heal, G.R., Carbon, 1967, 5, 65.

7.10 Glass, H.D., Fuel, 1955, 34, 253.

7.11 Hossain, T., Ph.D. Thesis, Salford University England, 1981.

7.12 Jahan, S.T., M. Phil. Thesis, BUET, 1985.